METABOLISM AND METABOLIC DISEASE

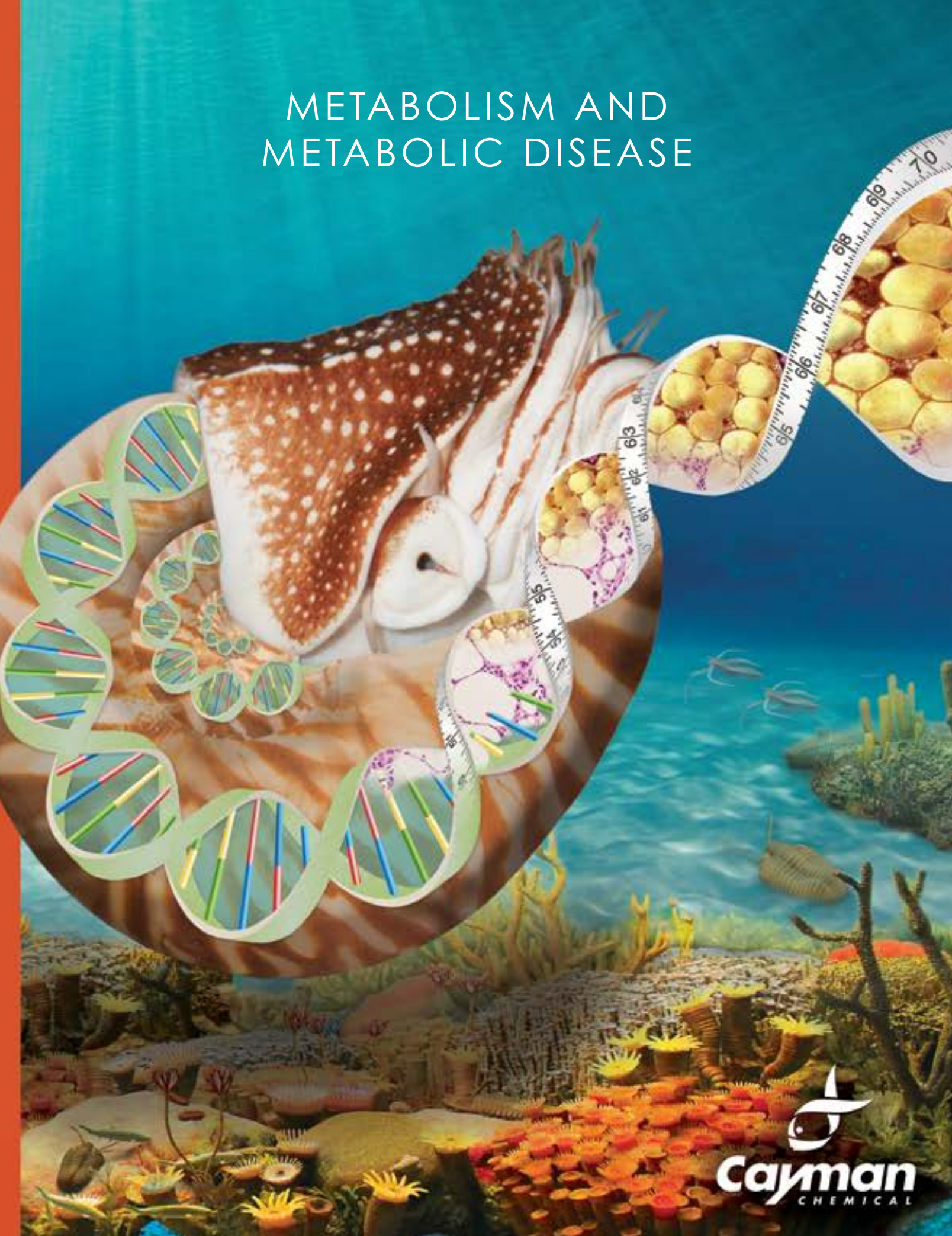

Cayman CHEMICAL

Thomas G. Brock, Ph.D.

Introduction to

Metabolism and Metabolic Disease

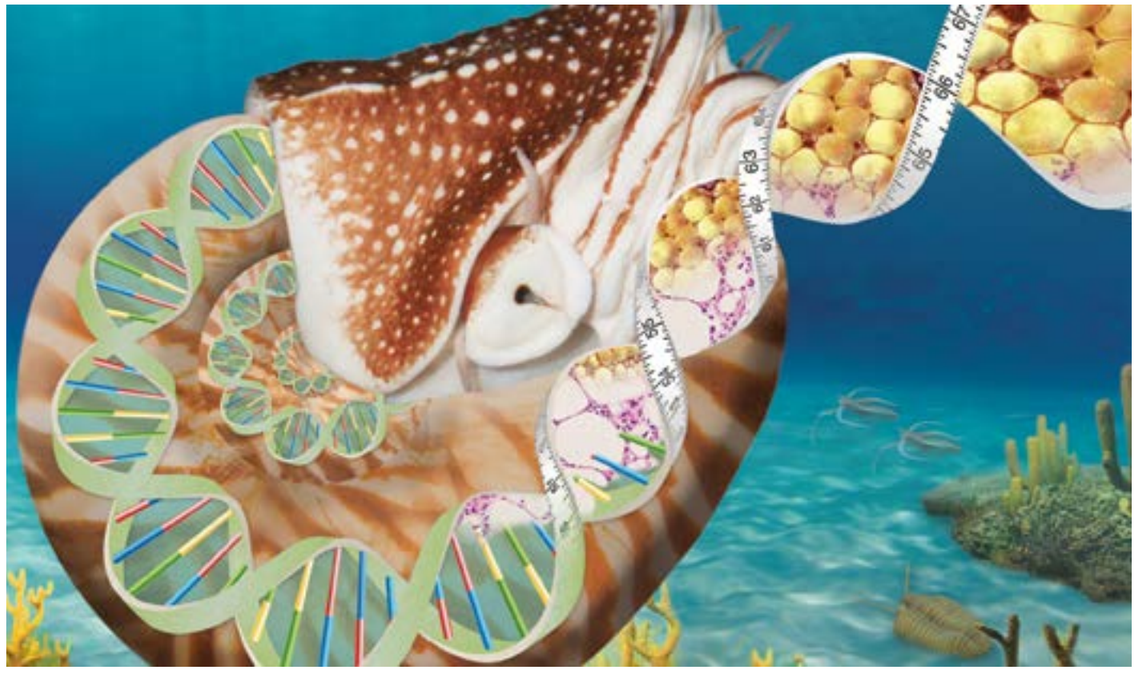

Of all of the cephalopods, the nautilus (our current cover creature) perhaps suffers most from lack of face recognition. Sure, many are familiar with the iconic shell, with its colorful patterning and intriguing spiral. However, squids and octopi are much better known, having landed major roles in movies, cartoons, and menus. Still, the curious scientist would do well to ponder the eye of the nautilus, peeking out from under its mantle, and the collection of tentacles organized around the mouth. These features emerged, along with a wide variety of diverse lifeforms, during the Cambrian explosion, some 500 million years ago. While many organisms either evolved or went extinct, the nautilus has proven to have a truly exceptional body plan that has prospered with little need for modification to this day.

The nautilus may be the perfect poster creature for metabolism, representing millions of years of successful health with no evidence of obesity, diabetes, or hypertension. Compare that track record with the checkered past of certain hominids. *Homo sapiens*, the most recent of a series of *Homo* species that can be traced back to the Pliocene some 2 million years ago, is also the only *Homo* species that has not yet become extinct. Today, over 75% of American adults over 20 years of age are overweight or obese, while some 20% of children aged 6-19 have a BMI-for-age at the 95th percentile or higher. Among American adults, obese individuals, comprising greater than 40% of the total population, surpass the number of overweight adults, at around 34%. As obesity increases the likelihood of developing heart disease, type 2 diabetes, and a host of other diseases, the condition represents one of the leading preventable causes of morbidity and mortality.

Homo Sapiens paradoxically finds itself metabolically maladapted for a nutritional environment that is largely of its own making – but there is hope through research. Cayman's goal is to make your research possible. In this catalog, you will find the best reagents, assay kits, proteins, and antibodies for research related to metabolism. Many more products can be found on our website (caymanchem.com). We are constantly expanding our product line, so feel free to register for new product emails that are tailored to your specific area of interest. We want to help you with your next great discovery!

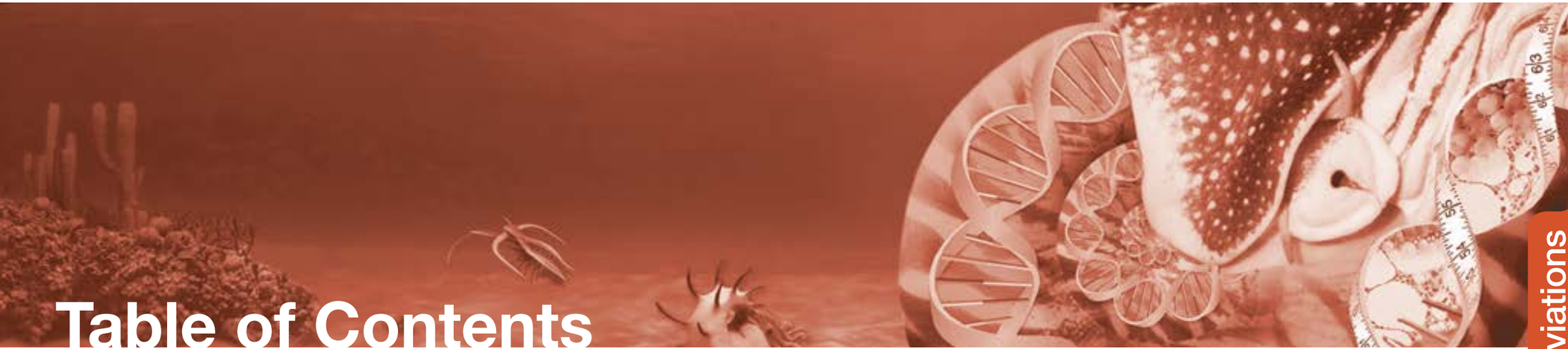

Table of Contents

vol. 16
Me
Metabolism and Metabolic Disease

abbreviations

ACAT	Acyl-coenzyme A:Cholesterol Acyltransferase
AEA	Arachidonoyl Ethanolamide; Anandamide
A-FABP	Adipocyte Fatty Acid Binding Protein
AMPK	AMP-activated Protein Kinase
aP2	Adipocyte Protein 2
CB	Cannabinoid
CDCA	Chenodeoxycholic Acid
COX	Cyclooxygenase
DHA	Docosahexaenoic Acid
EC_{50}	Effective Concentration
ED_{50}	Effective Dose
EIA	Enzyme Immunoassay
ELISA	Enzyme-linked Immunosorbent Assay
EPA	Eicosapentaenoic Acid
FAS	Fatty Acid Synthase
FFA	Free Fatty Acid
FITC	Fluorescein Isothiocyanate
FP	Prostaglandin F Receptor
FXR	Farnesoid X Receptor
GPCR	G Protein-Coupled Receptor
HDL	High-Density Lipoprotein
HIV	Human Immunodeficiency Virus
HMG-CoA	3-Hydroxy-3-methylglutaryl-coenzyme A
ICC	Immunocytochemistry
IHC	Immunohistochemistry
IP	Immunoprecipitation
K_d	Dissociation Constant
K_i	Dissociation Constant
LDL	Low-Density Lipoprotein
LO	Lipoxygenase
LXR	Liver X Receptor
NAD^+	Nicotinamide Adenine Dinucleotide
Nampt	Nicotinamide Phosphoribosyltransferase
OEA	Oleoyl Ethanolamide
PG	Prostaglandin
PGRN	Progranulin
PPAR	Peroxisome Proliferator-activated Receptor
SEAP	Secreted Alkaline Phosphatase
SIRT	Silent Information Regulator
SREBP	Sterol Regulatory Element-Binding Protein
TG	Triglyceride
TNF	Tumor Necrosis Factor
TZD	Thiazolidinedione
mRNA	Messenger Ribonucleic Acid
WB	Western Blot

vol. 16 Me

Thomas G. Brock, Ph.D.

Targeting PPARβ/δ For Weight Loss: Exercise in a Pill

First, understand this: history tells us to beware of the side effects of therapeutic drugs. In the early 1990's, Fen Phen was approved by the FDA for weight control in the seriously obese. Heavily marketed to the weight-conscious "Me" generation, Fen Phen became known as the "miracle pill" and was used by millions for quick and effective weight loss. Fen Phen is a combination of fenfluramine, which suppresses appetite, and with phentermine, a stimulant. Fenfluramine, an amphetamine introduced two decades earlier with little fanfare, increases serotonin levels, which, in the central nervous system, produces the desired effect on food intake (Figure 1). Unfortunately, by the time Fen Phen was released, the dark side of fenfluramine was beginning to be revealed. Serotonin also activates receptors on cardiovascular tissues, slowly stimulating mitogenesis. By the 1990's, evidence was accumulating that prolonged use of fenfluramine caused serious, if not fatal, cardiac and pulmonary complications. Specifically, fenfluramine produced heart valve defects through abnormal growth of heart tissue as well as primary pulmonary hypertension, which may have been related to changes in heart function secondary to the valve defects. Naturally, these changes in cardiovascular function were not reversed when drug use stopped. With 18 million prescriptions written for Fen Phen in 1996 in the United States alone, the public served as unwitting guinea pigs, demonstrating that the same side effects of fenfluramine were evident in Fen Phen. Law suits providing tens of billions in claims only begin to reflect the damages resulting from persistent cardiovascular disease, the cost of trying to lose a few pounds with a pill.

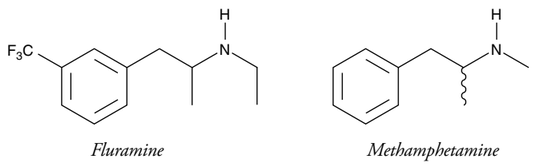

Fluramine *Methamphetamine*

Figure 1. Structures of two amphetamines

Now banned, Fen Phen has faded from public parlance; this is unfortunate, because the next "miracle pills" are already emerging. The Fen Phen experience provides a deeper understanding of how to anticipate potential side effects. Fenfluramine was known to increase serotonin levels. On the one hand, side effects due to serotonin-independent actions of fenfluramine could not be anticipated. The many known actions of serotonin, through its different receptors in different tissues, could be expected to result from taking fenfluramine. Similarly, other drugs that broadly elevate serotonin levels (*e.g.,* methamphetamine) can suppress appetite but should be expected to, like Fen Phen, evoke undesirable serotonin-mediated effects. For this reason, new drugs must modulate pathways other than serotonin signaling.

GW 1516: Actions through PPARβ/δ

The peroxisome proliferator-activated receptors (PPARs) are nuclear receptors which bind, with retinoid X receptors (RXR), to specific peroxisome proliferator response elements (PPRE) to regulate gene expression. PPARα is abundant in liver as well as in kidney, heart, brown adipose, intestine, and muscle. Activated by the synthetic agonists known as fibrates (*e.g.,* fenofibrate, clofibrate), PPARα alters gene expression relevant to altered lipid metabolism, lowering triglycerides, and raising HDL in dyslipidemia. PPARγ, abundant in adipose and other tissues, is activated by glitazones (*e.g.,* troglitazone, rosiglitazone) to reduce hyperglycemia associated with type 2 diabetes. PPARβ, described by a European group studying *Xenopus* (frog), was found to be identical to PPARδ, identified by an American group studying mice.[1,2] Less is known about this isoform. A cursory review of the PPAR signaling pathways (Figure 2) suggests that this isoform is less focused on lipid metabolism than either PPARα or PPARγ. However, a selective partial agonist for PPARβ/δ was found to correct plasma lipid parameters and improve insulin sensitivity in high fat fed ApoB100/CETP-transgenic mice, suggesting that partial agonists of PPARβ/δ might be useful in treating dyslipidemia.[3] Intriguingly, PPARβ/δ activation stimulated free fatty acid oxidation in muscle cells. Could a PPARβ/δ agonist be a fat burner?

GW 1516 (*aka* GW 501516) was first described in 2001 to be a potent, selective agonist of PPARβ/δ, binding the receptor with a K_i of 1.1 nM.[4]. In insulin-resistant middle-aged obese primates, GW 1516 increased reverse cholesterol transport, dramatically increasing serum HDL cholesterol while lowering LDL cholesterol, fasting triglycerides and insulin.[4] Similar improvements in multiple abnormalities associated with metabolic syndrome occurred in overweight men given GW 1516 for two weeks.[5] Part of this effect was thought to be due to increased fatty acid oxidation, a process that might spur weight loss. Perhaps most remarkably, GW 1516 significantly reduced weight gain in mice fed a high-fat diet for two months, specifically reducing fat accumulation in all depots by approximately 70%.[6] Similarly, mice engineered to express an activated form of PPARβ/δ in skeletal muscle demonstrated resistance to high-fat induced weight gain, indicating that some of the effects of GW 1516 were through this receptor in skeletal muscle.[6] These results recapitulated those of a previous study, where expression of an activated form of PPARβ/δ, this time in adipose tissue, induced fatty acid oxidation and utilization to prevent obesity in both high-fat diet-induced and genetically predisposed ($Lepr^{db/db}$) mice.[7] While this represented prevention of weight gain, rather than true weight loss, it suggested that, with a PPARβ/δ activator like GW 1516, some of the drawbacks of the Western diet could be avoided.

One 'side effect' of PPARβ/δ activation was its effects on muscle performance. The transgenic mice described above, expressing activated PPARβ/δ in skeletal muscle, developed more fatigue-resistant type I muscle fibers than wild type mice. When run on enclosed treadmills until exhaustion, transgenic mice ran approximately 60 min. (or ~70%) longer and almost twice the distance of wild type mice![6] In a subsequent study, mice given GW 1516 by oral gavage for five weeks and regularly exercised showed dramatic improvements in running endurance compared to similarly exercised mice given vehicle.[8] As with the transgenic mice, the gain in distance run was greater than that in time endured in response to GW 1516, suggesting that the mice also ran faster. Importantly, the improvements in performance in response to GW 1516 were only observed in mice that were regularly exercise-trained: sedentary mice given GW 1516 for five weeks performed like sedentary mice given vehicle.[8] Combining the finding that regular ingestion of GW 1516 can greatly improve muscle performance with studies showing that this compound is bioactive in humans has produced two major effects. First, the World Anti-Doping Agency added GW 1516 to its prohibited list in 2009. Second, a robust black market for GW 1516 has emerged.

AICAR Instead of Exercise

The study demonstrating that GW 1516 boosted performance when taken with exercise involved treadmill running with "progressively increasing intensity and time", ultimately running 50 min/day at 18 m/min. For the strain and sex of mice used, 18 m/min represented its 'critical speed', the speed that would result in exhaustion over the given interval.[9] This is less like mall walking and more like world class half marathon running. This suggests that GW 1516 might not benefit the weekend warrior as much as Olympians, racehorses, and greyhounds. How can this help the average Joe?

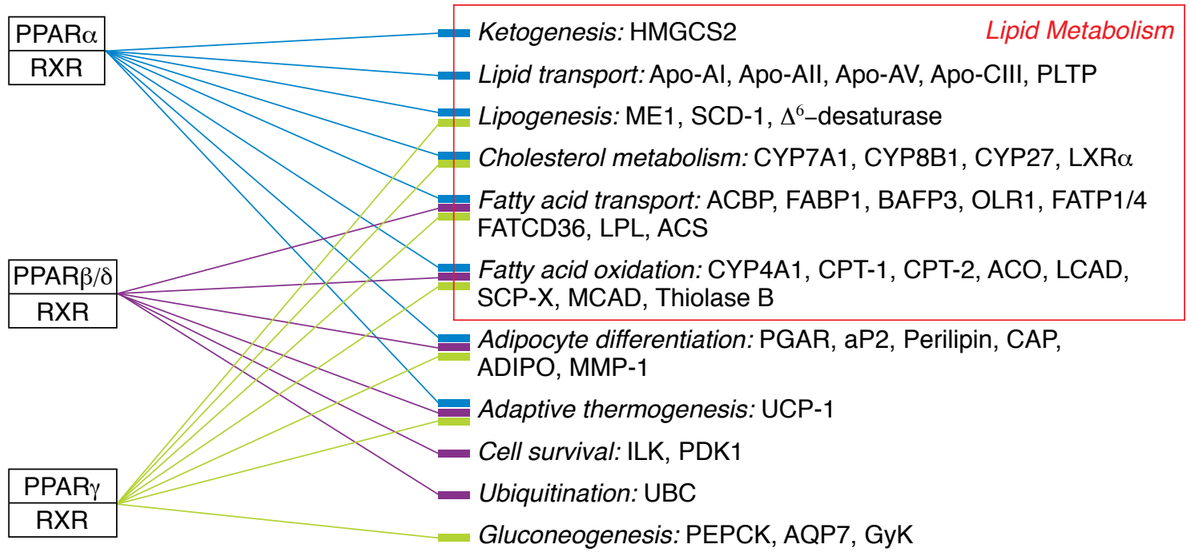

Figure 2. Biochemical and cellular pathwasy regulated by the PPARs. Adapted from the Kyoto Encyclopedia of Genes and Genomes (KEGG: www.genome.jp/kegg)

Exercise activates specific physiological pathways; one of the important ones involves AMP-activated protein kinase (AMPK), a master regulator of cellular and organismal metabolism. In mammals, AMPK contributes to glucose homeostasis and exercise physiology, and it also protects against metabolic stress.[10] The compound AICAR selectively activates AMPK.[11] Surprisingly, mice given AICAR for 4 weeks, without added exercise, experienced induced metabolic gene expression and enhanced running endurance by 44%.[8] Although AICAR did not completely mimic exercise in terms of its effects on gene expression, the majority of the oxidative genes (30 out of 32) upregulated by AICAR are active in mice with constitutively active PPARβ/δ in skeletal muscle, perhaps reflecting genes that are crucial to improved muscle performance.

The key to combining PPARβ/δ with AMPK lies in their synergy. Several genes induced by either pathway are super-induced when both pathways are activated. Also, the combination of GW 1516 plus AICAR stimulated novel biochemical pathways. PPARβ/δ, when activated alone and in the absence of physical activity, signals heavily through lipid metabolism, β-oxidation of free fatty acids, cholesterol efflux, and energy uncoupling.[6,7,12] When PPARβ/δ is activated either with exercise or with AICAR-mediated stimulation of AMPK, fat metabolism is supercharged and numerous additional, complementary pathways supporting energy consumption and tissue remodeling are put in play (Figure 3).[8] The net effect combines weight loss with muscle endurance enhancement.

An interesting caveat relates to the side effects of treatment with GW 1516 plus AICAR. The GW 1516-plus-training (GW+Tr) signature of genes induced in mouse quadriceps includes 130 genes and the GW 1516-plus-AICAR (GW+AI) signature includes 189 genes. Remarkably, only 52 genes are on both lists. This means that GW+AI treatment induces 137 genes that are not generated by GW+Tr. This leaves plenty of room for unwanted side effects, through either AMPK-dependent or AMPK-independent effects of AICAR. Remember Fen Phen.

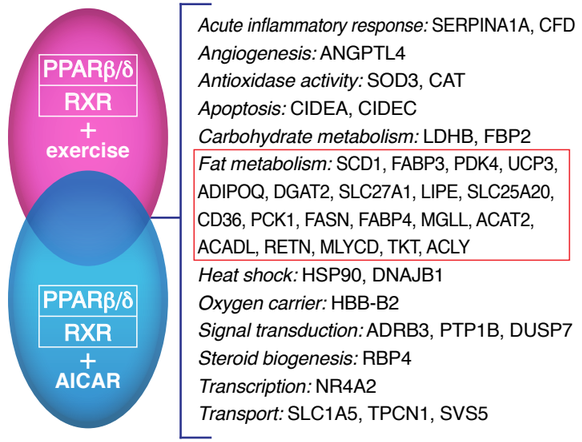

Figure 3. Biochemical and cellular pathways common to PPARβ/δ+exercise and PPARβ/δ +AICAR signaling in mouse skeletal muscle. Adapted from Table S4.[8]

References

1. Dreyer, C., Krey, G., Keller, H., *et al. Cell* **68,** 879-887 (1992).
2. Kliewer, S.A., Forman, B.M., Blumberg, B., *et al. Proc. Natl. Acad. Sci. USA* **91,** 7355-7359 (1994).
3. Sauerberg, P., Olsen, G.S., Jeppesen, L., *et al. J. Med. Chem.* **50,** 1495-1503 (2007).
4. Oliver, W.R., Shenk, J.L., Snaith, M.R., *et al. Proc. Natl. Acad. Sci. USA* **98(9),** 5306-5311 (2001).
5. Risérus, U., Sprecher, D., Johnson, T., *et al. Diabetes* **57(2),** 332-339 (2008).
6. Wang, Y.-X., Zhang, C.-L., Yu, R.T., *et al. PLoS Biol.* **2(10),** 1532-1539 (2004).
7. Wang, Y.-X., Lee, C.-H., Tiep, S., *et al. Cell* **113,** 159-170 (2003).
8. Narkar, V.A., Downes, M., Yu, R.T., *et al. Cell* **134,** 1-11 (2008).
9. Billat, V.L., Mouisel, E., Roblot, N., *et al. J. Appl. Physiol.* **98,** 1258-1263 (2005).
10. Hardie, D.G. and Carling, D. *Eur. J. Biochem.* **246,** 259-273 (1997).
11. Corton, J.M., Gillespie, J.G., Hawley, S.A., *et al. Eur. J. Biochem.* **229,** 558-565 (1995).
12. Dressel, U., Allen, T.L., Pippal, J.B., *et al. Mol. Endocrinol.* **17(12),** 2477-2493 (2003).

Antibodies

ACAT-1 Polyclonal Antibody 100028

Cholesterol Acyltransferase 1, SOAT1, Sterol O-Acyltransferase 1
Peptide affinity-purified IgG **Stability:** ≥1 year at -20°C
Summary: Antigen: human ACAT-1 amino acids 6-23 • Host: rabbit • Cross Reactivity: (+) mouse, rat, porcine, and human ACAT-1 • Application(s): IF and WB • ACAT-1 catalyzes the formation of cholesterol esters from cholesterol and long chain fatty acyl-CoA, and may play a role in the development of atherosclerosis.

500 µl

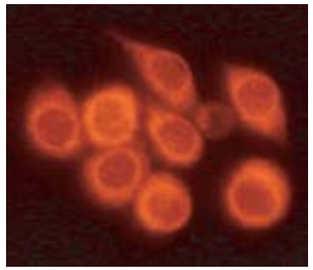

Immunofluorescent staining of RAW 264.7 cells with anti-human ACAT-1 polyclonal antibody. The positive staining was visualized with an anti-rabbit secondary antibody conjugated to Cy3. Note the very intense perinuclear staining.

•Also Available: **ACAT-1 Blocking Peptide** (10005090)

ACAT-2 Polyclonal Antibody 100027

Sterol O-Acyltransferase 2
Peptide affinity-purified IgG **Stability:** ≥1 year at -20°C
Summary: Antigen: human ACAT-2 amino acids 3-20 • Host: rabbit • Cross Reactivity: (+) human, mouse, rat, porcine, and ovine ACAT-2 • Application(s): ICC, IHC, and WB • ACAT-2 catalyzes the formation of cholesterol esters from cholesterol and long chain fatty acyl-CoA.

500 µl

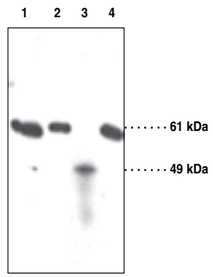

Lane 1: Murine liver (30 µg)
Lane 2: Human fibroblast cell lysate (30 µg)
Lane 3: Jurkat (human) cell lysate (30 µg)
Lane 4: Rat liver (60 µg)

•Also Available: **ACAT-2 Blocking Peptide** (10005091)

Adipose Triglyceride Lipase Polyclonal Antibody 10006409

ATGL, Desnutrin, PLA$_2$ζ
Peptide affinity-purified IgG **Stability:** ≥1 year at -20°C
Summary: Antigen: human ATGL amino acids 382-400 • Host: rabbit • Cross Reactivity: (+) human, mouse, and rat ATGL • Application(s): IHC (paraffin-embedded sections) and WB • ATGL is one of the key enzymes involved in the mobilization of fatty acids from triglyceride stores in adipose tissue, catalyzing the conversion of triacylglycerols to diacylglycerols.

500 µl

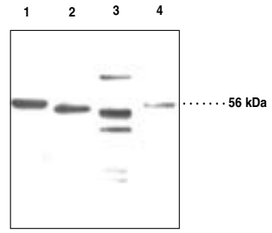

Lane 1: Human liver microsome (50 µg)
Lane 2: HepG2 cell lysate (50 µg)
Lane 3: Rat brown fat homogenate (50 µg)
Lane 4: Mouse liver 100,000 x g pellet (50 µg)

•Also Available: **Adipose Triglyceride Lipase Blocking Peptide** (10008492)

AdPLA$_2$ Polyclonal Antibody 10337

Adipose PLA$_2$, HRAS-Like Suppressor 3
Peptide affinity-purified IgG **Stability:** ≥1 year at -20°C
Summary: Antigen: human AdPLA$_2$ amino acids 147-162 • Host: rabbit • Cross Reactivity: (+) human and mouse AdPLA$_2$ • Application(s): WB • AdPLA$_2$ is highly expressed in adipose tissue, is associated with adipocyte differentiation and lipolysis, and has been implicated as a major player in the development of obesity. This antibody was raised against the C-terminal region of the human protein.

500 µl

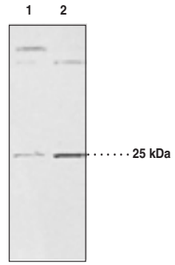

Lane 1: 3T3 Control Lysate Day 7 (50 µg)
Lane 2: 3T3 Differentiated Adipocyte Lysate Day 7 (50 µg)

•Also Available: **AdPLA$_2$ Blocking Peptide** (10338)

ANGPTL3 (human) Monoclonal Antibody (Clone Kairos-37) 10805

Angiopoietin-5, Angiopoietin-Like Protein 3, ANGPT5, FHBL2
A 1 mg/ml solution in PBS, pH 7.4 **Stability:** ≥6 months at -20°C
Summary: Antigen: recombinant human ANGPTL3 • Host: mouse, clone Kairos-37 • Cross Reactivity: (+) human ANGPTL3; (-) human ANGPTL isoforms 1, 2, 4, 6, and 7 • Application(s): ELISA and WB • ANGPTL3 regulates angiogenesis and also directly regulates lipid, glucose, and energy metabolism.

50 µg
100 µg

Lane 1: Recombinant ANGPTL3 (human)

ANGPTL3 (mouse) Monoclonal Antibody (Clone Kairos3-1541) 10806

ANG-5, Angiopoietin-5, Angiopoietin-Like 3, Angiopoietin-Related Protein 3, ANGPT5, FHBL2
A 1 mg/ml solution in PBS, pH 7.4 **Stability:** ≥6 months at -20°C
Summary: Antigen: recombinant mouse ANGPTL3 • Host: rat, clone Kairos3-1541 • Cross Reactivity: (+) mouse ANGPTL3; (-) mouse ANGPTL4 and human ANGPTL3 • Application(s): ELISA and WB • ANGPTL3 regulates angiogenesis and also directly regulates lipid, glucose, and energy metabolism.

50 µg
100 µg

Lane 1: Recombinant ANGPTL3 (mouse)

ANGPTL3 (mouse) Monoclonal Antibody (Clone Kairos3-3741) 10807

ANG-5, Angiopoietin-5, Angiopoietin-Like 3, Angiopoietin-Related Protein 3, ANGPT5, FHBL2
A 1 mg/ml solution in PBS, pH 7.4 **Stability:** ≥6 months at -20°C
Summary: Antigen: recombinant mouse ANGPTL3 • Host: rat, clone Kairos3-3741 • Cross Reactivity: (+) mouse ANGPTL3; (-) mouse ANGPTL4 and human ANGPTL3 • Application(s): ELISA and WB • ANGPTL3 regulates angiogenesis and also directly regulates lipid, glucose, and energy metabolism.

50 µg
100 µg

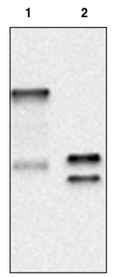

Lane 1: Recombinant ANGPTL3 (mouse)
Lane 2: Recombinant ANGPTL3 (mouse) (FLD)

ANGPTL6 (human) Monoclonal Antibody (Clone Kairos-60) 10808

AGF, Angiopoietin-Like Protein 6, Angiopoietin-Related Growth Factor
A 0.5 mg/ml solution in PBS, pH 7.4 **Stability:** ≥6 months at -20°C
Summary: Antigen: recombinant human ANGPTL6 • Host: mouse, clone Kairos-60 • Cross Reactivity: (+) human ANGPTL6; (-) human ANGPTL isoforms 1, 2, 3, 4, and 7 • Application(s): ELISA and WB • ANGPTL6 regulates angiogenesis and also directly regulates lipid, glucose, and energy metabolism.

50 µg
100 µg

Lane 1: Recombinant human ANGPTL6

Endothelial Lipase Polyclonal Antibody 100030

EDL, EL
Peptide affinity-purified IgG **Stability:** ≥1 year at -20°C
Summary: Antigen: human EL amino acids 19-32 • Host: rabbit • Cross Reactivity: (+) human, mouse, rat, porcine, and ovine EL • Application(s): IHC and WB • EL is a major genetic determinant for the concentration, structure, and metabolism of HDL, which protects against atherosclerosis.

500 µl

•Also Available: **Endothelial Lipase (human) Blocking Peptide** (10004111)

FTO (human) Monoclonal Antibody (Clone FT 86-4) 10816

Fat Mass- and Obesity-associated Protein, FATSO
A 1 mg/ml solution in PBS, pH 7.4 **Stability:** ≥6 months at -20°C
Summary: Antigen: recombinant human FTO • Host: mouse, clone FT 86-4 • Isotype: IgG$_{1κ}$ • Cross Reactivity: (+) human, mouse, and rat FTO • Application(s): ELISA, IP, and WB • FTO is associated with type 2 diabetes and positively correlated with other symptoms of the metabolic syndrome, including higher fasting insulin, glucose, and triglycerides, and lower HDL-cholesterol.

50 µg
100 µg

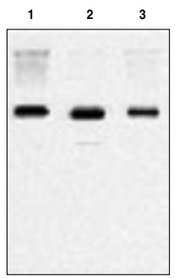

Lane 1: Recombinant human FTO (100 ng)
Lane 2: Recombinant mouse FTO (100 ng)
Lane 3: Recombinant rat FTO (100 ng)

FTO (mouse) Monoclonal Antibody (Clone FT 62-6) 10814

Fat Mass- and Obesity-associated Protein, FATSO
A 1 mg/ml solution in PBS, pH 7.4 **Stability:** ≥6 months at -20°C
Summary: Antigen: recombinant human FTO • Host: mouse, clone FT 62-6 • Isotype: $IgG_{1\kappa}$ • Cross Reactivity: (+) mouse FTO, (-) rat FTO • Application(s): ELISA, IHC, IP, and WB • FTO is associated with type 2 diabetes and positively correlated with other symptoms of the metabolic syndrome, including higher fasting insulin, glucose, and triglycerides, and lower HDL-cholesterol.

50 µg
100 µg

Lane 1: Recombinant mouse FTO (10 ng)
Lane 2: 3T3L1 cell lysate (100 µg)

FTO (mouse) Monoclonal Antibody (Clone FT 342-1) 10815

Fat Mass- and Obesity-associated Protein, FATSO
A 1 mg/ml solution in PBS, pH 7.4 **Stability:** ≥6 months at -20°C
Summary: Antigen: recombinant mouse FTO • Host: rat, clone FT 342-1 • Isotype: $IgG_{2a\kappa}$ • Cross Reactivity: (+) mouse and rat FTO; (-) human FTO • Application(s): ELISA and WB • FTO is associated with type 2 diabetes and positively correlated with other symptoms of the metabolic syndrome, including higher fasting insulin, glucose, and triglycerides, and lower HDL-cholesterol.

50 µg
100 µg

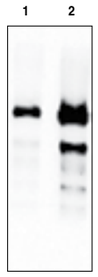

Lane 1: Recombinant rat FTO
Lane 2: Recombinant mouse FTO

GPR40 Polyclonal Antibody 10007205

FFAR1, Free Fatty Acid Receptor, G Protein-Coupled Receptor 40
Peptide affinity-purified IgG **Stability:** ≥1 year at -20°C
Summary: Antigen: human GPR40 amino acids 210-222 • Host: rabbit • Cross Reactivity: (+) human GPR40 • Application(s): IHC • GPR40 is a GPCR found predominantly in the β-cells of pancreatic islets that has been implicated in the regulation of insulin secretion. Overexpression of GPR40 in mouse β-cells leads to glucose intolerance suggesting a link between GPR40 expression and diabetes.

500 µl

•Also Available: **GPR40 Blocking Peptide** (10007206)

Hormone Sensitive Lipase Polyclonal Antibody 10006371

LIPE
Peptide affinity-purified IgG **Stability:** ≥1 year at -20°C
Summary: Antigen: human HSL amino acids 731-741 • Host: rabbit • Cross Reactivity: (+) human, mouse, and rat HSL • Application(s): WB • HSL catalyzes the hydrolysis of tri-, di-, and monoacylglycerols, as well as cholesterol esters.

500 µl

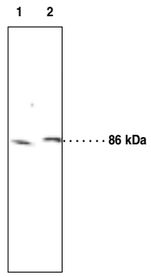

Lane 1: Rat brown fat lysate (40 µg)
Lane 2: RAW 264.7 cell lysate (40 µg)

11β-Hydroxysteroid Dehydrogenase (Type 1) Polyclonal Antibody 10004303

Corticosteroid 11β-Dehydrogenase Isozyme 1, 11β-HSD1
Peptide affinity-purified IgG **Stability:** ≥1 year at -20°C
Summary: Antigen: human 11β-HSD1 amino acids 77-92 • Host: rabbit • Cross Reactivity: (+) human, mouse, and rat 11β-HSD1 • Application(s): IHC (paraffin-embedded sections) and WB • 11β-HSD1 catalyzes the conversion of inactive cortisone to active cortisol in adipose tissue. Over-expression of 11β-HSD1 results in visceral obesity and metabolic syndrome including insulin-resistant diabetes, hyperlipidemia, and hyperphagia.

Trial
500 µl

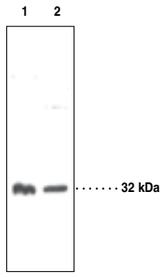

Lane 1: Rat liver microsomes (50 µg)
Lane 2: Mouse liver microsomes (50 µg)

•Also Available: **11β-Hydroxysteroid Dehydrogenase (Type 1) Blocking Peptide** (10005729)

11β-Hydroxysteroid Dehydrogenase (Type 2) Polyclonal Antibody 10004549

Corticosteroid 11β-Dehydrogenase Isozyme 2, 11β-HSD2
Peptide affinity-purified IgG **Stability:** ≥1 year at -20°C
Summary: Antigen: human 11β-HSD2 amino acids 25-40 • Host: rabbit • Cross Reactivity: (+) human, mouse, and rat 11β-HSD2 • Application(s): ICC and WB • 11β-HSD2 plays a critical role in normal physiology in the corticosteroid regulation of sodium homeostasis and the pathophysiology of hypertension by converting active cortisol to inactive cortisone. Mutation in the gene encoding 11β-HSD2 results in cortisol induction of hypertension and hypokalemia, a syndrome of apparent mineralocorticoid excess.

500 µl

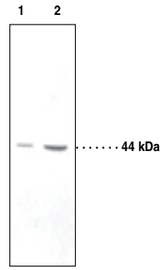

Lane 1: Mouse kidney 100,000 x g pellet resuspension (22.5 µg)
Lane 2: Mouse kidney 100,000 x g pellet resuspension (45 µg)

•Also Available: **11β-Hydroxysteroid Dehydrogenase (Type 2) Blocking Peptide** (10242)

LDL Receptor Polyclonal Antibody 10007665

LDLR
Affinity-purified IgG **Stability:** ≥1 year at -20°C
Summary: Antigen: mouse LDL receptor amino acids 499-511 • Host: rabbit • Cross Reactivity: (+) human, mouse, and rat LDL receptors • Application(s): ICC, IF, and WB • The LDLRs are cell surface glycoproteins that scavenge LDL from the blood and regulate plasma LDL cholesterol.

500 µl

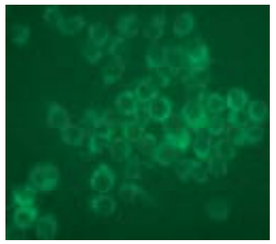

Immunofluorescent staining of RAW 264.7 cells with Cayman's LDLR polyclonal antibody at 4 µg/ml. The positive cytoplasm staining was visualized in green with Cayman's FITC conjugated goat anti-rabbit secondary antibody (Item No. 10006588).

•Also Available: **LDL Receptor Blocking Peptide** (10007672)

MCAD Polyclonal Antibody 101730

Medium-chain Fatty Acyl-CoA Dehydrogenase
Protein A-purified IgG **Stability:** ≥2 years at -20°C
Summary: Antigen: recombinant human MCAD • Host: rabbit • Cross Reactivity: (+) human, porcine, ovine, and mouse MCAD • Application(s): WB • MCAD is a mitochondrial enzyme that catalyzes the first step in the β-oxidation of fatty acids. Its expression is induced during periods of fasting and is regulated by PPARα, a ligand-activated transcription factor involved in the regulation of lipid homeostasis. MCAD expression can be used as a marker to evaluate the *in vivo* activity of PPARα.

500 µl

Melanocortin-4 Receptor Polyclonal Antibody 10006355

MC4R
Peptide affinity-purified IgG **Stability:** ≥1 year at -20°C
Summary: Antigen: mouse MC4R amino acids 21-33 • Host: rabbit • Cross Reactivity: (+) human, mouse, and rat MC4R • Application(s): IHC (formalin-fixed paraffin-embedded sections) and WB • MC4R receptor plays a critical role in appetite regulation and is a prime target for therapeutic intervention in obesity.

500 µl

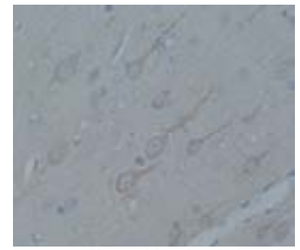

Immunoperoxidase staining of rat brain section with the MC4R polyclonal antibody. Note the tadpole like staining of cortex neurons.

•Also Available: **Melanocortin-4 Receptor Blocking Peptide** (10006356)

Nampt Monoclonal Antibody (Clone OMNI 379) 10813

Nicotinamide Phosphoribosyltransferase, PBEF1, Pre-B Cell Colony Enhancing Factor 1, Visfatin
A 1 mg/ml solution in PBS, pH 7.4 **Stability:** ≥6 months at -20°C
Summary: Antigen: recombinant human Nampt • Host: mouse, clone OMNI 379 • Cross Reactivity: (+) human, mouse, and rat Nampt • Application(s): ELISA, FC, ICC, IHC, IP, and WB • Nampt is an adipokine involved in the biosynthesis of NAD^+ and is highly expressed in visceral fat. It promotes vascular smooth muscle cell maturation, inhibits neutrophil apoptosis, and activates the insulin receptor with insulin-mimetic effects, lowering blood glucose and improving insulin sensitivity. Serum levels of Nampt correlate with obesity.

50 µg
100 µg

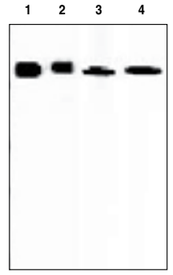

Lane 1: Recombinant human Nampt (His-tagged)
Lane 2: Recombinant human Nampt (FLAG®-tagged)
Lane 3: Recombinant mouse Nampt (His-tagged)
Lane 4: Recombinant rat Nampt (His-tagged)

PCSK9 Monoclonal Antibody (Clone 15A6) 10218

NARC-1, Proprotein Convertase Subtilisin Kexin 9
Lyophilized IgG_1 **Stability:** ≥1 year at -20°C
Summary: Antigen: recombinant human PCSK9 • Host: mouse, clone 15A6 • Isotype: IgG_1 • Cross Reactivity: (+) human recombinant PCSK9 • Application(s): PCSK9 ligand blotting and WB • PCSK9 is a member of the subtilisin serine protease family with an important role in lipoprotein metabolism. Gain-of-function mutations in the PCSK9 gene are associated with autosomal dominant hypercholesterolemia which is characterized by an increase in LDL cholesterol levels.

1 ea

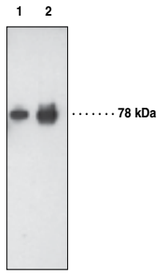

Lane 1: PCSK9 Western Ready Control (1 µg)
Lane 2: PCSK9 Western Ready Control (2 µg)

PCSK9 Polyclonal Antibody 10240

NARC-1, Proprotein Convertase Subtilisin Kexin 9
Protein-A purified IgG **Stability:** ≥1 year at -20°C
Summary: Antigen: recombinant human PCSK9 • Host: rabbit • Cross Reactivity: (+) human, rat, and mouse PCSK9 • Application(s): ICC and WB • PCSK9 is a member of the subtilisin serine protease family with an important role in lipoprotein metabolism. Gain-of-function mutations in the PCSK9 gene are associated with autosomal dominant hypercholesterolemia which is characterized by an increase in LDL cholesterol levels.

1 ea

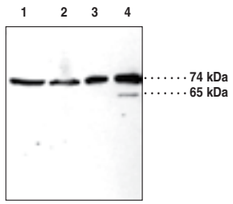

Lane 1: Mouse heart (10,000 x g supernatant) (40 µg)
Lane 2: Mouse liver (10,000 x g supernatant) (50 µg)
Lane 3: PCSK9 Western Ready Control (2 µl)
Lane 4: PCSK9 Western Ready Control (5 µl)

PCSK9 (human) Polyclonal Antibody 10007185

NARC-1, Proprotein Convertase Subtilisin Kexin 9
Peptide affinity-purified IgG **Stability:** ≥1 year at -20°C
Summary: Antigen: human PCSK9 amino acids 490-502 • Host: rabbit • Cross Reactivity: (+) human, mouse, and rat PCSK9 • Application(s): ICC, IF, and WB • PCSK9 is a member of the subtilisin serine protease family with an important role in lipoprotein metabolism. Several gain of function mutations in the PCSK9 gene are associated with hypercholesterolemia which is characterized by an increase in LDL cholesterol levels.

500 µl

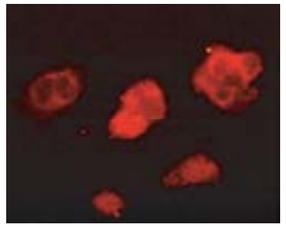

Immunofluorescent staining HepG2 cells with the PCSK9 polyclonal antibody at 16 µg/ml. The positive cytoplasm staining was visualized in red with a Cy3 conjugated goat anti-rabbit secondary antibody.

•Also Available: **PCSK9 (human) Blocking Peptide** (10007186)

PCSK9 (mouse) Polyclonal Antibody 10008811

NARC-1, Proprotein Convertase Subtilisin Kexin 9
Peptide affinity-purified IgG **Stability:** ≥1 year at -20°C
Summary: Antigen: mouse PCSK9 amino acids 152-163 • Host: rabbit • Cross Reactivity: human, mouse, and rat PCSK9 • Application(s): ICC, IF, and WB • PCSK9 is a member of the subtilisin serine protease family with an important role in lipoprotein metabolism. Several gain of function mutations in the PCSK9 gene are associated with hypercholesterolemia which is characterized by an increase in LDL cholesterol levels.

500 µl

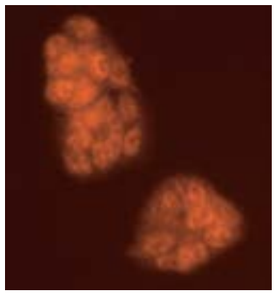

Indirect immunofluorescence of HepG2 cells incubated with the PCSK9 polyclonal antibody at 8 µg/ml. The positive cytoplasm staining was visualized in red with a Cy3 conjugated goat anti-rabbit secondary antibody.

•Also Available: **PCSK9 (mouse) Blocking Peptide** (10009581)

PEPCK Polyclonal Antibody 10004943

Pck1, PEPCK-c, Phosphoenolpyruvate carboxykinase
Peptide affinity-purified IgG **Stability:** ≥1 year at -20°C
Summary: Antigen: mouse and rat PEPCK protein amino acids 5-17 • Host: rabbit • Cross Reactivity: (+) mouse and rat PEPCK protein • Application(s): WB • PEPCK catalyzes the conversion of oxaloacetate to phosphoenolpyruvate, the first committed step in gluconeogenesis. Both non-insulin-dependent diabetes mellitus and streptozotocin-induced diabetes result in elevated PEPCK activity, protein, and mRNA. This antibody was generated against mouse cytosolic PEPCK.

500 µl

•Also Available: **PEPCK Blocking Peptide** (10007475)

PGC-1 Polyclonal Antibody 101707

PPARγ Coactivator 1
Protein-A purified IgG **Stability:** ≥2 years at -20°C
Summary: Antigen: human PGC-1α amino acids 75-90 • Host: rabbit • Cross Reactivity: (+) human, mouse, and rat PGC-1α and PGC-1β • Application(s): IHC (paraffin-embedded sections) and WB • Three PGC-1 isoforms have been characterized - PGC-1α, PGC-1β, and PGC-1-related coactivator. PGC-1α and PGC-1β are inducible transcriptional coactivators for certain nuclear receptors and play a key role in energy metabolism, hepatic gluconeogenesis, and cholesterol homoeostasis. Changes in PGC-1 levels may play a role in metabolic disorders such as type II diabetes and obesity.

500 µl

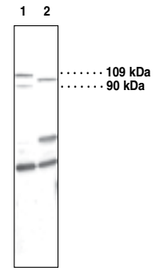

Lane 1: HEK293 cell lysate (40 µg)
Lane 2: Mouse kidney 100,000 x g pellet resuspension (40 µg)

•Also Available: **PGC-1 Blocking Peptide** (301707)

PPARα Polyclonal Antibody 101710

Peptide affinity-purified IgG **Stability:** ≥1 year at -20°C
Summary: Antigen: human, mouse, and rat PPARα amino acids 22-36 • Host: rabbit • Cross Reactivity: (+) human, mouse, rat, ovine, and porcine PPARα; (-) PPARγ • Application(s): WB • PPARα is a ligand-activated transcription factor involved in the regulation of lipid homeostasis.

500 µl

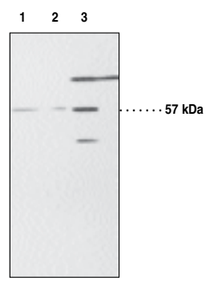

Lane 1: Baboon myometrium (100 µg)
Lane 2: Baboon myometrium (50 µg)
Lane 3: K-562 cell lysate (75 µg)

•Also Available: **PPARα Blocking Peptide** (301710)

PPARδ Polyclonal Antibody 101720

FAAR, NUC1, Nuclear Hormone Receptor 1, PPARβ
Peptide affinity-purified IgG **Stability:** ≥1 year at -20°C
Summary: Antigen: human PPARδ amino acids 39-54 • Host: rabbit • Cross Reactivity: (+) human, mouse, ovine, porcine, and rat PPARδ • Application(s): ICC, IHC, and WB • PPARδ is ubiquitously expressed but is particularly abundant in tissues such as liver, intestine, kidney, abdominal adipose, and skeletal muscle, all of which are involved in lipid metabolism. PPARδ is a mediator of diverse physiological functions including lipid and cholesterol homeostasis, embryo implantation, cancer development, and obesity.

500 µl

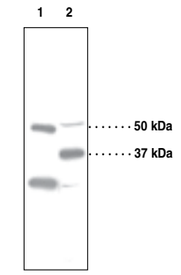

Lane 1: Human cerebral cortex (30 µg)
Lane 2: Mouse liver (30 µg)

•Also Available: **PPARδ Blocking Peptide** (10006247)

PPARγ Polyclonal Antibody 101700

Peptide affinity-purified IgG **Stability:** ≥1 year at -20°C
Summary: Antigen: human PPARγ1 amino acids 82-101 (amino acids 110-129 of PPARγ2) • Host: rabbit • Cross Reactivity: (+) human and mouse PPARγ1 and PPARγ2 • Application(s): WB • PPARγ is a ligand-activated transcription factor involved in the regulation of lipid homeostasis and may function as a master regulator of adipogenesis.

500 µl

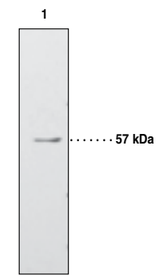

Lane 1: Rat adipose homogenate (30 µg)

•Also Available: **PPARγ Blocking Peptide** (301700)

Serum Retinol Binding Protein 4 Polyclonal Antibody 10007681

pRBP, Plasma Retinol Binding Protein 4, sRBP4
Peptide affinity-purified IgG **Stability:** ≥1 year at -20°C
Summary: Antigen: human sRBP4 amino acids 28-37 • Host: rabbit • Cross Reactivity: (+) human sRBP4 • Application(s): WB • sRBP4 binds one equivalent of vitamin A and is one of the major retinol carriers found in the blood of mammals. It is an adipocyte-derived 'signal' whose elevation causes systemic insulin resistance whereas reduction of serum concentrations improves insulin action. Thus, sRBP4 may contribute to the pathogenesis of type 2 diabetes.

500 µl

•Also Available: **Serum Retinol Binding Protein 4 Blocking Peptide** (10007682)
Serum Retinol Binding Protein 4 Western Ready Control (10009754)

SIRT7 Polyclonal Antibody 13477

Sir2, Sirtuin 7
Protein G-purified IgG **Stability:** ≥1 year at -20°C
Summary: Antigen: human SIRT7 amino acids 35-51 and 361-377 • Host: rabbit • Cross Reactivity: (+) human SIRT7 • Application(s): WB • SIRT7 is a member of the sirtuin family of proteins, which are able to metabolize NAD^+. Reports of histone-activated Sir2-mediated NAD^+ metabolism and NAD^+-activated Sir2-mediated histone deacetylation suggest a coupled reciprocal activation mechanism involving interactions of Sir2 with NAD^+ and the N-e-acetyl-lysine groups of acetylated histone.

1 ea

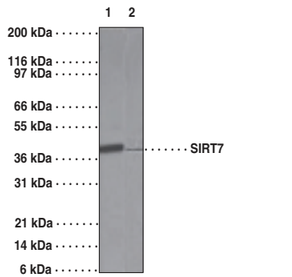

Lane 1: Human liver homogenate
Lane 2: PBMC lysate

SREBP-2 Polyclonal Antibody 10007663

SREBF2, Sterol Regulatory Element-binding Transcription Factor 2
Affinity-purified IgG **Stability:** ≥1 year at -20°C
Summary: Antigen: human SREBP-2 amino acids 455-469 • Host: rabbit • Cross Reactivity: (+) human, mouse, and rat SREBP-2 • Application(s): ICC and WB • SREBP-2 is a transcription factor that plays a critical role in lipid homeostasis by regulating genes involved in cholesterol and fatty acid metabolism.

500 µl

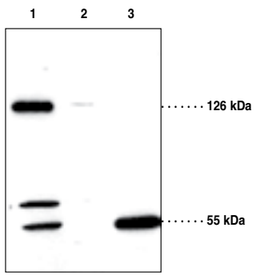

Lane 1: Human fibroblast cell lystate (60 µg)
Lane 2: Rat brown fat homogenate (60 µg)
Lane 3: Rat testis supernatant (60 µg)

•Also Available: **SREBP-2 Blocking Peptide** (10009266)

Vaspin (human) Monoclonal Antibody (Clone VP63) 10812

OL-64, Serpin A12, Visceral Adipose Tissue-Derived Serine Protease Inhibitor
A 1 mg/ml solution in PBS, pH 7.4 **Stability:** ≥6 months at -20°C
Summary: Antigen: recombinant human vaspin • Host: mouse, clone VP63 • Cross Reactivity: (+) human vaspin • Application(s): ELISA and WB • Vaspin is an insulin-sensitizing adipocytokine present in visceral and subcutaneous white adipose tissue that may regulate immune responses and inflammation and correlates with various metabolic parameters. Vaspin may represent a novel biomarker for obesity and impaired insulin sensitivity and might serve as a new therapeutic target of metabolic syndrome.

50 µg
100 µg

Lane 1: Recombinant human vaspin (His-tagged)
Lane 2: Recombinant human vaspin (FLAG®-tagged)

Biochemicals

A-922500 10012708

[959122-11-3]
MF: $C_{26}H_{24}N_2O_4$ **FW:** 428.5 **Purity:** ≥95%
A crystalline solid **Stability:** ≥1 year at -20°C
Summary: A potent inhibitor of diacylglycerol acyltransferase-1 (IC_{50}s = 7 and 24 nM, for human and mouse, respectively); confers significant weight loss within seven days and significantly reduces plasma and liver triglycerides when administered at 3 mg/kg to diet-induced obesity mice

1 mg
5 mg
10 mg
25 mg

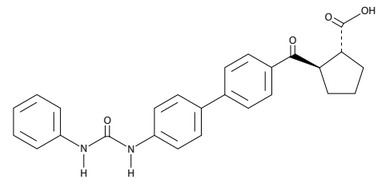

Acetyl Podocarpic Acid Anhydride 10007686

[344327-48-6] APD
MF: $C_{38}H_{46}O_7$ **FW:** 614.8 **Purity:** ≥98%
A crystalline solid **Stability:** ≥2 years at -20°C
Summary: A potent, semi-synthetic LXR agonist derived from extracts of the mayapple; induces the expression of the ABCA1 reverse cholesterol transporter to increase the efflux of cholesterol from enterocytes and thus inhibits the overall absorption of cholesterol (ED_{50} = 1 nM)

1 mg
5 mg
10 mg
50 mg

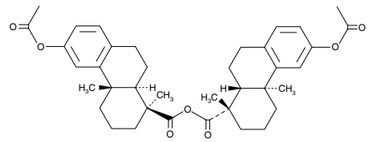

AICAR 10010241

[2627-69-2] Acadesine, AICA Riboside, NSC 105823
MF: $C_9H_{14}N_4O_5$ **FW:** 258.2 **Purity:** ≥98%
A crystalline solid **Stability:** ≥2 years at -20°C
Summary: A selective activator of AMPK; inhibits synthesis of fatty acids and sterols in hepatocytes and insulin-stimulated glucose uptake in adipocytes

5 mg
10 mg
50 mg
100 mg

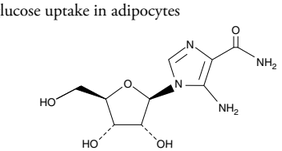

AM3102 13452

[213182-22-0] KDS-5104
MF: $C_{21}H_{41}NO_2$ **FW:** 339.6 **Purity:** ≥98%
A crystalline solid **Stability:** ≥2 years at -20°C
Summary: An OEA analog that stimulates PPARα transcriptional activity (EC_{50} = 100 nM) and prolongs feeding latency in rodents (ED_{50} = 2.4 mg/kg); as potent as OEA yet resistant to enzymatic hydrolysis; demonstrates weak affinity for the CB_1 and CB_2 receptors (K_i = 33 and 26 µM, respectively)

5 mg
10 mg
50 mg
100 mg

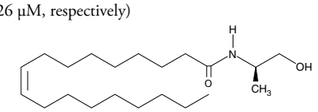

6-Aminonicotinamide 10009315

[329-89-5] 6-AN, NSC 21206, SR 4388
MF: $C_6H_7N_3O$ **FW:** 137.1 **Purity:** ≥98%
A crystalline solid **Stability:** ≥2 years at -20°C
Summary: A well-established inhibitor of the nicotinamide adenine dinucleotide phosphate-dependent enzyme, 6-phosphogluconate dehydrogenase (K_i = 0.46 µM) which interferes with glycolysis; through ATP depletion, synergizes with chemotherapy drugs, like cisplatin, in killing cancer cells (IC_{50} = 0.5 mM); reduces cardiovascular oxidative injury following ischemia/reperfusion; causes glial neurodegeneration

100 mg
250 mg
500 mg
1 g

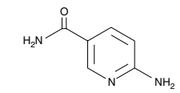

AMP-Deoxynojirimycin 10010332

[216758-20-2] Adamantane-pentyl-dNM, AMP-dNM, N-(5-adamantane-1-yl-methoxy-pentyl)-Deoxynojirimycin
MF: $C_{22}H_{39}NO_5$ **FW:** 397.6 **Purity:** ≥95%
A solution in ethanol **Stability:** ≥1 year at -20°C
Summary: A hydrophobic derivative of deoxynojirimycin that potently inhibits β-glucosidase 2 (IC_{50} = 0.3 nM), less potently antagonizes glucosylceramide synthase (IC_{50} = 25 nM), but only poorly inhibits other GCase isoforms; suppresses hapten-induced colitis, enhances insulin sensitivity, and induces SREBP-regulated gene expression and cholesterol synthesis

500 µg
1 mg
5 mg
10 mg

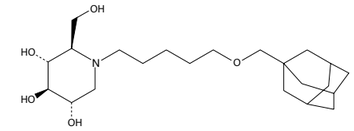

AN-7 10006212

[691410-93-2]
MF: $C_{19}H_{34}N_2O_2S_4$ **FW:** 450.7 **Purity:** ≥98%
A crystalline solid **Stability:** ≥2 years at -20°C
Summary: A more lipophilic analog of α-lipoic acid with enhanced potency to stimulate glucose transport

5 mg
10 mg
50 mg
100 mg

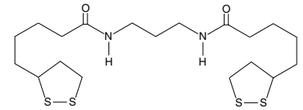

Apelin-13 13523

[217082-58-1]
MF: $C_{69}H_{111}N_{23}O_{16}S$ **FW:** 1,550.8 **Purity:** ≥95%
A crystalline solid **Stability:** ≥2 years at -20°C
Summary: Endogenous ligand of the APJ receptor, with an EC_{50} value of 0.37 nM; acts primarily in the periphery and CNS, playing important roles in regulating cardiovascular function, fluid homeostasis, hypertension, and insulin sensitivity **Amino Acid Sequence:** QRPRLSHKGPMPF

1 mg
5 mg
10 mg
25 mg

Apelin-36 13524

[252642-12-9]
FW: 4,195.9 **Purity:** ≥95%
A crystalline solid **Stability:** ≥2 years at -20°C
Summary: Full-length mature apelin peptide; acts primarily in the regulation of cardiovascular function, fluid homeostasis, hypertension, and insulin sensitivity; a less potent APJ agonist than either apelin-17 or apelin-13 (EC_{50} = 20, 2.5, and 0.37 nM, respectively); potently inhibits HIV-1 entry into cells expressing APJ and CD4
Amino Acid Sequence:
LVQPRGSRNGPGPWQGGRRKFRRQRPRLSHKGPMPF

500 µg
1 mg
5 mg

Thomas G. Brock, Ph.D.

Weight Loss: A New Star is Irisin

vol. 16 Me

What does a good workout have in common with Zeus, the Greek King of the Gods? A recent study suggests that a protein secreted during exercise targets adipose tissue, ultimately improving both obesity and glucose homeostasis. This protein has been named irisin, after the Greek goddess Iris, who acted as the messenger for Zeus. To help her fly between Mount Olympus and the land of mortals, Iris had golden wings (Figure 1). She was also considered the goddess of rainbows and could move along the colored spectrum between the clouds and the earth or sea. By both wings and rainbows, Iris moved swiftly to carry the directions of Zeus to mortals and immortals.

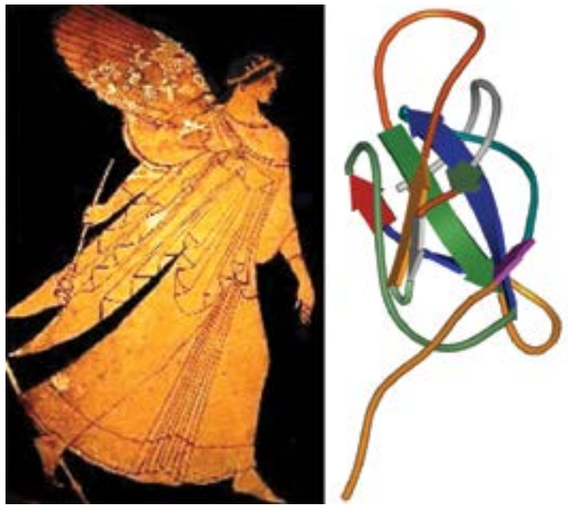

Figure 1. Potential likenesses of Iris (left) and irisin (right)

The hormone irisin looks and acts differently from Iris. This messenger is derived from fibronectin type III domain-containing protein 5 (FNDC5), a membrane-spanning protein of 196 aa. Aside from a short signal peptide, FNDC5 predominantly consists of an extracellular region containing the fibronectin type III (FnIII) domain, separated from a small cytoplasmic region by the helical transmembrane section. Irisin is a 112 aa peptide which includes the 91 aa extracellular FnIII domain, cleaved from the carboxy terminus of FNDC5. FnIII domains commonly consist of a combination of beta strands and random coils, as shown in the resolved structure of the FnIII domain of FNDC3 (1X5X.pdb, Figure 1).They are found in thousands of different proteins, usually serving to mediate interactions with other molecules (proteins, DNA, etc.) or cells. Whatever the mechanism, irisin is, like the goddess Iris, a powerful messenger, sending the signal to determine the function of specific cells.

The Background

Iris and irisin differ somewhat in their beginnings. While Iris was the daughter of Thaumas, a god of the seas, and Elektra, a nymph of the clouds, irisin is induced by PGC1α, also known as peroxisome proliferator-activated receptor-γ (PPAR-γ) coactivator 1-α. As suggested by its name, PGC1α is a transcriptional coactivator; it enhances the activity of nuclear receptors, like PPAR-γ. Predominantly expressed in tissues which are rich in mitochondria, like skeletal muscle, brown adipose tissue, and heart, PGC1α helps

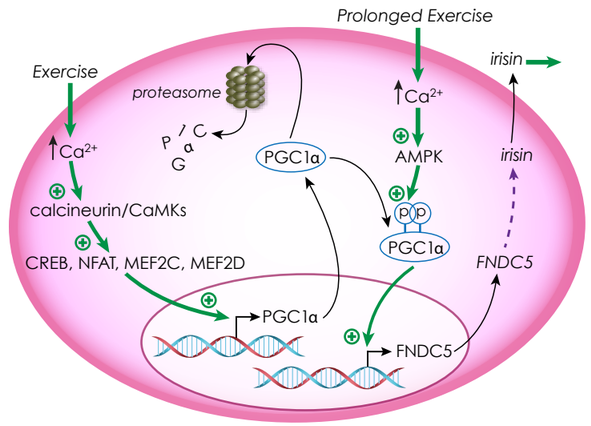

Figure 2. Exercise activates signaling that triggers transient expression of PGC1α. Prolonged exercise drives AMPK activation, phosphorylation of PGC1α, and FNDC5 production, followed by cleavage of FNDC5 to generate secretable irisin.

regulate transcriptional programs that are important for energy homeostasis by enhancing fatty acid oxidation and stimulating mitochondrial biogenesis. Exercise increases the expression of PGC1α in heart and skeletal muscle, stimulating muscle respiratory capacity. More specifically, contraction of skeletal muscle is initiated by motor neuron-induced calcium signaling (Figure 2). Elevated calcium activates the protein phosphatase calcineurin and the calcium/calmodulin-dependent protein kinases, which then alter the phosphorylation state of several transcription factors and coactivators, including CREB, NFAT, MEF2C, and MEF2D.[1] Exercise rapidly and robustly increases the expression of PGC1α, but this effect is transient as both mRNA and protein levels of PGC1α quickly revert to pre-exercise values.[2] Exercise also activates AMP-activated protein kinase (AMPK), a master regulator of cellular and organismal metabolism. AMPK directly phosphorylates PGC1α, which is required for PGC1α-dependent induction of the PGC1α promoter.[3] While brief training produces only a transient rise in PGC1α, endurance training results in persistent PGC1α elevation.[4] Expression of PGC1α in muscle stimulates an increase in FNDC5, as does exercise alone.[5] Irisin is then cleaved from the carboxy terminus of FNDC5 and secreted from muscle cells; glycosylated forms of irisin can be detected in the plasma after exercise.[5] Thus, myocontraction during exercise drives the expression of PGC1α, which in turn elicits the production of FNDC5 and subsequent secretion of irisin from muscle.

Actions of Note

Perhaps the most interesting things about irisin are its effects and potential applications. One approach to studying the specific effects of elevated levels of irisin in the plasma involves ectopically expressing FNDC5 using adenoviral vectors. When this was done in mice in such a way as to increase plasma levels of irisin 3-4 fold (a modest increase, since basal concentrations are very low), the mRNA levels for UCP1 and Cidea were significantly increased in the subcutaneous fat depot ten days later.[5] This was accompanied by a clear increase in the number of UCP1-positive, multilocular adipocytes in that particular adipose tissue. This demonstrated that a moderate increase in circulating irisin can induce browning of white adipose tissues *in vivo*.

To help clarify, all adipose tissues, and, indeed, all adipocytes, are not identical. Fats are deposited in 'depots' or pads in specific sites, which may be identified generally (subcutaneous or visceral) or more specifically by location (*e.g.,* inguinal (groin), epididymal, perirenal). Each site contains a variety of cell types in addition to the adipocytes and has unique features regarding its development and function. More relevant to this article, distinctive types of adipocytes exist. White adipocytes, which contain a single large lipid droplet, populate white adipose tissue. This most familiar form, the bane of dieters, stores excess energy as fat. When other energy sources have been exhausted, white adipocytes hydrolyze triglycerides and export fatty acids to be utilized for energy by other cells. Brown adipocytes, on the other hand, burn fatty acids to generate heat through uncoupled respiration. Cytologically, these cells are described as 'multilocular', as they store fat in many small subcellular droplets which appear as empty compartments in histological cross-sections. Brown adipocytes also contain numerous mitochondria, which provide the distinctive color. The mitochondria of brown adipocytes express a unique uncoupling protein, UCP1, a multi-pass inner membrane protein which uncouples oxidative phosphorylation from ATP synthesis so that energy is dissipated in the form of heat. These cells are abundant in brown adipose tissue (BAT), which is most commonly found in newborns and hibernating animals. Functional, classical BAT also occurs in a supraclavicular depot in healthy adult humans.[6,7]

Recently, a new type of adipocyte which expresses UCP1 and metabolizes, rather than stores, lipids has been described. Like brown adipocytes, these new cells have many mitochondria and locular lipid droplets, albeit fewer than true brown cells. However, they differ in their origin. Brown adipocytes are derived from the same precursor as skeletal muscle, termed a dermomyotome, which expresses the homeobox transcription factor Engrailed 1 (En1) and myogenic factor 5 (Myf5)(Figure 3). Differentiation of dermomyotomes to either myocytes or adipocytes is determined by signaling *via* bone morphogenetic protein 7 (Bmp7) and Wnt. White adipocytes, on the other hand, differentiate from a different precursor which lacks Myf5, presumably a mesodermal stem cell. Again, adipocyte development is promoted by Bmps and blocked by Wnt. The new type of adipocyte can be induced *in vivo* in WAT depots by chronic β-adrenergic stimulation or by chronic PPARγ-agonist treatment, particularly in the inguinal depot of the mouse.[8,9] As this cell type is morphologically and functionally similar to brown cells but shares a precursor with white adipocytes, it has been called a 'brite' (brown-in-white) adipocyte.[10] Alternatively, it may be referred to as a 'beige' adipocyte or a recruitable or inducible brown adipocyte-like cell. More important than the name, this cell type may serve an important role in regulating energy balance, glucose metabolism, and lipid homeostasis.

Significant Impact

Iris and irisin differ in their actions. Iris affected the course of the Trojan War, one of the great Greek clashes, by carrying Zeus' advice to the Trojan leader Hector (although the Trojan Horse ultimately led to the fall of Troy). Irisin, by way of contrast, may alter the course of diseases like diabetes, obesity, and other pathologies that benefit from exercise. 'Browned' WAT, produced either by irisin (from FNDC5-expressing adenovirus) or by transgenic expression of Prdm16, protects against diet-induced obesity and diabetes.[5,11] Whether irisin can be developed into a deliverable therapeutic that mimics exercise-induced irisin production remains a major hurdle.

References

1. Berchtold, M.W., Brinkmeier, H., and Müntener, M. *Physiol. Rev.* **80(3),** 1215-1265 (2000).
2. Pilegaard, H., Saltin, B., and Neufer, P.D. *J. Physiol.* **546,** 851-858 (2003).
3. Jäger, S., Handschin, C., St.-Pierre, J., *et al. Proc. Natl. Acad. Sci. USA* **104(29),** 12017-12022 (2007).
4. Russell, A.P., Feilchenfeldt, J., Schreiber, S., *et al. Diabetes* **52(12),** 2874-2881 (2012).
5. Boström, P., Wu, J., Jedrychowski, M.P., *et al. Nature* **481,** 463-468 (2012).
6. Zingaretti,M.C., Crosta,F., Vitali,A., *et al. FASEB J.* **23,** 3113-3120 (2009).
7. Ouellet, V., Labbé, S.M., Blondin, D.P., *et al. J. Clin. Invest.* **122(2),** 545-552 (2012).
8. Guerra, C., Koza, R.A., Yamashita, H., *et al. J. Clin. Invest.* **102(2),** 412-420 (1998).
9. Carmona, M.C., Louche, K., Lefebvre, B., *et al. Diabetes* **56,** 2797-2808 (2007).
10. Petrovic, N., Walden, T.B., Shabalina, I.G., *et al. J. Biol. Chem.* **285(10),** 7153-7164 (2010).
11. Seale, P., Conroe, H.M., Estall, J., *et al. J. Clin. Invest.* **121(1),** 96-105 (2011).
12. Waldén,T.B., Hansen,I.R., Timmons,J.A., *et al. Am. J. Physiol. Endocrinol. Metab.* **302,** E19-E31 (2012).

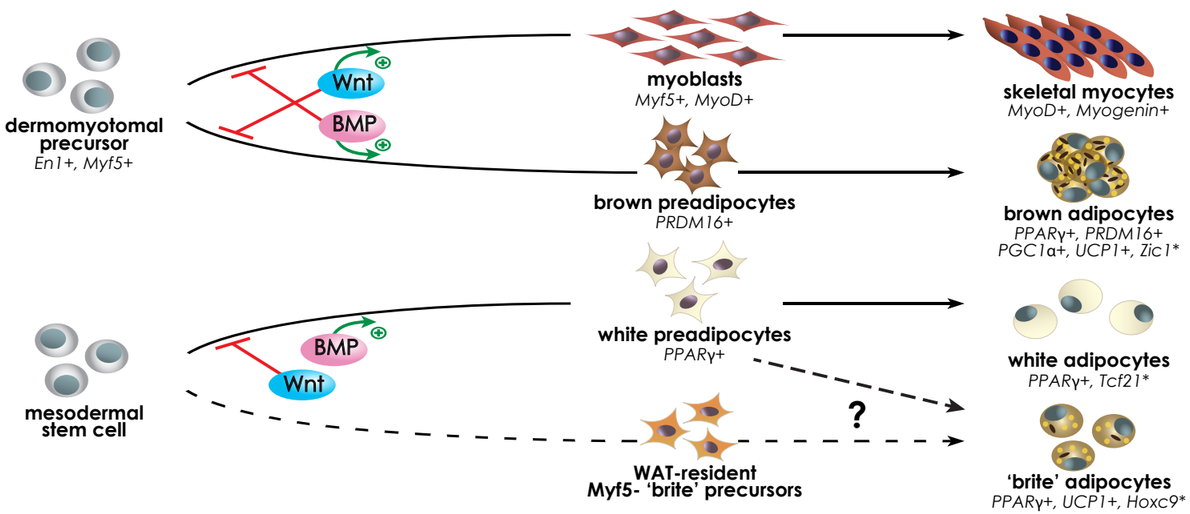

Figure 3. The differentiation of skeletal myocytes and known types of adipocytes, with markers indicated. *see Ref. [12]

Arachidonic Acid 90010

[506-32-1]
MF: $C_{20}H_{32}O_2$ **FW:** 304.5 **Purity:** ≥98%
A solution in ethanol **Stability:** ≥1 year at -20°C
Summary: Keystone essential fatty acid that is converted by COX, LO, and epoxygenase enzymes into more than 150 potent metabolites in species ranging from fungi to plants to mammals

50 mg
100 mg
250 mg
500 mg

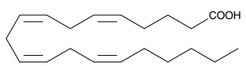

AS-1269574 10626

[330981-72-1]
MF: $C_{13}H_{14}BrN_3S$ **FW:** 308.2 **Purity:** ≥98%
A solution in ethanol **Stability:** ≥1 year at -20°C
Summary: An agonist of GPR199 that is effective both in isolated cells and *in vivo*; increases cyclic adenosine monophosphate levels in human embryonic kidney 293 cells transfected with human GPR119 (EC_{50} = 2.5 µM) and promotes glucose-stimulated insulin secretion in mice (100 mg/kg)

1 mg
5 mg
10 mg
25 mg

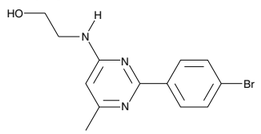

Berberine 10006427

[633-65-8] BBR, Umbellatine
MF: $C_{20}H_{18}ClNO_4$ **FW:** 371.8 **Purity:** ≥95%
A crystalline solid **Stability:** ≥2 years at -20°C
Summary: An akaloid natural product that reduces total cholesterol, LDL cholesterol, and triglycerides in humans and hamsters; enhances LDL-receptor protein and mRNA levels in hepatocytes

1 g
5 g
10 g
25 g

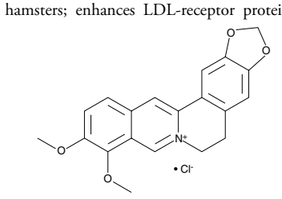

Bezafibrate 10009145

[41859-67-0] Benzofibrate, Bezalip, Bezatrol, BM 15075, Difaterol
MF: $C_{19}H_{20}ClNO_4$ **FW:** 361.8 **Purity:** ≥98%
A crystalline solid **Stability:** ≥2 years at -20°C
Summary: A well-established pan PPAR agonist; activates human PPARα, PPARδ, and PPARγ with EC_{50} values of 50, 20, and 60 µM, respectively; helps lower LDL cholesterol and triglycerides while raising HDL cholesterol levels

500 mg
1 g
5 g
10 g

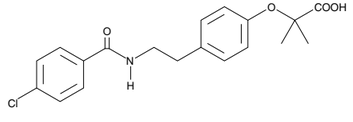

BIBB 515 10010517

[156635-05-1]
MF: $C_{22}H_{21}ClN_2O_2$ **FW:** 380.9 **Purity:** ≥98%
A crystalline solid **Stability:** ≥2 years at -20°C
Summary: A selective and potent inhibitor of 2,3-oxidosqualene cyclase *in vivo* with an ED_{50} value of 0.2-0.5 and 0.36-33.3 mg/kg in rats and mice, respectively; reduced total cholesterol by 19% in normolipemic hamsters at a dose of 55 mg/kg/day for 11 days and 25% in hyperlipemic hamsters at a dose of 148 mg/kg/day for 25 days

1 mg
5 mg
10 mg
25 mg

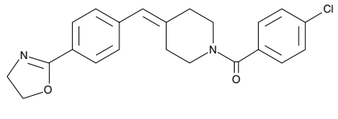

C75 10005270

[191282-48-1]
MF: $C_{14}H_{22}O_4$ **FW:** 254.3 **Purity:** ≥98%
A crystalline solid **Stability:** ≥2 years at -20°C
Summary: A stable inhibitor of FAS that leads to profound weight loss and feeding inhibition in both high-fat diet wild type obese and leptin-deficient *ob/ob* mice

1 mg
5 mg
10 mg
50 mg

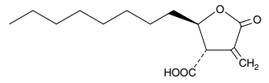

•Also Available: **(+)-*trans*-C75** (9000783)
(-)-*trans*-C75 (9000784)

Candesartan cilexetil 10489

[145040-37-5] TCV-116
MF: $C_{33}H_{34}N_6O_6$ **FW:** 610.7 **Purity:** ≥98%
A crystalline solid **Stability:** ≥2 years at -20°C
Summary: A prodrug of the potent, long-acting, and selective angiotensin II receptor type 1 receptor antagonist, candesartan; 4-16 mg/day effectively reduces diastolic blood pressure and has proved useful in the treatment of hypertension and diabetes

500 mg
1 g
5 g
10 g

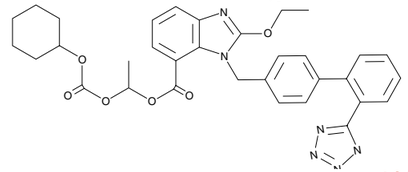

CAY10410 18590

[596104-94-8] 9,10-dihydro-15-deoxy-$\Delta^{12,14}$-PGJ_2
MF: $C_{20}H_{30}O_3$ **FW:** 318.5 **Purity:** ≥98% (isomer mixture)*
A solution in methyl acetate **Stability:** ≥1 year at -20°C
Summary: An analog of PGD_2/PGJ_2 with structural modifications intended to give it PPARγ ligand activity and resistance to metabolism

500 µg
1 mg
5 mg
10 mg

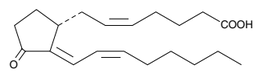

CAY10415 71748

[146062-49-9]
MF: $C_{19}H_{18}N_2O_4$ **FW:** 370.4 **Purity:** ≥98%
A crystalline solid **Stability:** ≥2 years at -20°C
Summary: A potent, antidiabetic drug of the TZD structural class that lowers blood glucose leves in obese, hyperglycemic, hyperinsulinemic, and insulin-resistant KKA$_γ$ mice at a dose of 100 mg/kg for four days; increases the rate of insulin-stimulated lipogenesis in 3T3-L1 adipocytes in a dose-dependent manner.

1 mg
5 mg
10 mg
50 mg

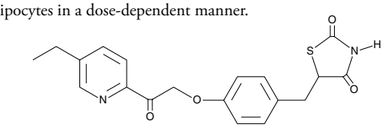

CAY10485 10006482

[615264-62-5] 3,4-dihydroxy Hydrocinnamic Acid (L-Aspartic Acid dibenzyl ester) amide
MF: $C_{27}H_{27}NO_7$ **FW:** 477.1 **Purity:** ≥98%
A crystalline solid **Stability:** ≥2 years at -20°C
Summary: An inhibitor of human ACAT-1 and ACAT-2 with an IC_{50} values of 95 and 81 µM, respectively; inhibits copper-mediated oxidation of LDL by 91% at a concentration of 2 µM

5 mg
10 mg
50 mg
100 mg

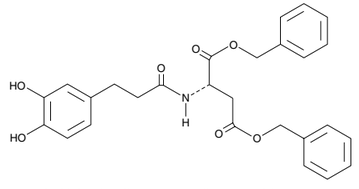

**All 5-cis 2-series PGs (those containing a 5,6-double bond) will contain a small amount of the 5-trans isomer. This isomer is generally undetectable using normal phase silica columns and plates, but may be resolved using RP-HPLC. The purity for all such 2-series PGs excludes the 1-3% trans isomer which will generally be present.*

Inhibitors of Lipoprotein Modifying Enzymes

Item No.	Item Name	Target Enzyme	IC_{50} values	Sizes
10006482	**CAY10485**	ACAT-1 and 2	96 µM ACAT-1; 81 µM ACAT-2	5 mg • 10 mg • 50 mg • 100 mg
10006452	**CAY10486**	ACAT-1 and 2	60 µM (both enzymes)	5 mg • 10 mg • 25 mg • 50 mg
10007875	**CAY10499**	Hormone Sensitive Lipase	90 nM (human)	1 mg • 5 mg • 10 mg • 25 mg
10006782	**Oleic Acid-2,6-diisopropylanilide**	ACAT	7 nM	5 mg • 10 mg • 50 mg • 100 mg
10006529	**Oleyl Anilide**	ACAT	26 µM	5 mg • 10 mg • 50 mg • 100 mg

CAY10486 10006452

[615264-52-3] 4-Hydroxycinnamic Acid (L-phenylalanine methyl ester) amide
MF: $C_{19}H_{19}NO_4$ **FW:** 325.4 **Purity:** ≥98%
A crystalline solid **Stability:** ≥2 years at -20°C
Summary: An inhibitor of human ACAT-1 and ACAT-2 with an IC_{50} value of approximately 60 µM for both enzymes; also inhibits copper-mediated oxidation of LDL by about 28% at a concentration of 3 µM

5 mg
10 mg
50 mg
500 mg

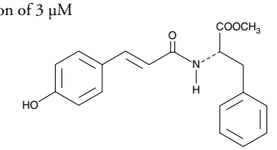

CAY10499 10007875

[359714-55-9]
MF: $C_{18}H_{17}N_3O_5$ **FW:** 355.3 **Purity:** ≥98%
A crystalline solid **Stability:** ≥2 years at -20°C
Summary: A potent inhibitor of human hormone sensitive lipase (IC_{50} = 90 nM)

1 mg
5 mg
10 mg
25 mg

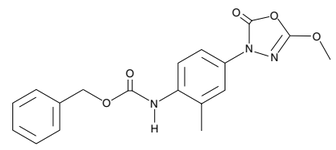

CAY10506 10009079

[292615-75-9]
MF: $C_{20}H_{26}N_2O_4S_3$ **FW:** 454.6 **Purity:** ≥98%
A solution in methyl acetate **Stability:** ≥1 year at -20°C
Summary: A hybrid lipoic acid-TZD derivative that transactivates human PPARγ with an EC_{50} value of 10 µM

1 mg
5 mg
10 mg
50 mg

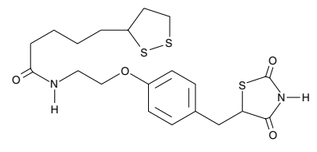

CAY10514 10009017

[868526-38-9] Methyl-8-hydroxy-8-(2-pentyl-oxyphenyl)-oct-5-ynoate
MF: $C_{20}H_{28}O_4$ **FW:** 332.4 **Purity:** ≥98%
A solution in methyl acetate **Stability:** ≥1 year at -20°C
Summary: An aromatic analog of 8(S)-HETE; acts as a dual agonist of PPARα and PPARγ with EC_{50} values of 0.17 and 0.64 µM, respectively

1 mg
5 mg
10 mg
50 mg

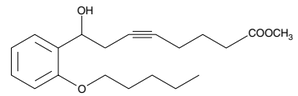

CAY10566 10012562

[944808-88-2]
MF: $C_{18}H_{17}ClFN_5O_2$ **FW:** 389.8 **Purity:** ≥98%
A crystalline solid **Stability:** ≥2 years at -20°C
Summary: A potent, selective inhibitor of stearoyl-CoA desaturase 1 that demonstrates IC_{50} values of 4.5 and 26 nM in mouse and human enzymatic assays, respectively

1 mg
5 mg
10 mg
25 mg

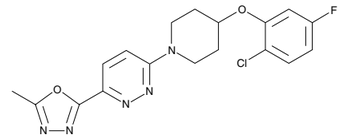

CAY10573 10008846

[853652-40-1]
MF: $C_{33}H_{33}NO_5$ **FW:** 521.6 **Purity:** ≥98%
A crystalline solid **Stability:** ≥2 years at -20°C
Summary: A PPAR agonist that displays potent binding at PPARα, γ, and δ (IC_{50}s = 113, 50, and 223 nM, respectively) and potently transactivates PPARα, γ, and δ (EC_{50}s = 8, 70, and 500 nM, respectively); demonstrates stronger binding and functional activity for PPARγ than rosiglitazone

500 µg
1 m
5 mg
10 mg

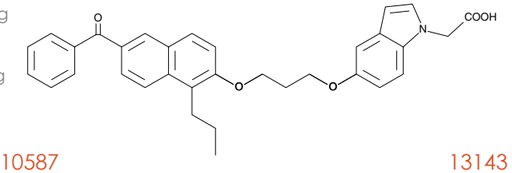

CAY10587 13143

[1082058-99-8]
MF: $C_{18}H_{16}O_2$ **FW:** 264.3 **Purity:** ≥98%
A crystalline solid **Stability:** ≥2 years at -20°C
Summary: A selective FFA1/GPR40 agonist (EC_{50} = 32nM) that does not exhibit activity on the related FFA receptors FFA2/GPR43 or FFA3/GPR41; increases glucose-stimulated insulin secretion at a concentration of 100 nM in the rat

1 mg
5 mg
10 mg
25 mg

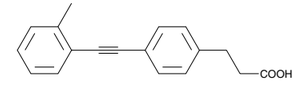

CAY10592 10012536

[685139-10-0]
MF: $C_{23}H_{17}Br_2ClO_3S$ **FW:** 568.7 **Purity:** ≥98%
A crystalline solid **Stability:** ≥2 years at -20°C
Summary: A selective PPARδ agonist that acts as a partial agonist (EC_{50} = 53 nM) in transactivation assays and as a full agonist (EC_{50} = 30 nM) in the oxidation of free fatty acid; increases HDL levels, decreases LDL and TG levels, and improves insulin sensitivity in high fat fed ApoB100/CETP-transgenic mice at a dose of 20 mg/kg

1 mg
5 mg
10 mg
50 mg

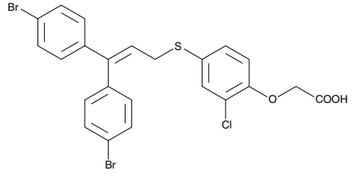

CAY10599 13282

[1143573-33-4]
MF: $C_{38}H_{41}NO_5$ **FW:** 591.7 **Purity:** ≥98%
A crystalline solid **Stability:** ≥2 years at -20°C
Summary: A PPARγ agonist that is 4-fold more potent than rosiglitazone at the PPARγ receptor demonstrating an EC_{50} value of 0.05 µM; shows high selectivity for PPARγ over PPARα (EC_{50} = 3.99 µM) or PPARδ (EC_{50} > 10 µM)

1 mg
5 mg
10 mg
25 mg

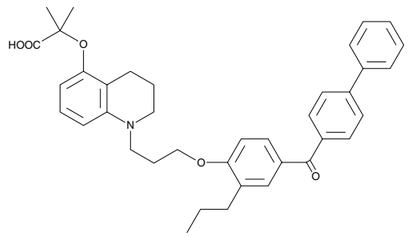

CAY10618 13670

[1202580-59-3] NMPRTase Inhibitor
MF: $C_{27}H_{29}N_5O$ **FW:** 439.6 **Purity:** ≥95%
A solution in methanol **Stability:** ≥1 year at -20°C
Summary: A potent inhibitor of Nampt (IC_{50} = 3.0 nM); induces cell death in the neuroblastoma cell line SH-SY5Y with an IC_{50} value of 3.8 nM through a process that appears to involve autophagy

500 µg
1 mg
5 mg
10 mg

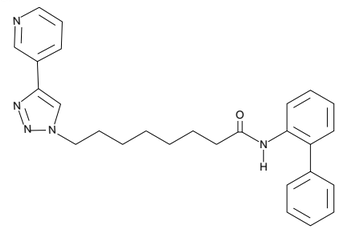

Cerulenin 10005647

[17397-89-6]
MF: $C_{12}H_{17}NO_3$ **FW:** 223.3 **Purity:** ≥98%
A crystalline solid **Stability:** ≥2 years at -20°C
Summary: An irreversible inhibitor of FAS; causes cytotoxicity and apoptosis in human cancer cell lines; causes weight loss and feeding inhibition in both high-fat diet wild type obese and leptin-deficient *ob/ob* mice

5 mg
10 mg
50 mg

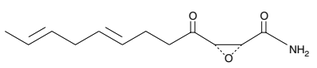

Cetaben 10007171

[55986-43-1] Hexadecylamino-p-amino Benzoic Acid
MF: $C_{23}H_{39}NO_2$ **FW:** 361.6 **Purity:** ≥98%
A crystalline solid **Stability:** ≥2 years at -20°C
Summary: A unique, PPARα-independent peroxisome proliferator with hypolipidemic activity characterized by reduction in serum triglyceride and cholesterol

5 mg
10 mg
50 mg
100 mg

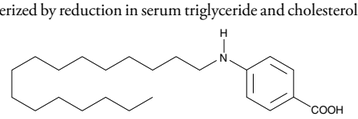

Chenodeoxycholic Acid 10011286

[474-25-9] Anthropodeoxycholic Acid, CDCA, Fluibil, Hekbilin, Kebilis, Ulmenide
MF: $C_{24}H_{40}O_4$ **FW:** 392.6 **Purity:** ≥95%
A crystalline solid **Stability:** ≥2 years at -20°C
Summary: A bile acid and FXR ligand (EC_{50} = 13-34 µM) that is a key regulator of cholesterol homeostasis; exhibits toxicity that is linked to increased glutathione and increased oxidative stress; excess CDCA contributes to liver and intestinal cancers

1 g
5 g
10 g
25 g

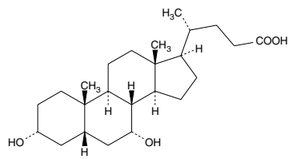

3-dodecanoyl-NBD Cholesterol 13220

3-C_{12}-NBD Cholesterol
MF: $C_{45}H_{70}N_4O_5$ **FW:** 747.1 **Purity:** ≥98%
A solution in ethanol **Stability:** ≥1 year at -20°C
Summary: A fluorescently-tagged cholesterol with the hydrophilic NBD fluorophore attached to the hydrophilic end of cholesterol, separated by a 2-carbon spacer; allows the cholesterol to properly orient in membrane bi-layers while the fluorescent tag is presented outside of the bi-layer

500 µg
1 mg
5 mg
10 mg

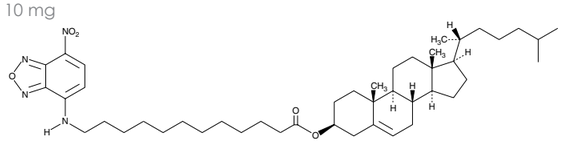

3-hexanoyl-NBD Cholesterol 13221

3-C_6-NBD Cholesterol
MF: $C_{39}H_{58}N_4O_5$ **FW:** 662.9 **Purity:** ≥98%
A solution in ethanol **Stability:** ≥1 year at -20°C
Summary: A fluorescently-tagged cholesterol with the hydrophilic NBD fluorophore attached to carbon 3, at the hydrophilic end of cholesterol, separated by a 6-carbon spacer; allows the cholesterol to properly orient in membrane bi-layers while the fluorescent tag is presented outside of the bi-layer

250 µg
500 µg
1 mg
5 mg

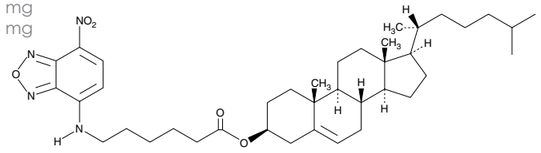

25-hydroxy Cholesterol 11097

[2140-46-7]
MF: $C_{27}H_{46}O_2$ **FW:** 402.7 **Purity:** ≥98%
A crystalline solid **Stability:** ≥2 years at -20°C
Summary: A side-chain substituted oxysterol derived from dietary cholesterol that inhibits the cleavage of SREBPs; has been implicated in a variety of metabolic events including cholesterol homeostasis and atherosclerosis as well as antitumor and immunomodulating activities

5 mg
10 mg
25 mg
100 mg

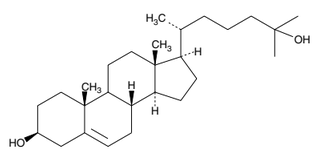

•Also Available: **25-hydroxy Cholesterol-d_6** (11099)

5α-hydroxy-6-keto Cholesterol 10007601

[13027-33-3] Cholestane-6-oxo-3β,5α-diol, 6-Oxo-3,5-diol
MF: $C_{27}H_{46}O_3$ **FW:** 418.7 **Purity:** ≥98%
A crystalline solid **Stability:** ≥2 years at -20°C
Summary: A major metabolite of cholesterol formed during exposure of lung epithelial cells to ozone; potent inhibitor of cholesterol synthesis in human bronchial epithelial cells (IC_{50} = 350 nM); exhibits significant cytotoxicity in the low µM range

1 mg
5 mg
10 mg
50 mg

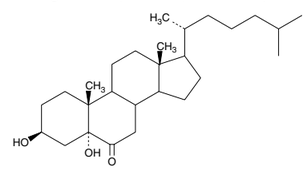

Cholesteryl Linoleate Hydroperoxides 48001

MF: $C_{45}H_{76}O_4$ **FW:** 681.1 **Purity:** ≥98% hydroperoxide content
A solution in ethanol **Stability:** ≥6 months at -80°C
Summary: A product derived from the autoxidation of cholesteryl linoleate containing a mixture of racemic 9- and 13-HpODE cholesteryl esters

100 µg
500 µg
1 mg
5 mg

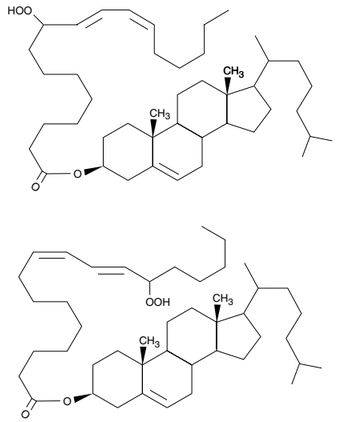

Ciglitazone 71730

[74772-77-3] ADD 3878, U-63287
MF: $C_{18}H_{23}NO_3S$ **FW:** 333.4 **Purity:** ≥98%
A crystalline solid **Stability:** ≥1 year at -20°C
Summary: An antidiabetic drug and selective PPARγ agonist (EC_{50} = 3.0 µM); active *in vivo* as an anti-hyperglycemic agent in the *ob/ob* mouse model

1 mg
5 mg
10 mg
50 mg

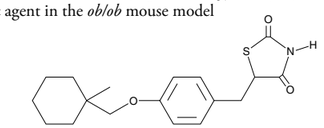

Clofibrate 10956

[637-07-0]
MF: $C_{12}H_{15}ClO_3$ **FW:** 242.7 **Purity:** ≥98%
A colorless liquid **Stability:** ≥1 year at -20°C
Summary: A PPARα agonist used clinically to treat dyslipidemia and cardiovascular disease; exhibits EC_{50} values of 50 and 55 µM for mouse and human PPARα, respectively

500 mg
1 g
5 g
10 g

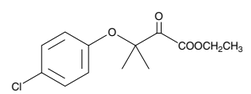

17-keto-4(Z),7(Z),10(Z),13(Z),15(E),19(Z)-Docosahexaenoic Acid 9000346

MF: $C_{22}H_{30}O_3$ **FW:** 342.5 **Purity:** ≥98%
A solution in ethanol **Stability:** ≥6 months at -80°C
Summary: A metabolite of lipoxygenase-mediated oxidation of DHA; activates Nrf2-dependent antioxidant gene expression, acts as a PPARγ agonist (EC_{50} ~200nM), and inhibits pro-inflammatory cytokine and nitric oxide production at biological concentration ranges (5-25 µM)

25 µg
50 µg
100 µg
250 µg

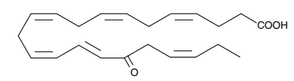

17-keto-7(Z),10(Z),13(Z),15(E),19(Z)-Docosapentaenoic Acid 9000347

MF: $C_{22}H_{32}O_3$ **FW:** 344.5 **Purity:** ≥95%
A solution in ethanol **Stability:** ≥6 months at -80°C
Summary: A metabolite of lipoxygenase-mediated oxidation of DPA; activates Nrf2-dependent antioxidant gene expression, acts as a PPARγ agonist (EC_{50} ~200nM), and inhibits pro-inflammatory cytokine and nitric oxide production at biological concentration ranges (5-25 µM)

100 µg
250 µg
500 µg
1 mg

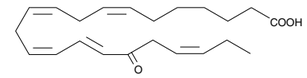

Eicosapentaenoic Acid 90110

[10417-94-4] EPA, Timnodonic Acid
MF: $C_{20}H_{30}O_2$ **FW:** 302.5 **Purity:** ≥98%
A solution in ethanol **Stability:** ≥1 year at -20°C
Summary: An ω-3 fatty acid abundantly available in marine organisms

50 mg
100 mg
250 mg
500 mg

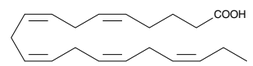

Eicosapentaenoic Acid ethyl ester 10008884

[86227-47-6] EPA-EE, EPA ethyl ester
MF: $C_{22}H_{34}O_2$ **FW:** 330.5 **Purity:** ≥98%
A solution in ethanol **Stability:** ≥1 year at -20°C
Summary: A stabilized ethyl ester form of this ω-3 C20:5 polyunsaturated fatty acid; dietary EPA-EE in rats increases fatty acid β-oxidation enzyme levels, down-regulates lipogenic genes, and decreases plasma cholesterol and triglyceride levels; blocks induced insulin resistance and corrects changes in adiponectin levels and TNF-α expression in rats fed a high-fat diet

10 mg
50 mg
100 mg
500 mg

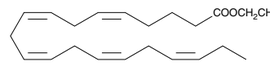

Fenofibrate 10005368

[49562-28-9]
MF: $C_{20}H_{21}ClO_4$ **FW:** 360.8 **Purity:** ≥98%
A crystalline solid **Stability:** ≥2 years at -20°C
Summary: A PPARα agonist and hypolipidemic drug used clinically to treat dyslipidemia and cardiovascular disease; exhibits EC_{50} values of 18 and 30 µM for mouse and human PPARα, respectively

1 g
5 g
10 g
50 g

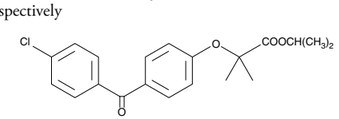

FK-866 13287

[658084-64-1] K 22.175
MF: $C_{24}H_{29}N_3O_2$ **FW:** 391.5 **Purity:** ≥98%
A crystalline solid **Stability:** ≥2 years at -20°C
Summary: A highly specific non-competitive inhibitor of Nampt (K_i = 0.4 nM), causing gradual NAD^+ depletion; directs delayed cell death by apoptosis in HepG2 cells (IC_{50} = ~1 nM)

5 mg
10 mg
25 mg
50 mg

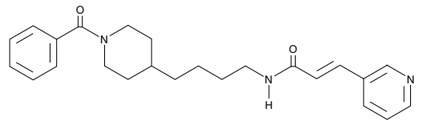

Fluvastatin (sodium salt) 10010337

[93957-55-2]
MF: $C_{24}H_{25}FNO_4$ • Na **FW:** 433.5 **Purity:** ≥98%
A crystalline solid **Stability:** ≥2 years at -20°C
Summary: A potent, competitive inhibitor of HMG-CoA reductase (K_i = 0.3 nM)

10 mg
25 mg
50 mg
100 mg

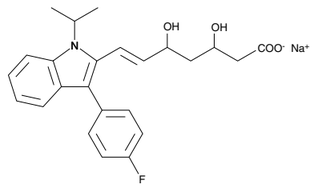

FMOC-L-Leucine 10004888

[35661-60-0] FMOC-Leu, NPC 15199, NSC 334290
MF: $C_{21}H_{23}NO_4$ **FW:** 353.4 **Purity:** ≥98%
A crystalline solid **Stability:** ≥2 years at room temperature
Summary: A partial agonist of PPARγ; activates PPARγ with a lower potency (K_i = 15 µM *versus* 0.035 µM) but a similar maximal efficacy compared to rosiglitazone; improves insulin resistance in normal, diet-induced glucose-intolerant, and in diabetic *db/db* mice, yet reduced adipogenic activity

25 g
50 g
100 g

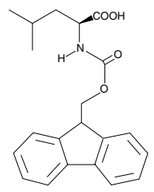

Fucoxanthin 13068

[3351-86-8] α-Carotene
MF: $C_{42}H_{58}O_6$ **FW:** 658.9 **Purity:** ≥98%
A crystalline solid **Stability:** ≥2 years at -20°C
Summary: A carotenoid that occurs naturally in certain algae; significantly reduces abdominal white adipose tissue (WAT) in mice and rats when included in their diet; increases the amount of UCP1 protein in WAT; decreases blood glucose and plasma insulin levels in diabetic mice

500 µg
1 mg
5 mg
10 mg

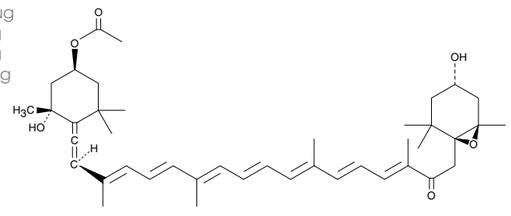

Cholesterol Synthesis Inhibitors

Item No.	Item Name	Target Enzyme	K_i
10010337	Fluvastatin (sodium salt)	HMG-CoA Reductase	0.3 nM
10010338	Lovastatin	HMG-CoA Reductase	0.6 nM
10010339	Lovastatin Hydroxy Acid (sodium salt)	HMG-CoA Reductase	0.6 nM
10010340	Mevastatin	HMG-CoA Reductase	1 nM
10010343	Pravastatin (sodium salt)	HMG-CoA Reductase	2.3 nM
10006415	Ro 48-8071	Oxidosqualene Cyclase	IC_{50} = 1.5-6.5 nM
10010334	Simvastatin	HMG-CoA Reductase	0.12 nM

GSK264220A 13009

[685506-42-7]
MF: $C_{17}H_{21}N_3O_4S$ **FW:** 363.4 **Purity:** ≥98%
A crystalline solid **Stability:** ≥2 years at -20°C
Summary: A potent inhibitor of endothelial lipase (IC_{50} = 16 nM)

1 mg
5 mg
10 mg
25 mg

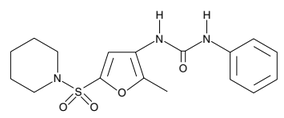

(E)-Guggulsterone 10011296

[39025-24-6]
MF: $C_{21}H_{28}O_2$ **FW:** 312.5 **Purity:** ≥98%
A crystalline solid **Stability:** ≥2 years at -20°C
Summary: A competitive antagonist of FXR (IC_{50} = 15 µM) that inhibits CDCA-induced transactivation of FXR; lowers LDL cholesterol and triglyceride levels in rodents fed a high cholesterol diet

1 mg
5 mg
10 mg

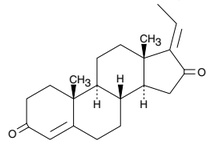

(Z)-Guggulsterone 71800

[39025-23-5]
MF: $C_{21}H_{28}O_2$ **FW:** 312.5 **Purity:** ≥98%
A crystalline solid **Stability:** ≥2 years at -20°C
Summary: A competitive antagonist of FXR (IC_{50} = 17 µM) that lowers LDL cholesterol and triglyceride levels in rodents fed a high cholesterol diet; demonstrates antitumor-promoting effects in human multiple myeloma and DU145 human prostate cancer cells

1 mg
5 mg
10 mg

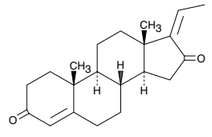

GW 0742 10006798

[317318-84-6]
MF: $C_{21}H_{17}F_4NO_3S_2$ **FW:** 471.5 **Purity:** ≥98%
A crystalline solid **Stability:** ≥2 years at -20°C
Summary: A selective PPARδ agonist (EC_{50} = 1.1 nM) that exhibits 1,000-fold selectivity over the other human PPAR subtypes

5 mg
10 mg
25 mg
50 mg

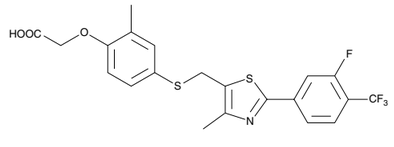

GW 7647 10008613

[265129-71-3]
MF: $C_{29}H_{46}N_2O_3S$ **FW:** 502.8 **Purity:** ≥98%
A crystalline solid **Stability:** ≥2 years at -20°C
Summary: A potent, selective PPARα agonist; activates human PPARα, PPARγ, and PPARδ with EC_{50} values of 0.006, 1.1, and 6.2 µM, respectively

1 mg
5 mg
10 mg
25 mg

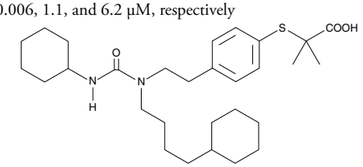

GW 9508 10008907

[885101-89-3]
MF: $C_{22}H_{21}NO_3$ **FW:** 347.4 **Purity:** ≥98%
A crystalline solid **Stability:** ≥1 year at -20°C
Summary: A small-molecule agonist of GPR40 (EC_{50} = 47 nM) and GPR120 (EC_{50} = 2.2 µM), GPCRs that are activated by medium and long-chain fatty acids; potentiates glucose-stimulated insulin secretion and the KCl-mediated increase in insulin secretion in MIN6 cells

5 mg
10 mg
50 mg
100 mg

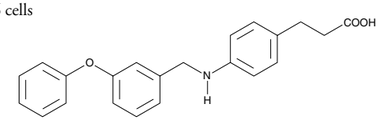

GW 9578 10011211

[247923-29-1]
MF: $C_{26}H_{34}F_2N_2O_3S$ **FW:** 492.6 **Purity:** ≥98%
A solution in methyl acetate **Stability:** ≥1 year at -20°C
Summary: A potent, selective PPARα agonist that activates mouse and human PPARα with EC_{50} values of 0.005 and 0.05 µM, respectively; 0.2 mg/kg given orally once daily for three days decreased serum total LDL cholesterol 40-60% in male Sprague-Dawely rats

500 µg
1 mg
5 mg
10 mg

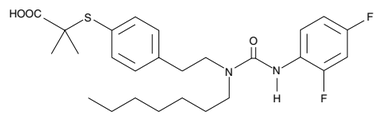

GW 9662 70785

[22978-25-2]
MF: $C_{13}H_9ClN_2O_3$ **FW:** 276.7 **Purity:** ≥98%
A crystalline solid **Stability:** ≥2 years at -20°C
Summary: A potent PPARγ antagonist; blocks the PPARγ-induced differentiation of monocytes to osteoclasts by >90% at a dose of 0.1 µM

1 mg
5 mg
10 mg
50 mg

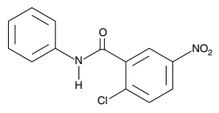

•Also Available: **GW 9662-d_5** (9000497)

GW 590735 10009880

[622402-22-6]
MF: $C_{23}H_{21}F_3N_2O_4S$ **FW:** 478.5 **Purity:** ≥98%
A crystalline solid **Stability:** ≥2 years at -20°C
Summary: A potent and selective PPARα agonist (EC_{50} = 4 nM) that is at least 500-fold selective for PPARα over PPARγ and PPARδ

1 mg
5 mg
10 mg
25 mg

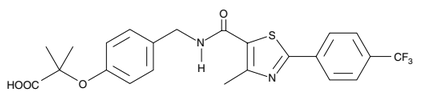

Harmine 10010324

[442-51-3]
MF: $C_{13}H_{12}N_2O$ **FW:** 212.1 **Purity:** ≥98%
A crystalline solid **Stability:** ≥2 years at -20°C
Summary: A unique regulator of PPARγ expression that acts by inhibiting the Wnt signaling pathway in a cell-specific manner

250 mg
500 mg
1 g
5 g

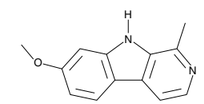

Hesperetin 10006084

[520-33-2]
MF: $C_{16}H_{14}O_6$ **FW:** 302.3 **Purity:** ≥98%
A crystalline solid **Stability:** ≥2 years at room temperature
Summary: A citrus flavonoid that lowers plasma cholesterol; reduces the transcription of ACAT-2 mRNA in HepG2 cells and reduces ApoB protein synthesis (EC_{50} ~ 50 µM)

25 g
50 g
100 g
500 g

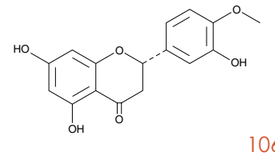

HTS 01037 10699

[682741-29-3]
MF: $C_{14}H_{11}NO_5S_2$ **FW:** 337.4 **Purity:** ≥98%
A crystalline solid **Stability:** ≥2 years at -20°C
Summary: A high-affinity ligand of A-FABP/aP2 (K_i = 0.67 µM); shown to antagonize the protein-protein interaction of A-FABP/aP2 with hormone sensitive lipase in cultured C8PA lipocytes; presumably competes with fatty acids for functional binding in the ligand-binding cavity of A-FABP/aP2

1 mg
5 mg
10 mg
25 mg

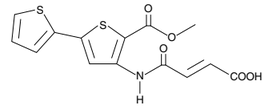

5-Iodotubercidin 10010375

[24386-93-4] Itu, NSC 113939
MF: $C_{11}H_{13}IN_4O_4$ **FW:** 392.2 **Purity:** ≥95%
A solution in ethanol **Stability:** ≥1 year at -20°C
Summary: Initiates glycogen synthesis in hepatocytes by causing inactivation of phosphorylase α and activation of glycogen synthase α (maximal effects with ~20 µM Itu)

100 µg
250 µg
1 mg
5 mg

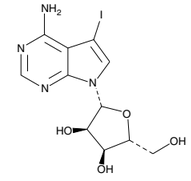

JMV3002 10012699

[925239-03-8]
MF: $C_{35}H_{34}N_6O_3$ **FW:** 586.7 **Purity:** ≥98%
A solution in methyl acetate **Stability:** ≥1 year at -20°C
Summary: A potent ghrelin receptor antagonist (IC_{50} = 1.1 nM) that inhibits hexarelin-stimulated food intake by as much as 98% in rats at 80 µg/kg; does not affect growth hormone release when tested in infant rats

100 µg
500 µg
1 mg
5 mg

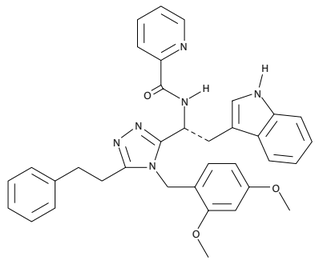

KB2115 10011054

[355129-15-6]
MF: $C_{18}H_{17}Br_2NO_5$ **FW:** 487.1 **Purity:** ≥98%
A crystalline solid **Stability:** ≥2 years at -20°C
Summary: A synthetic thyroid hormone mimetic that lowers total and LDL cholesterol up to 40% when administered to humans at a dose of 50-200 µg once daily for 14 days; stimulates cholesterol catabolism to bile acids without affecting cholesterol synthesis

500 µg
1 mg
5 mg
10 mg

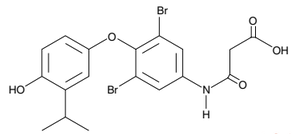

(R)-Lisofylline 13616

[100324-81-0] (-)-Lisofylline, (R)-LSF
MF: $C_{13}H_{20}N_4O_3$ **FW:** 280.3 **Purity:** ≥98%
A crystalline solid **Stability:** ≥2 years at -20°C
Summary: A potent inhibitor of the generation of phosphatidic acid (IC_{50} = 0.6 µM) from cytokine-activated lysophosphatidic acyl transferase (LPAAT), which has been shown to protect mice from endotoxic shock; suppresses the production of the proinflammatory cytokine IFN-γ, inhibits IL-12 signaling, and enhances glucose-stimulated β-cell insulin secretion; reduces the onset of diabetes in a non-obese diabetic mouse model

1 mg
5 mg
10 mg
25 mg

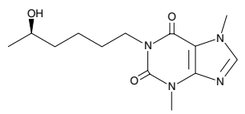

Lovastatin 10010338

[75330-75-5]
MF: $C_{24}H_{36}O_5$ **FW:** 404.5 **Purity:** ≥98%
A crystalline solid **Stability:** ≥2 years at -20°C
Summary: A potent, competitive inhibitor of HMG-CoA reductase (K_i = 0.6 nM)

5 mg
10 mg
25 mg
50 mg

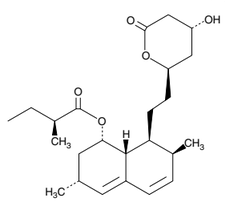

•Also Available: **Lovastatin Hydroxy Acid (sodium salt)** (10010339)

Mevastatin 10010340

[73573-88-3] Compactin, CS 500, L-637,312, ML 236B, NSC 281245, Statin I
MF: $C_{23}H_{34}O_5$ **FW:** 390.5 **Purity:** ≥98%
A crystalline solid **Stability:** ≥2 years at -20°C
Summary: A reversible, competitive HMG-CoA reductase inhibitor (K_i = 1 nM)

5 mg
10 mg
25 mg
50 mg

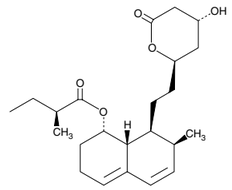

2-NBDG 11046

[186689-07-6] NBD-Glucose
MF: $C_{12}H_{14}N_4O_8$ **FW:** 342.3 **Purity:** ≥98% (mixture of α and β)
A crystalline solid **Stability:** ≥2 years at -20°C
Summary: A fluorescently-labeled deoxyglucose analog that is used primarily to directly monitor glucose uptake by living cells and tissues; also used as a topical contrast reagent for the detection of neoplasia

1 mg
5 mg
10 mg

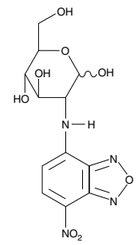

N-Octadecyl-N'-propyl-sulfamide 10009661

MF: $C_{21}H_{46}N_2O_2S$ **FW:** 390.7 **Purity:** ≥95%
A crystalline solid **Stability:** ≥2 years at -20°C
Summary: A selective and potent activator of PPARα with an EC_{50} value of 100 nM; induces satiety, decreases food-intake, reduces body weight, and lowers plasma triglyceride concentration in free-feeding Wistar and obese Zucker (*fa/fa*) rats

5 mg
10 mg
25 mg
50 mg

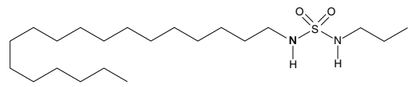

Oleic Acid-2,6-diisopropylanilide 10006782

[140112-65-8]
MF: $C_{30}H_{51}NO$ **FW:** 441.7 **Purity:** ≥98%
A solution in methyl acetate **Stability:** ≥1 year at -20°C
Summary: An inhibitor of ACAT with an IC_{50} value of 7 nM

5 mg
10 mg
50 mg
100 mg

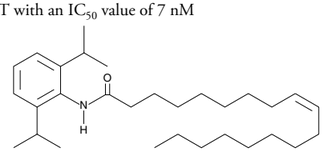

Oleoyl Ethanolamide 90265

[111-58-0] OEA, Oleic Acid Ethanolamide
MF: $C_{20}H_{39}NO_2$ **FW:** 325.5 **Purity:** ≥98%
A crystalline solid **Stability:** ≥1 year at -20°C
Summary: An analog of AEA found in brain tissue and chocolate; accumulates rapidly in infarcted tissue; an endogenous, potent PPARα agonist (EC_{50} = 120 nM); suppresses food intake and reduces weight gain in rats

5 mg
10 mg
50 mg
100 mg

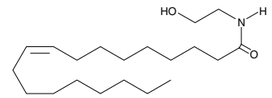

•Also Available: **Oleoyl Ethanolamide-d_2** (10007823)
Oleoyl Ethanolamide-d_4 (9000552)

Oleyl Anilide 10006529

[5429-85-6] OA, Oleic Acid Anilide
MF: $C_{24}H_{39}NO$ **FW:** 357.6 **Purity:** ≥95%
A crystalline solid **Stability:** ≥2 years at -20°C
Summary: A weak ACAT inhibitor with an IC_{50} value of 26 µM

5 mg
10 mg
50 mg
100 mg

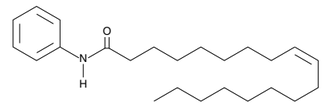

Orlistat 10005426

[96829-58-2] Alli, Tetrahydrolipstatin, Xenical ™
MF: $C_{29}H_{53}NO_5$ **FW:** 495.7 **Purity:** ≥98%
A crystalline solid **Stability:** ≥2 years at -20°C
Summary: An anti-obesity drug that inhibits gastric, pancreatic, and carboxyl ester lipases, preventing hydrolysis of triglycerides to free fatty acids and monoglycerides; potently inhibits human recombinant diacylglycerol lipase-α (IC_{50} = 60 nM) and at 1 µM inhibits the formation of 2-arachidonoyl glycerol in intact cells

50 mg
100 mg
250 mg
500 mg

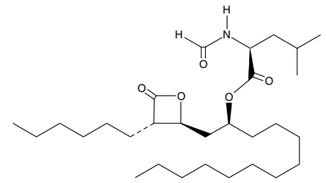

Palmitoleic Acid 10009871

[373-49-9] 9-cis-Hexadecenoic Acid, Palmitoleate, n-7 Palmitoleate, cis-Palmitoleic Acid
MF: $C_{16}H_{30}O_2$ **FW:** 254.4 **Purity:** ≥99%
A neat oil **Stability:** ≥1 year at -20°C
Summary: An ω-7 monounsaturated fatty acid that is a common constituent of the triglycerides of human adipose tissue; raises LDL cholesterol and lowers HDL cholesterol much like that of a saturated fatty acid, even when dietary intake of cholesterol is maintained at a low level

100 mg
500 mg
1 g
5 g

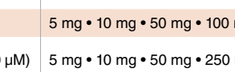

•Also Available: **Palmitoleic Acid-d_{14}** (9000431)
Palmitoleic Acid ethyl ester (10008204)

PPAR Ligands

Item No.	Product Name	Target	Mode of Action	Effective Concentration	Sizes
13452	**AM3102**	PPARα	Agonist	EC_{50} = 100 nM	5 mg • 10 mg • 25 mg • 50 mg
60924	**Azelaoyl PAF**	PPARγ	Agonist	~ Equal to Rosiglitazone	500 µg • 1 mg • 5 mg • 10 mg
10009145	**Bezafibrate**	pan PPAR	Agonist	EC_{50} = 20-60 µM	500 mg • 1 g • 5 g • 10 g
10009017	**CAY10514**	PPARα PPARγ	Dual Agonist	EC_{50} = 0.173 µM (PPARα) EC_{50} = 0.642 µM (PPARγ)	1 mg • 5 mg • 10 mg • 50 mg
10008846	**CAY10573**	pan-PPAR	Agonist	IC_{50} = 50-225 µM	500 µg • 1 mg • 5 mg • 10 mg
10012536	**CAY10592**	PPARδ	Agonist	EC_{50} = 53 nM (rat)	1 mg • 5 mg • 10 mg • 50 mg
13282	**CAY10599**	PPARδ	Agonist	EC_{50} = 50 nM	1 mg • 5 mg • 10 mg • 25 mg
71730	**Ciglitazone**	PPARγ	Agonist	EC_{50} = 3 µM	1 mg • 5 mg • 10 mg • 50 mg
10956	**Clofibrate**	PPARα	Agonist	EC_{50} = 55 µM (human)	500 mg • 1 g • 5 g • 10 g
10005368	**Fenofibrate**	PPARα	Agonist	EC_{50} = 30 µM (human)	1 g • 5 g • 10 g • 50 g
10006798	**GW 0742**	PPARδ	Agonist	EC_{50} = 1.1 nM	5 mg • 10 mg • 25 mg • 50 mg
10008613	**GW 7647**	PPARα	Agonist	EC_{50} = 6 nM (human)	1 mg • 5 mg • 10 mg • 25 mg
10011211	**GW 9578**	PPARα	Agonist	EC_{50} = 50 nM (human)	500 µg • 1 mg • 5 mg • 10 mg
70785	**GW 9662**	PPARγ	Antagonist	Blocks differentiation of monocytes to osteoclasts by >90% at a dose of 0.1 µM	1 mg • 5 mg • 10 mg • 50 mg
10009880	**GW 590735**	PPARα	Agonist	EC_{50} = 4 nM	1 mg • 5 mg • 10 mg • 25 mg
10009661	**N-Octadecyl-N'-propyl-sulfamide**	PPARα	Agonist	EC_{50} = 100 nM	5 mg • 10 mg • 25 mg • 50 mg
90265	**Oleoyl Ethanolamide**	PPARα	Agonist	EC_{50} = 120 nM	5 mg • 10 mg • 50 mg • 100 mg
18570	**15-deoxy-$D^{12,14}$-Prostaglandin J_2**	PPARδ	Agonist	EC_{50} = 7 µM	100 µg • 500 µg • 1 mg • 5 mg
71740	**Rosiglitazone**	PPARγ	Agonist	K_d = 43 nM	5 mg • 10 mg • 50 mg • 100 mg
10026	**T0070907**	PPARγ	Antagonist	IC_{50} = 1 nM for inhibition of Rosiglitazone binding	1 mg • 5 mg • 10 mg • 50 mg
71750	**Troglitazone**	PPARγ	Agonist	EC_{50} = 0.55 µM (human)	5 mg • 10 mg • 50 mg • 100 mg
70730	**Wy 14643**	PPARα PPARδ	Agonist	Species dependent (PPARα: 0.1 - 10 µM)	5 mg • 10 mg • 50 mg • 250 mg

PPARγ Ligand Pack 71000

Purity: ≥98% **Stability:** ≥1 year at -20°C
Summary: Contains ciglitazone, GW 9662, 15-deoxy-$\Delta^{12,14}$-PGJ_2, rosiglitazone, and troglitazone

1 ea

Pravastatin (sodium salt) 10010343

[81131-70-6]
MF: $C_{23}H_{35}O_7$ • Na **FW:** 446.5 **Purity:** ≥98%
A crystalline solid **Stability:** ≥2 years at -20°C
Summary: A potent, competitive inhibitor of HMG-CoA reductase (K_i = 2.3 nM)

5 mg
10 mg
25 mg
50 mg

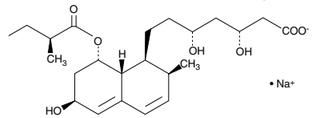

15-deoxy-$\Delta^{12,14}$-Prostaglandin J_2 18570

[87893-55-8]
MF: $C_{20}H_{28}O_3$ **FW:** 316.4 **Purity:** ≥97%*
A solution in methyl acetate **Stability:** ≥1 year at -20°C
Summary: A metabolite of PGD_2 formed by the elimination of two molecules of water; binds to PPARγ with an EC_{50} value of 2 µM

100 µg
500 µg
1 mg
5 mg

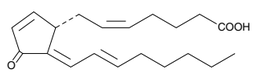

•Also Available: **15-deoxy-$\Delta^{12,14}$-Prostaglandin J_2-d_4** (318570)
15-deoxy-$\Delta^{12,14}$-Prostaglandin J_2-2-glycerol ester (10010132)
15-deoxy-$\Delta^{12,14}$-Prostaglandin J_2 Lipid Maps MS Standard (10007235)
15-deoxy-$\Delta^{12,14}$-Prostaglandin J_2-Quant-PAK (10006850)

15-deoxy-$\Delta^{12,14}$-Prostaglandin J_2 18570.1

[87893-55-8]
MF: $C_{20}H_{28}O_3$ **FW:** 316.4 **Purity:** ≥98% (isomer mixture)*
A solution in methyl acetate **Stability:** ≥1 year at -20°C
Summary: Formulation containing 90-95% of the *trans*,*trans*-$\Delta^{12,14}$ isomer, and 5-10% of other double bond isomers which have similar PPARγ ligand activity (see Item No. 18570)

1 mg
5 mg
10 mg
50 mg

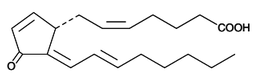

15-deoxy-$\Delta^{12,14}$-Prostaglandin J_2-biotin 10141

MF: $C_{35}H_{54}N_4O_4S$ **FW:** 626.9 **Purity:** ≥98%*
A solution in ethanol **Stability:** ≥1 year at -20°C
Summary: An affinity probe designed to allow 15-deoxy-$\Delta^{12,14}$-PGJ_2 to be detected in complexes with nuclear receptors and/or nucleic acid or protein binding partners

50 µg
100 µg
500 µg
1 mg

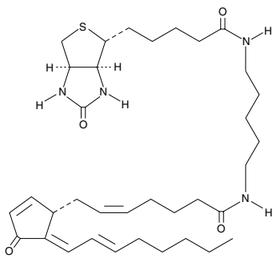

**All 5-cis 2-series PGs (those containing a 5,6-double bond) will contain a small amount of the 5-trans isomer. This isomer is generally undetectable using normal phase silica columns and plates, but may be resolved using RP-HPLC. The purity for all such 2-series PGs excludes the 1-3% trans isomer which will generally be present.*

PSN375963 10008593

[388575-52-8]
MF: $C_{17}H_{23}N_3O$ **FW:** 285.4 **Purity:** ≥98%
A crystalline solid **Stability:** ≥2 years at -20°C
Summary: A selective agonist of GPR119, a GPCR that mediates a reduction in food intake and body weight gain by oleoyl ethanolamide in rats; exhibits EC_{50} values of 8.4 and 7.9 µM at recombinant mouse and human GPR119 receptors, respectively

1 mg
5 mg
10 mg
25 mg

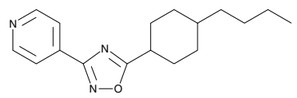

PSN632408 10008594

[857652-30-3]
MF: $C_{18}H_{24}N_4O_4$ **FW:** 360.4 **Purity:** ≥98%
A crystalline solid **Stability:** ≥2 years at -20°C
Summary: A selective agonist of GPR119, a GPCR that mediates a reduction in food intake and body weight gain by oleoyl ethanolamide in rats; exhibits EC_{50} values of 5.6 and 7.9 µM at recombinant mouse and human GPR119 receptors, respectively

1 mg
5 mg
10 mg
25 mg

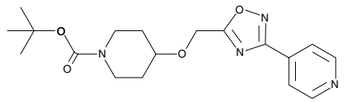

Rimonabant 9000484

[168273-06-1] SR141716
MF: $C_{22}H_{21}Cl_3N_4O$ **FW:** 463.8 **Purity:** ≥98%
A crystalline solid **Stability:** ≥2 years at -20°C
Summary: A selective CB_1 receptor inverse agonist (K_i = 1.8 nM)

5 mg
10 mg
25 mg
50 mg

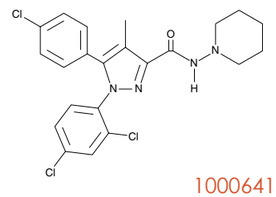

Ro 48-8071 10006415

[161582-11-2]
MF: $C_{23}H_{27}BrFNO_2$ **FW:** 448.4 **Purity:** ≥98%
A solution in methyl acetate **Stability:** ≥1 year at -20°C
Summary: An inhibitor of oxidosqualene cyclase (OSC) that has LDL cholesterol lowering activity; inhibits OSC from human liver microsomes and $HepG_2$ cells with IC_{50} values of approximately 6.5 and 1.5 nM, respectively

5 mg
10 mg
50 mg
100 mg

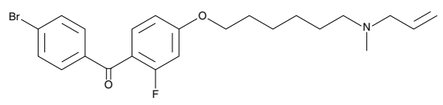

Rosiglitazone 71740

[122320-73-4] BRL 49653
MF: $C_{18}H_{19}N_3O_3S$ **FW:** 357.4 **Purity:** ≥98%
A crystalline solid **Stability:** ≥2 years at -20°C
Summary: A potent and selective PPARγ agonist; binds to the PPARγ ligand-binding domain with a K_d value of 43 nM

5 mg
10 mg
50 mg
100 mg

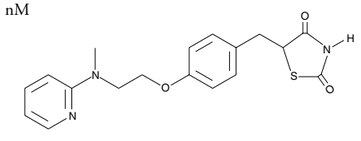

•Also Available: **Rosiglitazone-d_5 Maleate** (10011343)
Rosiglitazone (potassium salt) (71742)

Sesamin 70310

[607-80-7]
MF: $C_{20}H_{18}O_6$ **FW:** 354.4 **Purity:** ≥95%
A crystalline solid **Stability:** ≥1 year at -20°C
Summary: A non-competitive inhibitor of Δ^5-desaturase; inhibits the conversion of DGLA to arachidonic acid with a K_i value of 155 µM in rat liver microsomes

1 mg
5 mg
10 mg
50 mg

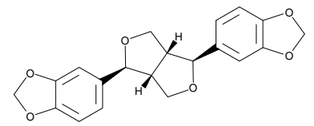

Simvastatin 10010344

[79902-63-9] MK 733
MF: $C_{25}H_{38}O_5$ **FW:** 418.6 **Purity:** ≥98%
A crystalline solid **Stability:** ≥2 years at -20°C
Summary: A potent, competitive inhibitor of HMG-CoA reductase (K_i = 0.12 nM)

5 mg
10 mg
25 mg
50 mg

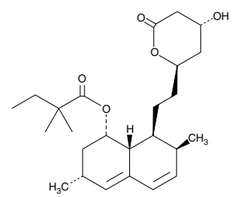

•Also Available: **Simvastatin (sodium salt)** (10010345)

Stearic Acid 10011298

[57-11-4]
MF: $C_{18}H_{34}O_2$ **FW:** 284.5 **Purity:** ≥98%
A crystalline solid **Stability:** ≥2 years at -20°C
Summary: A long-chain saturated fatty acid that does not affect plasma total cholesterol or LDL-cholesterol but may reduce HDL-cholesterol

500 mg
1 g
5 g
10 g

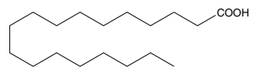

•Also Available: **Stearic Acid ethyl ester** (10008196)

Stearidonic Acid 90320

[20290-75-9] Moroctic Acid
MF: $C_{18}H_{28}O_2$ **FW:** 276.4 **Purity:** ≥98%
A solution in ethanol **Stability:** ≥1 year at -20°C
Summary: An 18-carbon, ω-3 fatty acid which is a dietary precursor to EPA and DHA present in small amounts in seed oils, especially black currant seed oil

1 mg
5 mg
25 mg

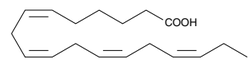

•Also Available: **Stearidonic Acid ethyl ester** (10006856)
Stearidonic Acid methyl ester (10005000)
Stearidonoyl Glycine (9000327)

T0070907 10026

[313516-66-4]
MF: $C_{12}H_8ClN_3O_3$ **FW:** 277.7 **Purity:** ≥98%
A crystalline solid **Stability:** ≥1 year at -20°C
Summary: A potent and selective PPARγ antagonist with an apparent IC_{50} value of 1 nM for the human receptor

1 mg
5 mg
10 mg
50 mg

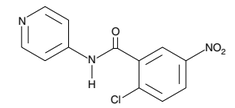

T0901317 71810

[293754-55-9]
MF: $C_{17}H_{12}F_9NO_3S$ **FW:** 481.3 **Purity:** ≥98%
A crystalline solid **Stability:** ≥1 year at -20°C
Summary: A potent and selective agonist for both LXRα and LXRβ (EC_{50} = 50 nM)

5 mg
10 mg
50 mg
100 mg

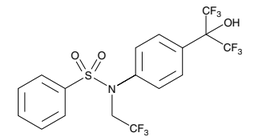

9-Thiastearic Acid 10007417

[106689-24-1]
MF: $C_{17}H_{34}O_2S$ **FW:** 472.3 **Purity:** ≥98%
A crystalline solid **Stability:** ≥2 years at -20°C
Summary: Inhibits desaturation of radiolabeled stearate to oleate in rat hepatocytes and hepatoma cells (>80% at a concentration of 25 µg)

5 mg
10 mg
50 mg
100 mg

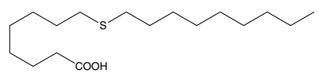

3-Thiatetradecanoic Acid 90500

[116296-31-2] 3-TDA
MF: $C_{13}H_{26}O_2S$ **FW:** 246.4 **Purity:** ≥98%
A crystalline solid **Stability:** ≥2 years at -20°C
Summary: An analog of myristic acid wherein the C-3 carbon has been replaced by sulfur in a thioether linkage; acts as a PPAR ligand, increases fatty acid oxidation, and lowers plasma lipid levels

1 mg
5 mg
10 mg
50 mg

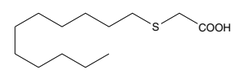

TOFA 10005263

[54857-86-2] RMI 14514, 5-(Tetradecyloxy)-2-furoic Acid
MF: $C_{19}H_{32}O_4$ **FW:** 324.5 **Purity:** ≥98%
A crystalline solid **Stability:** ≥2 years at -20°C
Summary: An inhibitor of fatty acid synthesis that blocks the synthesis of malonyl-CoA by acetyl-CoA carboxylase

5 mg
10 mg
50 mg
100 mg

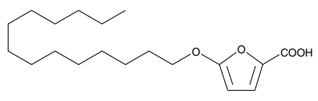

Troglitazone 71750

[97322-87-7] Resulin™
MF: $C_{24}H_{27}NO_5S$ **FW:** 441.5 **Purity:** ≥98%
A crystalline solid **Stability:** ≥1 year at -20°C
Summary: A selective PPARγ agonist with EC_{50} values of 0.55 and 0.78 µM for transactivation of human and mouse PPARγ, respectively

5 mg
10 mg
50 mg
100 mg

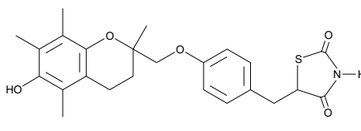

U-18666A 10009085

[3039-71-2]
MF: $C_{24}H_{41}NO_2$ • HCl **FW:** 412.1 **Purity:** ≥95%
A crystalline solid **Stability:** ≥2 years at -20°C
Summary: A cell permeable drug that inhibits cholesterol trafficking from late endosomes/lysosomes to the endoplasmic reticulum, but not to the plasma membrane

5 mg
10 mg
25 mg
50 mg

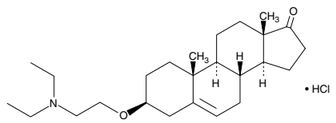

Wy 14643 70730

[50892-23-4] Pirinixic Acid
MF: $C_{14}H_{14}ClN_3O_2S$ **FW:** 323.8 **Purity:** ≥98%
A crystalline solid **Stability:** ≥2 years at room temperature
Summary: An agonist of PPARα and PPARγ

5 mg
10 mg
50 mg
250 mg

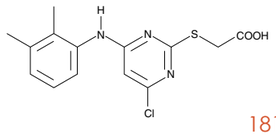

YM-53601 18113

[182959-33-7]
MF: $C_{21}H_{21}FN_2O$ • HCl **FW:** 372.9 **Purity:** ≥98%
A crystalline solid **Stability:** ≥2 years at -20°C
Summary: Inhibits squalene synthase activity in rat hepatic microsomes and human HepG2 cells (IC_{50} = 90 and 79 nM, respectively); inhibits cholesterol biosynthesis in rats, reducing both cholesterol and triglyceride levels in plasma

500 µg
1 mg
5 mg
10 mg

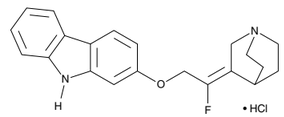

YM-201636 13576

[371942-69-7]
MF: $C_{25}H_{21}N_7O_3$ **FW:** 467.5 **Purity:** ≥95%
A crystalline solid **Stability:** ≥2 years at -20°C
Summary: A cell-permeable and selective inhibitor of PIKfyve (IC_{50} = 33 nM); reversibly impairs endosomal trafficking in NIH3T3 cells and blocks retroviral exit by budding from cells; inhibits basal and insulin-activated 2-deoxyglucose uptake (IC_{50} = 54 nM) in adipocytes

1 mg
5 mg
10 mg
25 mg

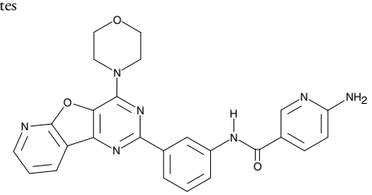

KITS

Adipogenesis Assay Kit 10006908

Stability: ≥1 year at -20°C
Summary: Cayman's Adipogenesis Assay provides the reagents required for studying the induction and inhibition of adipogenesis in the established 3T3-L1 model. This kit can also be used to screen drug candidates involved in adipogenesis. The classic Oil Red O staining for lipid droplets is used in this kit as an indicator of the degree of adipogenesis, and can be quantified with a plate reader after the dye is conveniently extracted from the lipid droplet.

1 ea

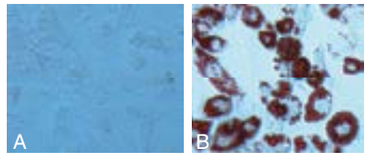

Panel A: Non-differentiated 3T3-L1 cells were not stained by Oil Red O Solution. *Panel B:* More than 80% of preadipocytes were differentiated four days after weaning the cells from induction media to insulin media. Different degrees of lipid droplet accumulation in the differentiated cells can be visualized by Oil Red O Solution staining.

Adipolysis Assay Kit 10009381

Stability: ≥1 year at -20°C
Summary: Cayman's Adipolysis Assay provides an easy to use tool for studying the hydrolysis of triglycerides to FFAs and glycerol in differentiated 3T3-L1 cells. This kit will allow investigators to screen compounds involved in lipid storage and metabolism. Isoproterenol is included in the kit as a positive control for screening pharmaceuticals that regulate FFA release from adipocytes.

1 ea

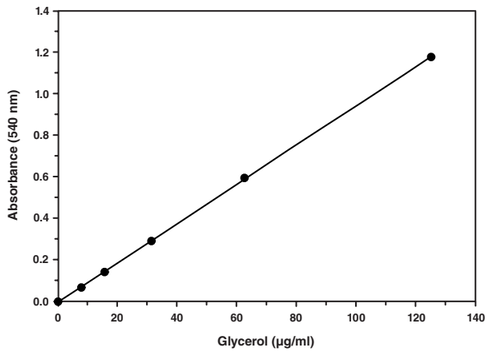

Adiponectin

Adiponectin, also known as Acpr30 and GPB-28, is a physiologically active protein which is specifically and highly expressed from adipose cells. Adipose tissue-expressed levels of adiponectin are inversely related to the degree of obesity and are correlated with insulin resistant states such as those found in obesity and type II diabetes mellitus. Adiponectin increases insulin sensitivity and decreases plasma glucose by increasing fat oxidation. The assay kits listed below are sensitive methods for the quantification of adiponectin from human or mouse samples.

Adiponectin (human) EIA Kit† 500641

Acpr30, AdipoQ, GBP-28
Stability: ≥6 months at 4°C **Limit of Detection:** 0.7 µg/ml
Summary: This EIA is based on the competition between free adiponectin and bound adiponectin (coated to the wells of a 96-well plate) for a fixed quantity of HRP-labeled adiponectin antibody.
Specificity:
For a full specificity profile, please go to www.caymanchem.com

96 wells

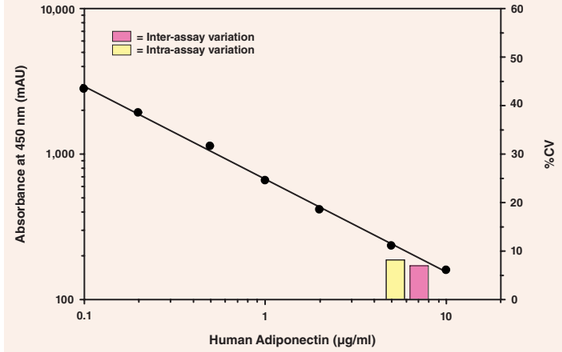

Adiponectin (human) EIA Kit (HS)† 10007619

Acpr30, AdipoQ, GBP-28
Stability: ≥6 months at 4°C **Limit of Detection:** 0.5 ng/ml
Summary: This EIA is based on a double antibody sandwich technique that is applicable to the quantification of both low molecular weight and high molecular weight polymers of adiponectin, but not adiponectin trimers.
Specificity:
For a full specificity profile, please go to www.caymanchem.com

96 wells

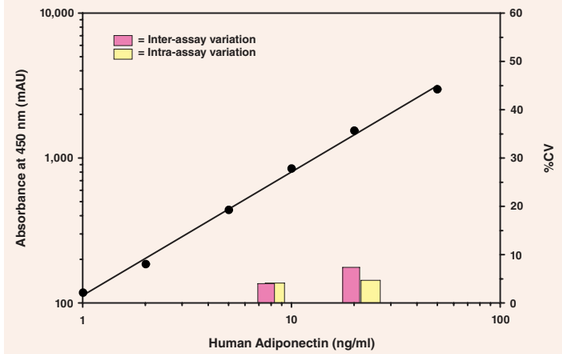

† *SPI-BIO Assays are available through Cayman Chemical only within North & South America and Asia; elsewhere contact Bertin Pharma.*

Adiponectin (mouse) EIA Kit† 10007620

Acpr30, AdipoQ, GBP-28
Stability: ≥6 months at 4°C **Limit of Detection:** 0.1 ng/ml
Summary: This EIA is based on a double-antibody sandwich technique which utilizes a mouse adiponectin-specific monoclonal capture antibody and a HRP-conjugated polyclonal antibody for detection.
Specificity:
For a full specificity profile, please go to www.caymanchem.com

96 wells

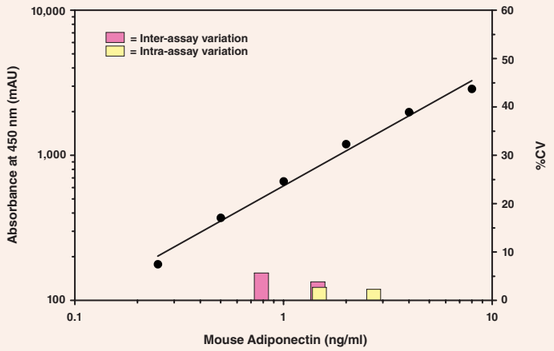

ANGPTL3 (human) EIA Kit 580170

Angiopoietin-like protein 3
Stability: ≥6 months at 4°C **Limit of detection:** 150 pg/ml
Summary: ANGPTL3 demonstrates pro-angiogenic effects by binding integrin αvβ3, which induces endothelial cell migration and adhesion. It also dually inhibits the catalytic activities of lipoprotein lipase, which catalyzes the hydrolysis of triglycerides, and endothelial lipase, which hydrolyzes HDL phospholipids. In hypolipidemic, yet obese, KK/Snk mice, a reduction in ANGPTL3 expression promotes the clearance of triglycerides, while human ANGPTL3 plasma concentrations positively correlate with plasma HDL cholesterol and HDL phospholipid levels. Cayman's Human ANGPTL3 EIA Kit is an immunometric (*i.e.*, sandwich) assay which can be used to measure ANGPTL3 in human serum, plasma, or cell culture supernatants.
Specificity:
For a full specificity profile, please go to www.caymanchem.com

1 ea

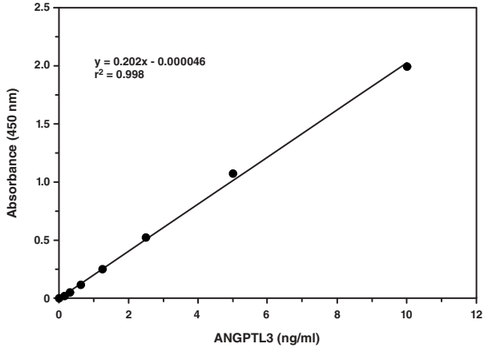

ANGPTL6 (human) EIA Kit 580190

Angiopoietin-like protein 6
Stability: ≥6 months at 4°C **Limit of detection:** 1.2 ng/ml
Summary: ANGPTL6 induces angiogenesis and arteriogenesis through activation of the ERK1/2-eNOS pathway. Transgenic mice that persistently overexpress ANGPTL6 have increased systemic energy expenditure counteracting high-fat diet-induced obesity and related insulin resistance, while onset of obesity in ANGPTL6 null mice is attributed to decreased energy expenditure and insulin resistance. Circulating levels of human ANGPTL6 are elevated in obese or diabetic conditions and positively correlate with fasting serum glucose levels. Cayman's Human ANGPTL6 EIA Kit is an immunometric (*i.e.*, sandwich) assay which can be used to measure ANGPTL6 in human serum, plasma, or cell culture supernatants.
Specificity:
For a full specificity profile, please go to www.caymanchem.com

1 ea

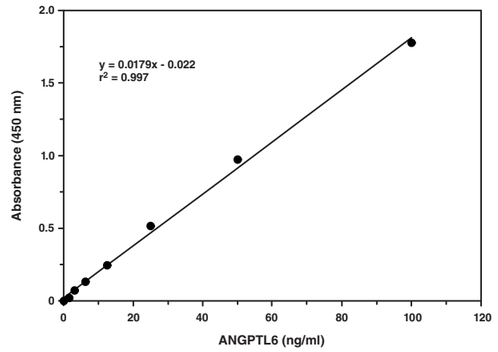

Cholesterol Assay Kit 10007640

Stability: ≥1 year at -20°C
Summary: Cholesterol, particularly in the form of LDLs, is well understood to be associated with increased risk of coronary heart disease. The measurement of cholesterol is one of the most common tests performed in the clinical laboratory setting. Cayman's Cholesterol Assay provides research labs with a simple fluorometric method for the sensitive quantitation of total cholesterol in plasma or serum.

96 wells
480 wells

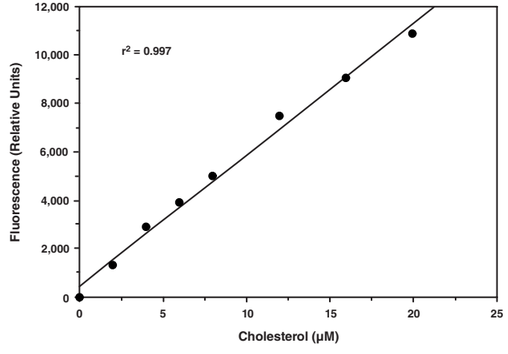

Cholesterol Cell-Based Detection Assay Kit 10009779

Stability: ≥6 months at -20°C
Summary: The mechanism for the movement of cholesterol from intracellular sites to their ultimate cellular destination is an unresolved question of fundamental importance to cell biology and medicine. Cayman's Cholesterol Cell-Based Detection Assay provides a simple fluorometric method to study mechanisms and biological factors that regulate cholesterol metabolism or movement within cells.

192 wells

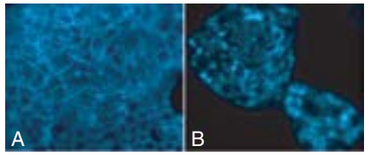

Accumulation of cholesterol in HepG2 cells. *Panel A:* Cells treated with DMSO (vehicle) demonstrate that the majority of cholesterol is localized on the plasma membrane. *Panel B:* U-18666A (1.25 µM) treatment for 48 hours induces intracellular accumulation of cholesterol droplets.

Cholesterol Uptake Cell-Based Assay Kit 600440

Stability: ≥6 months at -20°C
Summary: Maintaining body cholesterol homeostasis is critical for normal physiological functions and is achieved by a highly regulated balance of *de novo* synthesis, dietary cholesterol absorption, biliary clearance, and excretion. A better understanding of the relationship between cholesterol absorption and synthesis may allow for the development of powerful novel strategies for the prevention and treatment of hypercholesterolemia. Cayman's Cholesterol Uptake Cell-Based Assay Kit provides a convenient tool for studying cholesterol absorption modulators by employing NBD Cholesterol, a fluorescently-tagged cholesterol, as a probe for the detection of cholesterol taken up by cultured cells.

1 ea

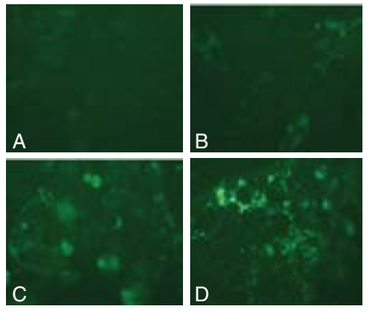

U-18666A increases NBD Cholesterol uptake in Caco-2 cells as measured by fluorescent microscopy. *Panel A:* Cells grown in culture medium containing 10% FBS and treated with vehicle. There is minimal NBD Cholesterol uptake in these cells. *Panel B:* Cells grown in culture medium containing 10% FBS and treated with 2.5 µM U-18666A. There is increasing NBD Cholesterol uptake in these cells, compared to those cells grown in culture medium containing 10% FBS. *Panel C:* Cells grown in culture medium containing no FBS and treated with vehicle. Note that there is an increase in fluorescence intensity in most of cells. *Panel D:* Cells grown in culture medium containing no FBS and treated with 2.5 µM U-18666A, show that when intracellular transportation of cholesterol was blocked, there was a dramatic increase in the uptake of NBD Cholesterol.

ChREBP Cell-Based Translocation Assay Kit 10010060

Stability: ≥1 year at -20°C
Summary: The identification of ChREBP activators is of great interest for drug discovery. The distinct translocation of the protein from the cytoplasm to the nucleus during activation makes it possible to study modulators of ChREBP through sub-cellular localization of the protein using conventional immunocytochemical staining with a specific antibody. Cayman's ChREBP Cell-Based Translocation Assay provides a highly specific ChREBP primary antibody together with a Dylight™ (product of Thermo Scientific, Inc.) conjugated secondary antibody in a ready to use format.

96 wells

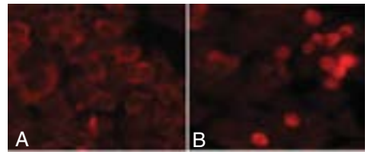

Translocation of ChREBP into nuclei induced by sucrose. *Panel A:* HepG2 cells treated with PBS (vehicle) demonstrate cytoplasmic localization of ChREBP. *Panel B:* Sucrose treatment for 24 hours induces ChREBP translocation into the nuclei.

ChREBP Transcription Factor Assay Kit 10006909

Stability: ≥6 months at -80°C
Summary: ChREBP is a transcription factor playing a critical role in the nutrient and hormonal regulation of genes encoding enzymes of glucose metabolism and lipogenesis pathways. Cayman's ChREBP Transcription Factor Assay Kit is a non-radioactive, sensitive method for detecting specific transcription factor DNA binding activity in nuclear extracts and whole cell lysates in a 96-well plate format.

96 wells

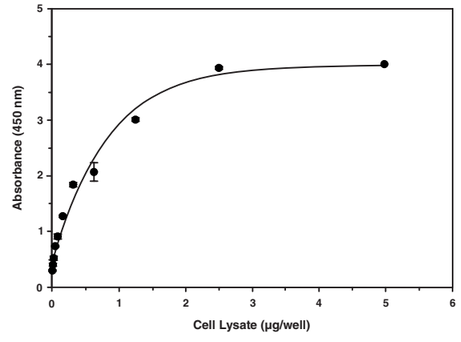

† *SPI-BIO Assays are available through Cayman Chemical only within North & South America and Asia; elsewhere contact Bertin Pharma.*

vol. 16 Me

Olivia L. May, Ph.D.

Sirtuins, to your health

Metabolic control is a delicate balance between energy intake, utilization, and storage. As researchers are discovering, sirtuins, a family of nicotinamide adenine dinucleotide (NAD^+)-dependent deacetylases, may be crucial sensors of the metabolic network that controls energy homeostasis, regulating fat and glucose metabolism in response to physiological changes in energy levels. Sirtuins not only deacetylate histones and several transcriptional regulators in the nucleus, but also modulate specific proteins in the cytoplasm and in mitochondria. Not too long ago, sirtuins gained major nutriceutical interest as the Holy Grail for extending longevity. The search was on to identify activators of this youth fountain, and the most notable sirtuin activator, resveratrol, a polyphenol found in red wine, berries, and peanuts became a household name. This was one more good reason to drink red wine, as you toasted to long life. Though not yet fully translatable to humans, in yeast, worms, flies, and mice, a further connection of sirtuins to longevity has been made related to caloric restriction.[1,2] Sirtuins can stimulate the activity of mitochondria, the powerhouses of cells, and of mitochondrial proteins, which have a key role in diseases relating to metabolism, such as type 2 diabetes and obesity, but also for neurodegenerative diseases, such as Alzheimer's disease and Parkinson's disease.[3] Thus, sirtuins may have a protective role in metabolic dysfunction. Much is still left to be understood before a modern Ponce de Leon can lay claim to this exact function of sirtuin activation. Meanwhile, you can still toast to good health as sirtuins are proving to play a key part in healthy metabolic maintenance.

Meet the Family

In mammals the sirtuin family includes seven proteins (SIRT1–SIRT7), which vary in tissue specificity, subcellular localization, enzymatic activity, and target (Table 1). They are divided into four classes: class I (SIRT1–SIRT3), class II (SIRT4), class III (SIRT5), and class IV (SIRT6 and SIRT7). In addition to their original role as histone deacetylases, they have recently been described as ADP-ribosyl transferases and also possess demalonylation and desuccinylation activity with a wide variety of target proteins.[1]

Sirtuin localization and function

Sirtuin	Class	Localization	Activity	Targets
SIRT1	**I**	Nucleus, cytosol	Deacetylation	PGC1α, FOXO, p53, HIF1α, LXR, SREBP1c and more
SIRT2	**I**	Cytosol	Deacetylation	PEPCK, FOXO1, PAR3
SIRT3	**I**	Mitochondria	Deacetylation	LCAD, HMGCS2, GDH, components of mitochondrial respiration, IDH2 and more
SIRT4	**II**	Mitochondria	ADP-ribosylation	GDH
SIRT5	**III**	Mitochondria	Deacetylation, demalonylation, desuccinylation	CPS1
SIRT6	**IV**	Nucleus	Deacetylation, ADP-ribosylation	IGF1 *via* Histones H3K9 and H3K56
SIRT7	**IV**	Nucleolus	Not known	Not known

Table 1. Sirtuin localization and function

SIRT1, the best-described sirtuin, has been studied for its role in caloric restriction, the prevention of aging-related diseases, and the maintenance of metabolic homeostasis. SIRT1 expression is upregulated during low energy states such as starvation and repressed with excess energy as with a high fat diet. In differentiated adipocyte cell lines, SIRT1 inhibits adipogenesis and enhances fat mobilization through lipolysis by suppressing the activity of PPARγ. SIRT1 promotes the assembly of a co-repressor complex, involving NCoR1 and SMRT, on the promoters of PPARγ target genes to repress their transcription and thus limit fat storage in situations of caloric restriction and fasting. SIRT1 deacetylation of PPARγ co-activator 1α (PGC1α), a transcriptional co-regulator that controls mitochondrial biogenesis and activity, leads to PGC1α activation and to the induction of downstream pathways that control mitochondrial gene expression.[4] Also, SIRT1 controls the acetylation of forkhead box O (FOXO) transcription factors, which are important regulators of lipid and glucose metabolism as well as of stress responses. SIRT1-mediated deacetylation of FOXO has been suggested to direct FOXO to its selective targets.

SIRT2 may play a role in metabolic homeostasis by deacetylating phosphoenolpyruvate carboxykinase, a kinase involved in gluconeogenesis, preventing its degradation through ubiquitylation. SIRT2 also deacetylates and activates FOXO1, which is involved in adipogenesis.[5]

Localized primarily to mitochondria, **SIRT3** is the major mitochondrial deacetylase. Several of its targets have important roles in metabolic homeostasis. Long-chain acyl CoA dehydrogenase (LCAD), a protein involved in fatty acid oxidation, is targeted by SIRT3 during prolonged fasting, preventing LCAD hyperacetylation and enabling fatty acid breakdown.[6] Deletion of SIRT3 in mice impairs fat breakdown, enhancing diet-induced obesity and impairing tolerance to cold exposure upon fasting. SIRT3 deacetylation sites have also been identified in 3-hydroxy-3-methylglutaryl CoA synthase 2, which regulates the production of ketone bodies, an important energy source for the brain when blood glucose levels are low. In response to caloric restriction, SIRT3 deacetylates/activates isocitrate dehydrogenase 2, which is involved in the Krebs cycle, and the Krebs cycle enzyme glutamate dehydrogenase (GDH).[7] SIRT3 also deacetylates components of the pathway involved in mitochondrial aerobic respiration.

SIRT4 functions in metabolism by ADP-ribosylating GDH, inhibiting its activity and blocking amino acid-induced insulin secretion. SIRT4 also regulates fatty acid oxidation in hepatocytes and myocytes. Short hairpin RNA-mediated knockdown of SIRT4 in the liver increases fatty acid oxidation.[8] It seems that SIRT3 and SIRT4 have opposing roles in the regulation of GDH, and fatty acid oxidation.

SIRT5 targets carbamoyl phosphate synthetase 1, whose deacetylation during fasting activates ammonia detoxification through the urea cycle.[9]

As well as being involved in DNA stability and repair, **SIRT6** has a role in metabolism and aging. $SIRT6^{-/-}$ mice die early in life, have reduced insulin growth factor (IGF) 1 levels and are severely hypoglycemic, with detrimental levels of glucose uptake in muscle and brown adipose tissue. Specifically ablating SIRT6 in mice at birth results in reduced body weight (due to reduced IGF1 levels) that normalizes at 1 year of age but then develops into obesity later in life.[10]

While **SIRT7** is known to activate RNA polymerase I transcription, its protein substrate is still not known.

Sirtuins as NAD^+ sensors and role for resveratrol

Sirtuins are thought to act as metabolic sensors by translating changes in NAD^+ levels into adaptive responses. The enzymatic reaction catalyzed by sirtuins requires NAD^+ as a substrate.[11] NAD^+ synthesis and bioavailability is determined by the nutritional state of the cell. Therefore, NAD^+ availability controls adaptive responses to energy stress by moderating the activity of sirtuins and their downstream effectors.[12] Sirtuins consume NAD^+, releasing nicotinamide (NAM), O-acetyl ADP ribose, and the deacetylated target protein (Figure 1). The K_m values of sirtuins for NAD^+ have been reported in the range of 100-300 µM.[13] At high concentrations, NAM will non-competitively bind and feedback-inhibit sirtuin activity.[14] Interestingly, as NAD^+ is salvaged and resynthesized, the expression of the NAM phosphoribosyltransferase (NAMPT) enzyme that converts NAM to NAD^+ is regulated in a circadian fashion by a sirtuin. SIRT1 is recruited to the NAMPT promoter to increase NAMPT expression and thus, NAD^+ biosynthesis.

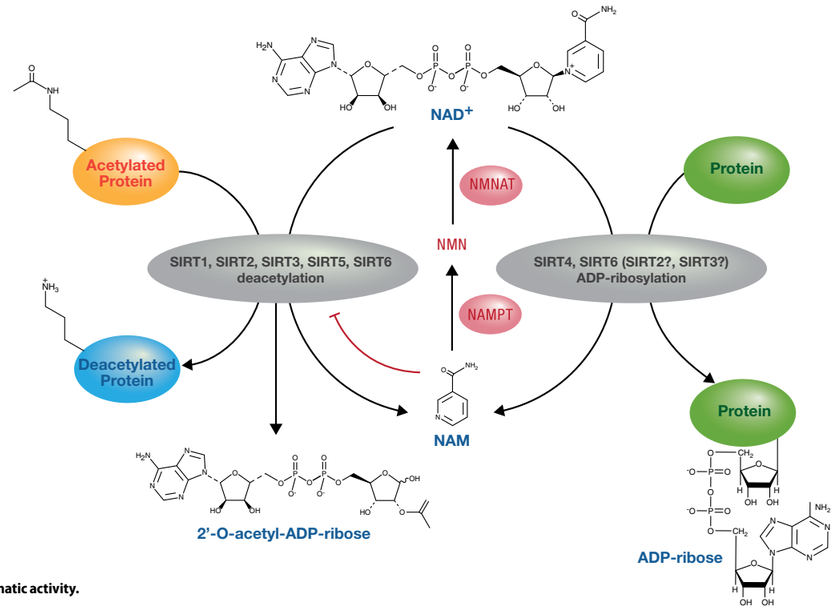

Figure 1. Sirtuin enzymatic activity.

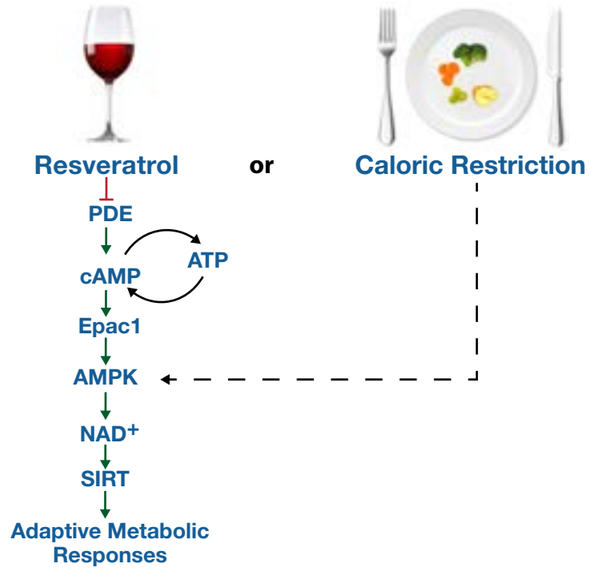

Figure 2. Proposed pathway of sirtuin activation.

NAD^+ levels, accompanied by sirtuin activation, rise in muscle, liver, and white adipose tissue during fasting, caloric restriction, and exercise, whereas a high-fat diet stimulates its conversion to a reduced form, NADH, decreasing relative NAD^+ levels. The sirtuin activator, resveratrol has been reported to mimic the effects of calorie restriction, to increase NAD^+ concentration, and to protect against obesity and insulin resistance in high-fat fed mice. Resveratrol also activates AMPK (AMP-activated protein kinase), a protein that senses nutrient deprivation by montinoring AMP/ATP and ADP/ATP ratios and increasing NAD^+ and SIRT1 as needed.[15] Elegant work by Park *et al.* has recently indentified the cAMP effector protein Epac1 as an upstream mediator of an AMPK→NAD^+→SIRT activation pathway.[16] They report that resveratrol increases cAMP levels by competitively inhibiting cAMP-specific phospodiesterases PDE1, PDE3, and PDE4 (IC_{50}s ~6-14 µM) which leads to an increase in AMPK activity (Figure 2).[16]

Conclusion

In general, sirtuins become active in nutritional or energetic deficit, promoting metabolic adjustments aimed at improving metabolic efficiency by utilizing all available energy sources. Working towards understanding the unique activities of each sirtuin member and their upstream activation should prove useful in managing metabolic and aging-related diseases. Cayman offers a complete set of highly pure, human recombinant sirtuin proteins and several convenient fluorescence-based assay kits for screening inhibitors or activators of SIRT1, SIRT2, SIRT3, or SIRT6 (see pages 50-51 and 47, respectively). We also offer a cell-based colorimetric assay for measuring intracellular NAD^+/NADH in culture cells (Item No. 600480). Finally, sirtuin activators such as resveratrol (Item No. 10004235) and sirtinol (Item No. 10523) are also available.

References

1. Houtkooper, R.H., Pirinen, E., and Auwerx, J. *Nature Reviews Mol. Cell Biol.* **13,** 225-238 (2012).
2. Demetrius, L. *EMBO Reports* **6,** S39-S44 (2005).
3. Houtkooper, R.H., Williams, R.W, and Aurwerx, J. *Cell* **142,** 9-14 (2010).
4. Rodgers, J.T., Lerin, C., Haas, W., *et al. Nature* **434,** 113–118 (2005).
5. Jing, E., Gesta, S., and Kahn, C.R. *Cell Metab.* **6,** 105–114 (2007).
6. Hirschey, M.D., Shimazu, T., Goetzman, E., *et al. Nature* **464,** 121-125 (2010).
7. Someya, S., Yu, W., Hallows, W. C., *et al. Cell* **143,** 802–812 (2010).
8. Nasrin, N., Wu, X., Fortier, E., *et al. J. of Biol. Chem.* **285(42),** 31995-32002 (2010).
9. Nakagawa, T., Lomb, D.J., Haigis, M.C., *et al. Cell* **137(3),** 560-570 (2009).
10. Schwer, B., Schumacher, B., Lombard, D.B., *et al. Proc. Natl Acad. Sci. USA* **107,** 21790–21794 (2010).
11. Denu, J.M. *TIBS* **28(1),** 41-48 (2003).
12. Cantó, C. and Auwerx, J. *Cold Spring Harb. Symp. Quant. Biol.* **LXXVI,** a010439 published in advance (2012).
13. Houtkooper, R.H., Cantó, C., Wanders, R.J., *et al. Endocr. Rev.* **31(2),** 194-223 (2010).
14. Rasler, M., Michel, S., and Breitenbach, M. *Front. Pharmacol.* **3,** article 32 (2012).
15. Price, N.L., Gomes, A.P., Ling, A.J.Y., *et al Cell Metab.* **15,** 675-690 (2012).
16. Park, S-J., Ahmad, F., Philip, A., *et al. Cell* **148**, 421-433 (2012).

Cortisol

Cortisol is a glucocorticoid produced by the adrenal cortex in response to adrenocorticotropic hormone (ACTH). It is secreted with a circadian periodicity, and peaks just prior to waking in the morning. Cortisol is often elevated in major depressive disorder, certain forms of hypertension, stress, AIDS, and in the visceral fat of obese individuals. Cortisol can be measured in many matrices including blood, urine, and saliva. In serum, approximately 90-95% of cortisol is bound to proteins. Urinary cortisol is not bound to proteins, but its levels are dependent on glomerular and tubular function. In saliva, approximately 67% of cortisol is unbound. There is generally good correlation between cortisol measurements in saliva and serum.

Cortisol EIA Kit 500360

Stability: ≥1 year at -20°C
Sensitivity: 50% B/B_0: 180 pg/ml • 80% B/B_0: 35 pg/ml
Summary: Cayman's Cortisol EIA Kit is a competitive assay that can be used for quantification of cortisol in urine, plasma, and other sample matrices.
Specificity:
For a full specificity profile, please go to www.caymanchem.com

96 solid wells
96 strip wells
480 solid wells
480 strip wells

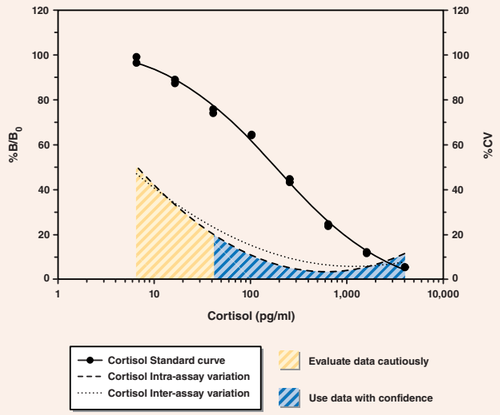

Coenzyme A Assay Kit 700440

CoA
Stability: ≥6 months at -20°C
Summary: Coenzyme A (CoA) is an indispensible cofactor in all living organisms, functioning as an acyl group carrier and carbonyl-activating group in a number of key biochemical reactions, including the TCA cycle and fatty acid metabolism. CoA is involved in over 100 different reactions in intermediary metabolism with approximately 4% of known enzymes utilizing CoA as a cofactor. Cayman's Coenzyme A Assay Kit can be used for assaying coenzyme A from plasma, serum, urine, cell lysates, and tissue homogenates. In this assay, CoA forms a fluorescent complex with europium chloride and tetracycline in the presence of periodic acid.

96 wells

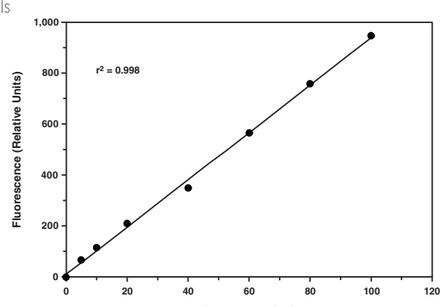

Cortisol Express EIA Kit 500370

Stability: ≥1 year at -20°C
Sensitivity: 50% B/B_0: 400 pg/ml • 80% B/B_0: 110 pg/ml
Summary: Cayman's Cortisol Express EIA is a competitive assay that permits the rapid measurement of cortisol from biological samples, requiring only a two hour incubation and one hour development times. This EIA offers the convenience of a fast assay while maintaining sensitivity.
Specificity: Refer to Cortisol EIA Kit (Item No. 500360)

96 solid wells
96 strip wells
480 solid wells
480 strip wells

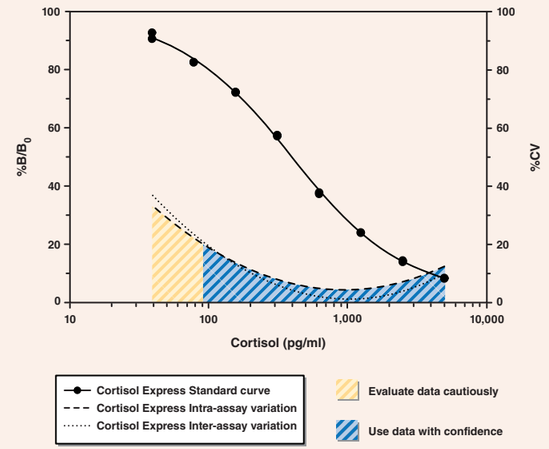

CTRP3 (human) EIA Kit 580200

Complement C1q TNF-related Protein 3
Stability: ≥6 months at 4°C **Limit of detection:** 10 ng/ml
Summary: CTRP3 is a glycoprotein secreted by adipocytes and leukocytes that has important roles in morphogenesis, metabolism, and cell function. It is induced during chondrogenic differentiation, contributing to bone and cartilage differentiation and angiogenesis *via* ERK1/2 signaling and has been shown to suppress hepatic glucose output *via* inhibition of gluconeogenesis and to lower blood glucose levels in both normal and *ob/ob* mice. Cayman's CTRP3 (Human) EIA Kit is a competitive assay which can be used to measure CTRP3 in human serum, plasma, or cell culture supernatants.
Specificity:
For a full specificity profile, please go to www.caymanchem.com

1 ea

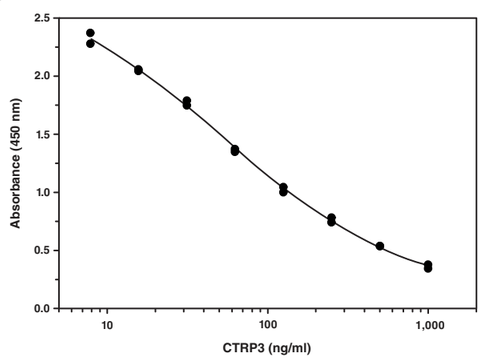

CTRP5 (human) EIA Kit 580120

C1QTNF, C1q tumor necrosis factor-α-related protein 5
Stability: ≥6 months at 4°C **Limit of detection:** 2.3 ng/ml
Summary: CTRP5 is a member of the C1q/tumor necrosis factor superfamily. Mutations in this gene are associated with late-onset retinal degeneration. CTRP5 is also abundantly expressed in adipose tissue and circulates in the blood. It is secreted as a glycoprotein, initially forming trimers then higher order oligomeric complexes. Extracellular, recombinant CTRP5 is a potent activator of AMPK, leading to increased cell surface recruitment of GLUT4 and increased glucose uptake. Serum CTRP5 levels are significantly elevated in obese or diabetic mice. Cayman's CTRP5 (Human) EIA Kit is a competitive assay which can be used to measure CTRP5 in human serum or plasma.
Specificity:
For a full specificity profile, please go to www.caymanchem.com

1 ea

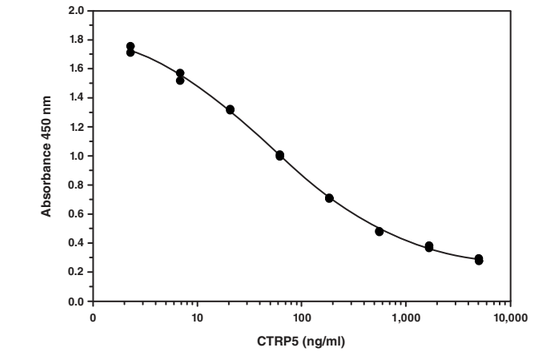

DPP (IV) Inhibitor Screening Assay Kit 700210

Stability: ≥1 year at -80°C
Summary: DPP (IV) inhibitors have emerged as a new class of oral antidiabetic agents. These inhibitors promote glucose homeostasis by inhibiting degradation of glucose-dependent insulinotropic polypeptide and glucagon-like peptide-1 (GLP-1) by DPP (IV). GLP-1 extends the action of insulin while suppressing the release of glucagon. Cayman's DPP (IV) Inhibitor Screening Assay provides a convenient fluorescence-based method for screening DPP (IV) inhibitors in a 96-well format.

96 wells

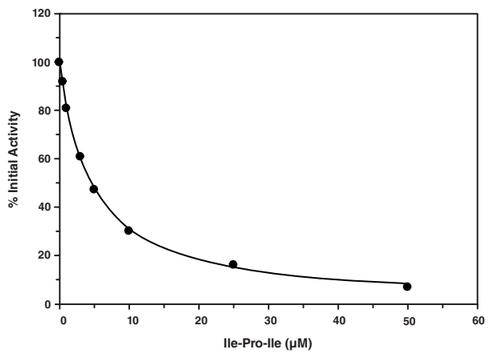

FABP4 (human) EIA Kit† 10007614

Adipocyte FABP, A-FABP, aP2
Stability: ≥6 months at 4°C **Limit of Detection:** 0.1 ng/ml
Summary: FAPB4 is a 15 kDa member of the intracellular FABP family, which is known for the ability to bind fatty acids and related compounds (bile acids or retinoids). FABP4 is expressed in a differentiation-dependent fashion in adipocytes and is a critical gene in the regulation of the biological function of these cells. This EIA uses a plate coated with a goat polyclonal antibody against human FABP4. Detection of bound FABP4 is achieved with biotin-labeled anti-human FABP4 polyclonal and streptavidin-HRP.
Specificity:
For a full specificity profile, please go to www.caymanchem.com

96 wells

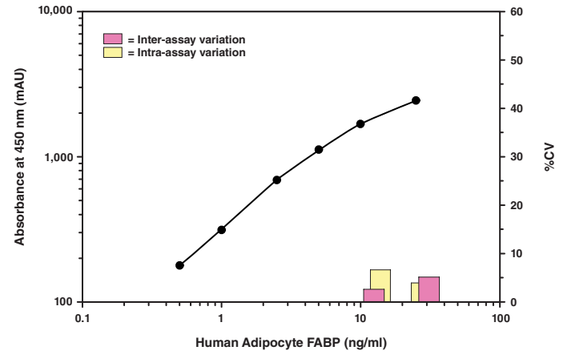

FABP4 Inhibitor/Ligand Screening Assay Kit 10010231

Adipocyte FABP, A-FABP, aP2
Stability: ≥1 year at -80°C
Summary: Cayman's FABP4 Ligand Binding Assay provides a sensitive method for the identification of FABP4 ligands. The assay makes use of a detection reagent that exhibits increased fluorescence when bound to FABP4. Any strong ligand and/or inhibitor of FABP4 will displace the detection reagent thereby reducing the fluorescence.

1 ea

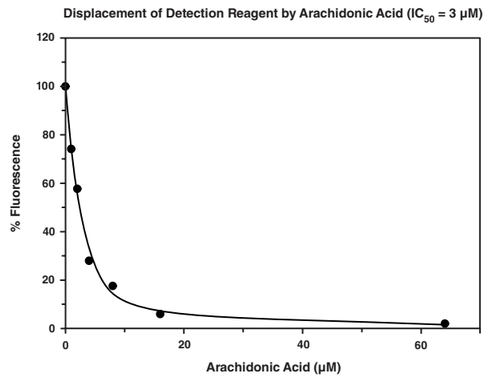

† *SPI-BIO Assays are available through Cayman Chemical only within North & South America and Asia; elsewhere contact Bertin Pharma.*

Free Fatty Acid Assay Kit 700310

FFA

Stability: ≥6 months at -20°C

Summary: The measurement of FFA can be useful in determining metabolic status. Cayman's FFA Assay can be used for measuring free fatty acids in plasma, serum, and urine. The FFA Assay utilizes a coupled enzymatic reaction that results in generation of the highly fluorescent product resorufin.

96 wells

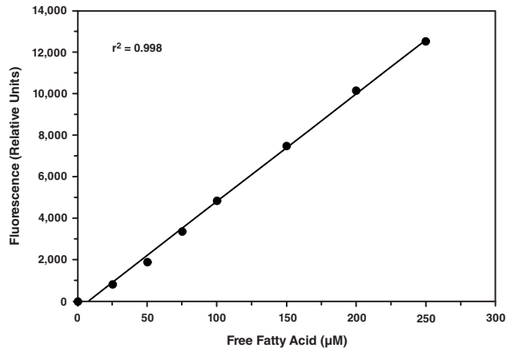

Fructose Fluorometric Assay Kit 700690

Stability: ≥6 months at -20°C

Summary: Fructose is a dietary monosaccharide directly absorbed into the bloodstream during digestion. Excess fructose consumption leads to various complications related to metabolic syndrome as well as contributes to the development of non-alcoholic fatty liver disease. Cayman's Fructose Fluorometric Assay provides a fluorescence-based method for detecting fructose in plasma, serum, urine, tissue homogenates, and cell lysates.

96 wells

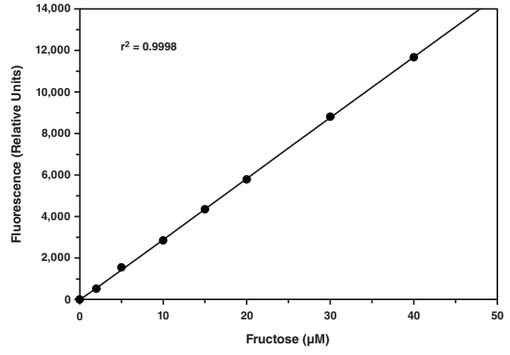

FTO

Fat Mass and Obesity-Associated Gene (FTO) is abundantly expressed in most organs. The gene product is an AlkB-like DNA/RNA demethylase with a strong preference for single stranded DNA and RNA. Single nucleotide polymorphisms in the first intron of the FTO gene contribute to childhood obesity and severe adult obesity. Knockout or loss-of-function of FTO produces an autosomal-recessive lethal syndrome with multiple malformations and severe growth retardation. FTO is the first locus unequivocally associated with adiposity, with activity within the central nervous system apparently regulating feeding behavior and energy expenditure.

FTO (intracellular; human) EIA Kit 579010

Fat Mass and Obesity-Associated Gene

Stability: ≥6 months at 4°C **Limit of detection:** 50 pg/ml

Summary: Cayman's FTO (intracellular; human) EIA Kit is an immunometric (*i.e.*, sandwich) assay which can be used to measure FTO in human cell lysates.

Specificity:

FTO (human)	100%

96 wells

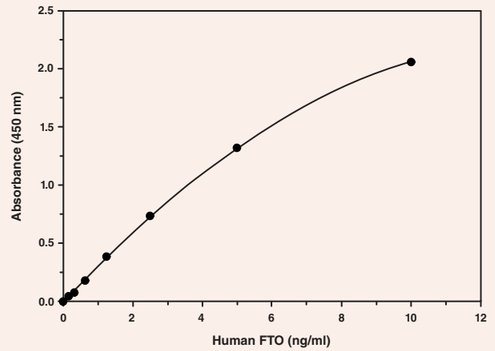

FTO (intracellular; mouse) EIA Kit 579060

Fat Mass and Obesity-Associated Gene

Stability: ≥6 months at 4°C **Limit of detection:** 20 pg/ml

Summary: Cayman's FTO (intracellular; mouse) EIA Kit is an immunometric (*i.e.*, sandwich) assay which can be used to measure FTO in mouse cell lysates.

Specificity:

FTO (mouse)	100%

96 wells

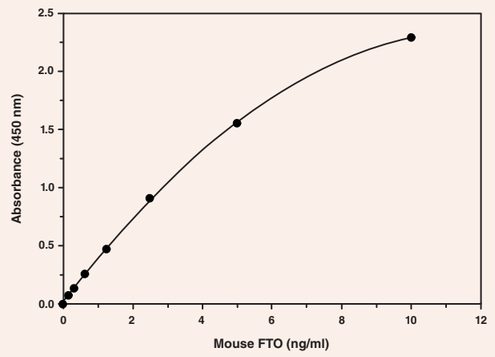

Ghrelin

Ghrelin, an endogenous ligand for the growth hormone secretagogue receptor, is synthesized principally in the stomach. It stimulates food intake and transduces signals to the hypothalamic regulatory nuclei that control energy homeostasis. The peptide consists of 28 amino acids with an octanoylation site at the serine-3 residue. Ghrelin is present in the peripheral circulation in acylated (octanoylated) and non-acylated forms in which the acylated form is biologically active. All of the kits below are based on a double-antibody sandwich technique designed to measure either the acylated or non-acylated forms of the peptide.

Ghrelin (human acylated) EIA Kit† 10006306

Stability: ≥6 months at -20°C

Limit of Detection: 1.5 pg/ml after 20 hour immunological incubation
4 pg/ml after 3 hour immunological incubation

Summary: This EIA kit specifically measures the acylated form of ghrelin.

Specificity:

Ghrelin (human)	100%
Ghrelin (rat)	118%

For a full specificity profile, please go to www.caymanchem.com

96 wells

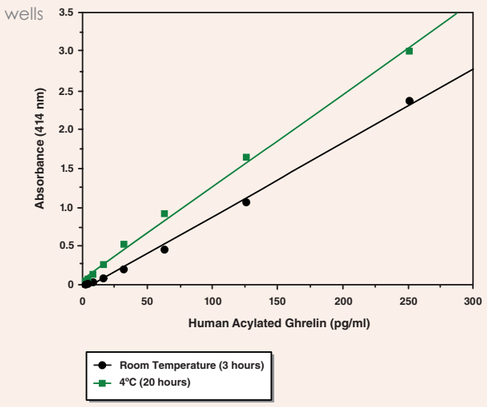

•Also Available: **Ghrelin (human unacylated) EIA Kit†** (10008952)

Ghrelin (rat acylated) EIA Kit† 10006307

Stability: ≥6 months at -20°C

Limit of Detection: 1 pg/ml after 20 hour immunological incubation
3.5 pg/ml after 3 hour immunological incubation

Summary: This EIA kit specifically measures the acylated form of ghrelin.

Specificity:

Ghrelin (human)	82%
Ghrelin (rat)	100%

For a full specificity profile, please go to www.caymanchem.com

96 wells

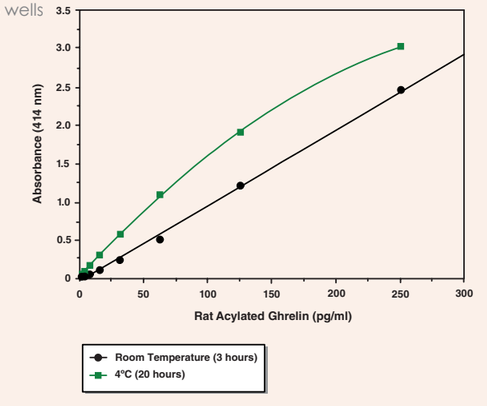

•Also Available: **Ghrelin (rat unacylated) EIA Kit** (10008953)

Glucose Fluorometric Assay Kit 700710

Stability: ≥1 year at -20°C

Summary: Glucose is the primary source of energy for the body's cells. Failure to maintain blood glucose in the normal range leads to conditions of hypoglycemia or hyperglycemia, such as diabetes mellitus. Cayman's Glucose Fluorometric Assay can be used to accurately quantify glucose in plasma, serum, and urine. This assay uses a glucose oxidase - peroxide reaction system to produce the highly fluorescent compound resorufin.

96 wells

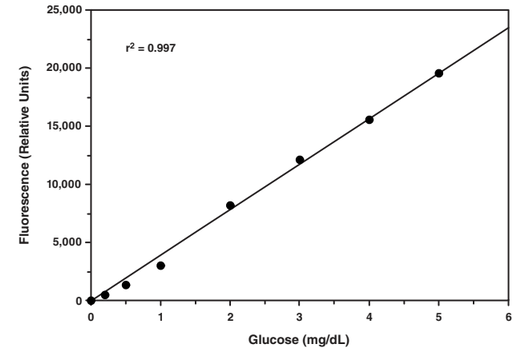

•Also Available: **Glucose Colorimetric Assay Kit** (10009582)

Glucose-6-Phosphate Dehydrogenase Activity Assay Kit 700300

G6PDH

Stability: ≥6 months at -20°C

Summary: G6PDH is a cytosolic enzyme that catalyzes the first step in the pentose phosphate pathway. G6PDH deficiency, the most common enzyme deficiency worldwide, causes a spectrum of diseases including neonatal hyperbilirubinemia, acute hemolysis, and chronic hemolysis. G6PDH activity has been shown to be upregulated in rat and mouse models of obesity, hyperglycemia, and hyperinsulinemia. Cayman's G6PDH Assay provides a fluorescence-based method for detecting G6PDH activity in a variety of samples including erythrocyte lysates, tissue homogenates, and cell culture samples.

96 wells

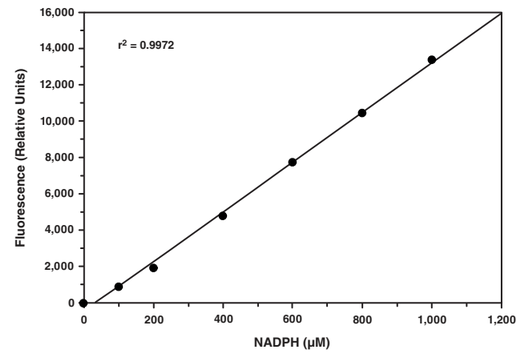

† *SPI-BIO Assays are available through Cayman Chemical only within North & South America and Asia; elsewhere contact Bertin Pharma.*

Glucose Uptake Cell-Based Assay Kit 600470

Stability: ≥6 months at -20°C
Summary: Glucose metabolism is a primary source of energy and biomaterials for the maintenance of cell homeostasis. The rate of glucose uptake in cells is dynamic and tightly regulated by hormones and/or growth factors including insulin. Cancer cells exhibit increased glucose uptake and metabolism by aerobic glycolysis in order to support a high rate of proliferation. Chemicals that block glucose uptake by cancer cells have been shown to have anti-cancer effects. Cayman's Glucose Uptake Cell-based Assay Kit provides a convenient tool for studying modulators of cellular glucose uptake. The kit employs 2-NBDG, a fluorescently-labeled deoxyglucose analog, as a probe for the detection of glucose taken up by cultured cells.

1 ea

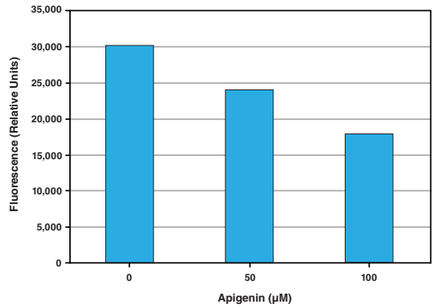

Measurement of 2-NBDG uptake in LS-180 cells grown in glucose- and serum-free medium and treated with various doses of Apigenin.

Glycerol Cell-Based Assay Kit 10011725

Stability: ≥1 year at -20°C
Summary: Cayman's Glycerol Cell-Based Assay provides a convenient tool for studying triglycerides/fatty acid cycling and its regulation in adipocytes or hepatocytes. This kit will allow investigators to screen compounds involved in lipid storage and metabolism. Chloroquine is included in the kit as a positive control for screening pharmaceuticals that induce lipid droplet accumulation and free glycerol release from hepatocytes.

1 ea

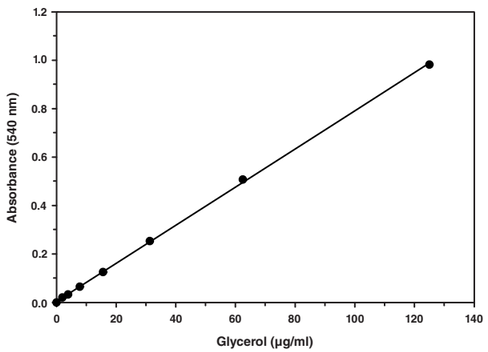

Glycerol Fluorometric Assay Kit 700720

Stability: ≥1 year at -20°C **Limit of Detection:** 0.2 mg/L (±0.05 mg/L)
Summary: Glycerol, the backbone of triglycerides, is an important metabolite in energy metabolism involved in both oxidation and synthetic processes. The measurement of circulating levels of glycerol and free fatty acids are considered to reflect lipolysis, and may be useful to evaluate lipolysis under various conditions in clinical studies. Cayman's Fluorometric Glycerol Assay Kit provides a fluorescence-based method for detecting glycerol in plasma and serum. The Fluorometric Glycerol Assay measures glycerol by a coupled enzymatic reaction system resulting in production of the fluorescent product of resorufin.

96 wells

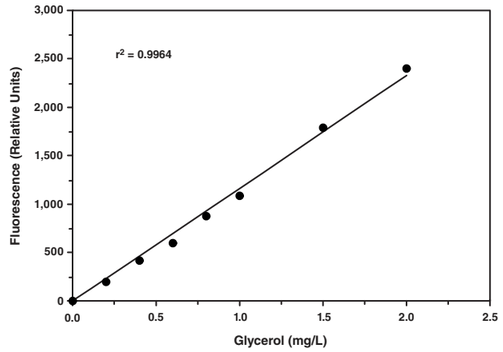

•Also Available: **Glycerol Colorimetric Assay Kit** (10010755)

Glycogen Assay Kit 700480

Stability: ≥6 months at -20°C
Summary: Glycogen is a polysaccharide that is the principal storage form of glucose in animal and human cells. Glycogen is made primarily by the liver and muscles, but it can also be made by glycogenesis within the brain and stomach. Cayman's Glycogen Assay provides a fluorescence-based method to quantify glycogen from tissue.

96 wells

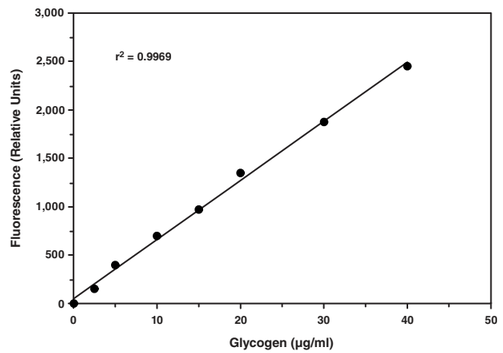

Glycolysis Cell-Based Assay Kit 600450

Stability: ≥6 months at -20°C
Summary: Cayman's Glycolysis Cell-Based Assay Kit provides a colorimetric method for detecting extracellular L-lactate, the end product of glycolysis, in cultured cells. In the assay, lactate dehydrogenase catalyzes the oxidation of lactate to pyruvate, in which the formed NADH reduces a tetrazolium substrate to a highly-colored formazan which absorbs strongly at 490-520 nm. The amount of formazan produced is proportional to the amount of lactate released into the culture medium and can be used as an indicator of the cellular glycolytic rate.

1 ea

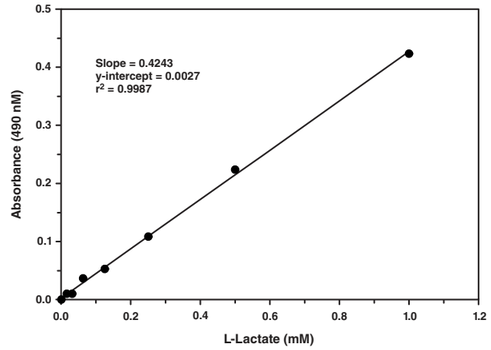

Growth Hormone (rat) EIA Kit† 589601

GH
Stability: ≥6 months at -20°C
Sensitivity: 50% B/B_0: 3.6 ng/ml • 80% B/B_0: 1 ng/ml
Summary: GH is a polypeptide hormone with a molecular weight of 23 kDa released from somatotropes of the anterior pituitary. It is regulated by several neurotransmitters and neuropeptides. Among other functions it plays an essential role in regulating body growth.
Specificity:

Rat Growth Hormone	100%
Mouse Growth Hormone	91%
Rat Prolactin	<1.0%

For a full specificity profile, please go to www.caymanchem.com

96 wells

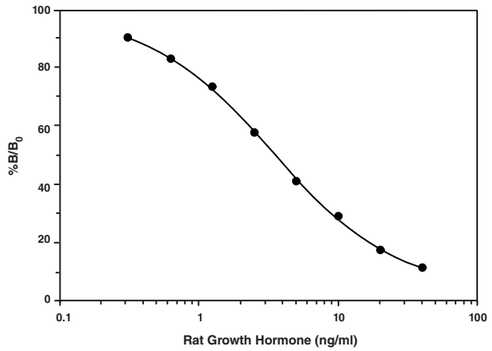

β-Hydroxybutyrate (Ketone Body) Assay Kit 700190

β-HB, 3-Hydroxybutric Acid
Stability: ≥1 year at -20°C
Summary: β-HB is a "ketone body" which is produced in the liver, mainly from the oxidation of fatty acids, and is exported to peripheral tissues for use as an energy source. Normally ketosis can indicate that lipid metabolism has been activated and the pathway of lipid degradation is intact. Cayman's β-HB (Ketone Body) Assay provides an accurate method for measuring β-HB levels in plasma, serum, or urine in a 96-well plate format with a colorimetric readout at 445-455 nm.

96 wells

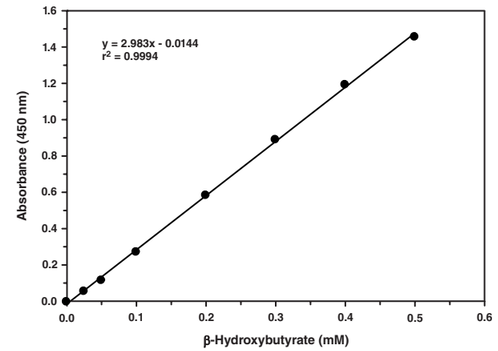

Insulin (rat) EIA Kit† 589501

Stability: ≥6 months at -20°C
Sensitivity: 50% B/B_0: 0.63 ng/ml
Summary: Insulin is a polypeptide hormone synthesized by the β cells of the islets of Langherans of the pancreas. Insulin's best known action is to lower the blood glucose concentration by increasing the rate at which glucose is converted to glycogen in the liver and muscle, and to fat in adipose tissue, by stimulating the rate of glucose metabolism, and by depressing gluconeogenesis.
Specificity:
For a full specificity profile, please go to www.caymanchem.com

96 wells

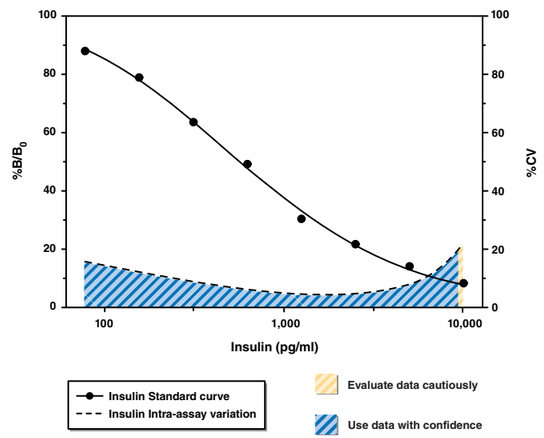

† *SPI-BIO Assays are available through Cayman Chemical only within North & South America and Asia; elsewhere contact Bertin Pharma.*

L-Lactate Assay Kit 700510

Stability: ≥6 months at -20°C
Summary: L(+)-Lactate is the major stereoisomer of lactate formed in human intermediary metabolism. The lactate to pyruvate ratio reflects the redox state of the cell and describes the balance between NAD^+ and NADH, which is dependent on the interconversion of lactate and pyruvate *via* LDH. Monitoring lactate levels is, therefore, a good way to evaluate the balance between tissue oxygen demand and utilization and is useful when studying cellular and animal physiology. Cayman's L-Lactate Assay provides a fluorescence-based method for detecting L-lactate in biological samples such as serum, plasma, blood, urine, and saliva. It can also be utilized to determine intracellular and extracellular lactate concentrations in cell culture samples.

96 wells

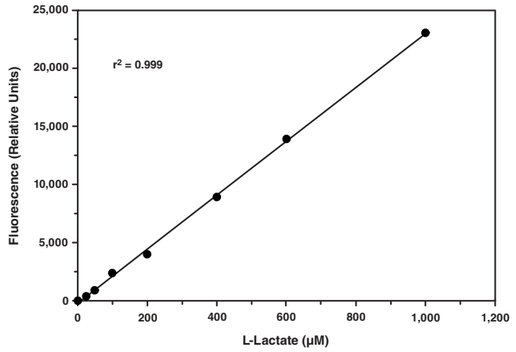

•Also Available: **D-Lactate Assay Kit** (700520)

LDL Uptake Cell-Based Assay Kit 10011125

Stability: ≥6 months at 4°C
Summary: LDL uptake and its regulation are important therapeutic targets for atherosclerosis and related diseases. Cayman Chemical's LDL Uptake Cell-Based Assay employs a preparation of human LDL conjugated to Dylight™ 549 as a fluorescent probe for detection of LDL uptake into cultured cells. A LDL receptor-specific antibody and a Dylight™ 488-conjugated secondary antibody are included in the kit for identifying the distribution of LDL receptors.

1 ea

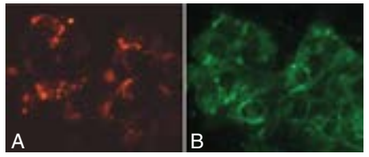

LDL Uptake in HepG2 cells. HepG2 cells were treated with 32 µM EGCG overnight followed by addition of LDL-DyLight™ 549 for four hours. *Panel A:* DyLight™ 549 taken into cells appear in red. *Panel B:* LDL receptors in green.

Leptin

Leptin is a 16 kDa protein hormone encoded by the obese (*ob*) gene with important effects in metabolism and regulation of body weight. Leptin has dual actions, decreasing appetite and increasing energy consumption. The primary effect of leptin appears to be mediated by leptin receptors expressed mainly in the hypothalamus. Mutations in the *ob* gene or leptin receptor gene causes hyperphagia, reduced energy expenditure, and severe obesity. The assays listed below are based on a double-antibody sandwich technique for sensitive measurement of leptin or leptin receptor.

Leptin (human) EIA Kit† 500010

Stability: ≥6 months at 4°C **Limit of Detection:** 0.5 ng/ml
Summary: This EIA is based on a double-antibody sandwich technique. The wells of the plate supplied with the kit are coated with a polyclonal antibody specific of human leptin. This antibody will bind any leptin introduced in the wells (sample or standard).
Specificity:
For a full specificity profile, please go to www.caymanchem.com

96 wells

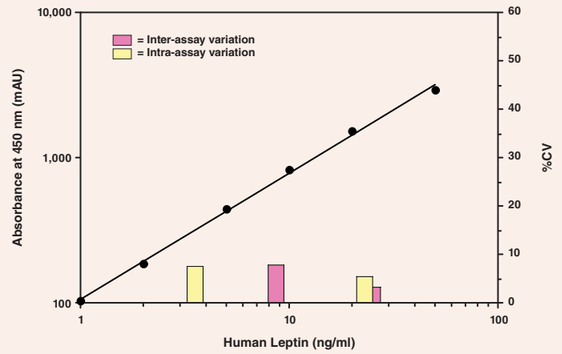

Leptin (mouse/rat) EIA Kit† 10007609

Stability: ≥6 months at 4°C **Limit of Detection:** 50 pg/ml
Summary: This EIA utilizes plates coated with a polyclonal antibody specific for mouse/rat leptin. A biotin-labeled polyclonal antibody and streptavidin-horseradish peroxidase are used for detection.
Specificity:
For a full specificity profile, please go to www.caymanchem.com

96 wells

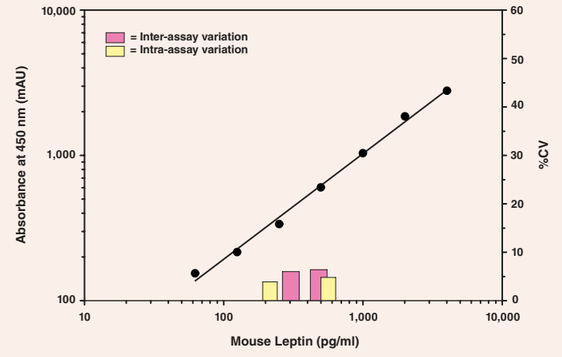

† *SPI-BIO Assays are available through Cayman Chemical only within North & South America and Asia; elsewhere contact Bertin Pharma.*

Leptin Receptor (human) EIA Kit† 10007608

Stability: ≥6 months at 4°C **Limit of Detection:** 0.4 ng/ml
Summary: The assay utilizes plates coated with a monoclonal capture antibody specific for the human leptin receptor and a HRP-conjugated monoclonal antibody for detection.
Specificity:
For a full specificity profile, please go to www.caymanchem.com

96 wells

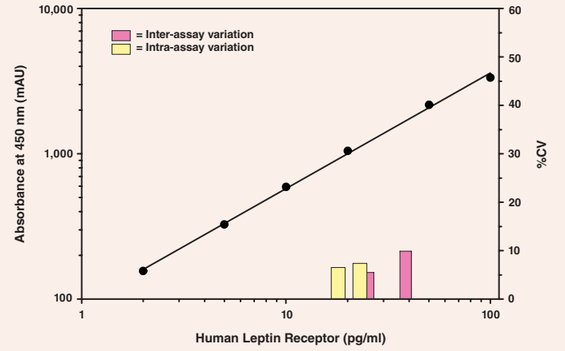

Lipid Droplets Fluorescence Assay Kit 500001

Stability: ≥1 year at -20°C
Summary: Lipid droplets are a fundamental component of intracellular lipid homeostasis in all cell types and they provide a rapidly mobilized lipid source for many important biological processes. Cayman's Lipid Droplets Fluorescence Assay can be used to study regulators of lipid droplet biogenesis. The main advantage of this assay is that the green fluorescence of Nile Red is both very sensitive and specific for lipid droplets.

480 tests

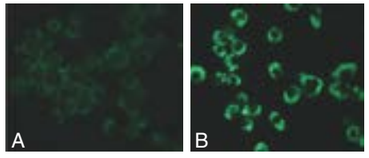

Oleic Acid dramatically induces lipid droplet accumulation in neuro-2a cells. Neuro-2a cells were treated with vehicle (*control*, *Panel A*) or 400 µM oleic acid *(treated*, *Panel B)* for 24 hours and then processed for lipid droplet staining.

Melanocortin-3 Receptor STEP Reporter Assay Kit (Luminescence) 600180

MC3R
Stability: ≥1 year at -20°C
Summary: MC3R helps regulate energy homeostasis and mice lacking MC3R have increased fat mass and reduced lean mass. Therefore, agonists that selectively activate MC3R might have beneficial effects related to weight gain and glucose metabolism. This assay consists of a 96-well plate coated with both MC3R and SEAP reporter constructs. Cells grown on the STEP complex will express MC3R at the cell surface. Binding of agonists to MC3R initiates a signaling cascade resulting in expression of SEAP. SEAP activity is measured following addition of a luminescence-based alkaline phosphatase substrate provided in the kit.

100 tests

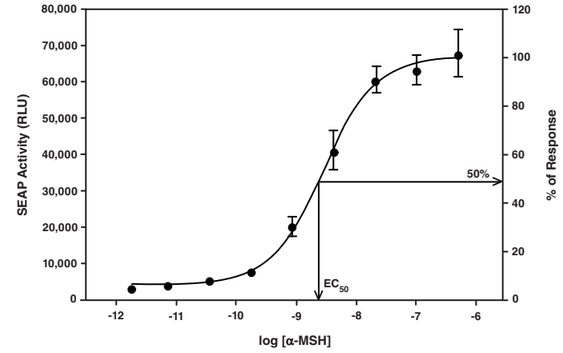

Melanocortin-4 Receptor STEP Reporter Assay Kit (Luminescence) 600190

MC4R
Stability: ≥1 year at -20°C
Summary: MC4R has important roles in weight regulation, sexual function, and inflammation. Mice deficient in MC4R have increased lipid deposition associated with elevated adiposity, while mutations in MC4R in humans are associated with early onset or severe obesity. This assay consists of a 96-well plate coated with both MC4R and SEAP reporter constructs. Cells grown on the STEP complex will express MC4R at the cell surface. Binding of agonists to MC4R initiates a signaling cascade resulting in expression of SEAP. SEAP activity is measured following addition of a luminescence-based alkaline phosphatase substrate provided in the kit.

100 tests

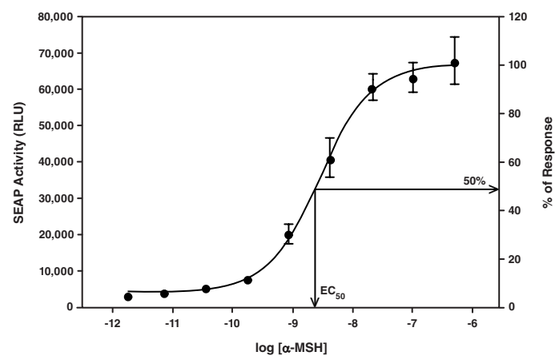

† *SPI-BIO Assays are available through Cayman Chemical only within North & South America and Asia; elsewhere contact Bertin Pharma.*

vol. 16 Me

Thomas G. Brock, Ph.D.

The PPARα Story

When peroxisomes were first studied, in the 1960's, as a subcellular organelle similar in structure to lysosomes, they were found to consume oxygen to initiate the metabolism of long chain fatty acids through β-oxidation. Additionally, peroxisomes use molecular oxygen to enzymatically produce hydrogen peroxide, which, with peroxidase, is used to oxidize a variety of substrates, including alcohols and toxic compounds. Excess hydrogen peroxide is decomposed by peroxisomal catalase. While peroxisomes may be found in many cells and tissues, they are particularly important in the liver and kidney.

Peroxisomes can multiply prior to cell division, doubling in number so that mother and daughter cells have a full complement.[1] More relevant to this article, peroxisomes can form *de novo* while a cell is in interphase. Specific peroxisomal membrane proteins are synthesized in the endoplasmic reticulum (ER), with pre-peroxisomes budding off from the ER to form immature organelles. These may fuse with each other or with mature peroxisomes, while enlarged mature peroxisomes may undergo fission to generate smaller peroxisomes. Lumenal (matrix) proteins and additional membrane proteins are imported from the cytoplasm directly into peroxisomes.[1]

As peroxisomal proliferation can coincide with mitosis and excess cell division is a hallmark of cancer, there was early interest that compounds that promoted peroxisomes to multiply might be associated with carcinogenesis. Moreover, it was known that clofibrate, a compound with lipid-lowering properties, causes enlargement of the liver (hepatomegaly) in rats that is associated with a profound increase in the number of peroxisomes in liver cells. Another lipid-lowering drug that causes peroxisomal proliferation, nafenopin, was found to cause hepatocellular carcinomas in mice with acatalasemia (a genetic disorder leading to a deficiency of catalase in erythrocytes) but not in wild type mice.[2] In the 1980's, concern moved from therapeutics to environmental factors when various phthalate and adipate esters, used as industrial plasticizers, were discovered to be peroxisome proliferator carcinogens in mice and rats.[3] None of these compounds were found to directly cause DNA damage, the prevalent modus operandi for known carcinogens at the time. By and large, it was thought that an overabundance of peroxisomes could lead to the generation of oxygen radicals, which then would produce the DNA damage necessary for carcinogenesis. Today, with a deeper understanding of how these compounds work, it is understood that normal proliferation of peroxisomes, like normal cell proliferation, does not cause cancer. Instead, it is only with dysfunctional signaling that pathologies occur. In fact, enhanced peroxisomal proliferator signaling is, for some diseases, therapeutic.

The First Peroxisome Proliferator-Activated Receptor

By the end of the 1980's, it was known that clofibrate, phthalate esters, and other compounds that caused dramatic proliferation of hepatic peroxisomes as well as liver hyperplasia also increased transcription of genes required for the peroxisomal β-oxidation of long chain fatty acids and genes of the cytochrome p450 IV family. Narendra Lalwani had discovered a clofibrate- and nafenopin-binding protein in rat liver, suggesting that peroxisome proliferators might act *via* soluble receptors, like steroid hormones.[4] In 1990, Isabelle Issemann and Stephen Green reported the cloning of a novel member of the steroid hormone receptor superfamily that was activated by peroxisome proliferators.[5] This protein, named a peroxisome proliferator activated receptor (PPAR), had a DNA-binding domain (DBD) with high sequence identity (46-64%) with known nuclear receptors (Figure 1). A distinct putative ligand-binding domain (LBD) shared highest identity (38%) with the human *erb*-A-related (ear) receptor hear1. Highest expression of the PPAR message was found in liver, kidney, and heart, with very weak expression in brain and testis. Expression was also reported to occur in brown adipose tissue. Chimeric reporters engineered to combine the putative ligand-binding domain of this new receptor with DNA-binding domains of either the estrogen receptor or the glucorticoid receptor, were used to show that hypolipidemic peroxisome proliferators, including nafenopin, clofibrate, and phthalate esters, activated gene expression as expected. Thus, the first PPAR, later renamed PPARα, was discovered.

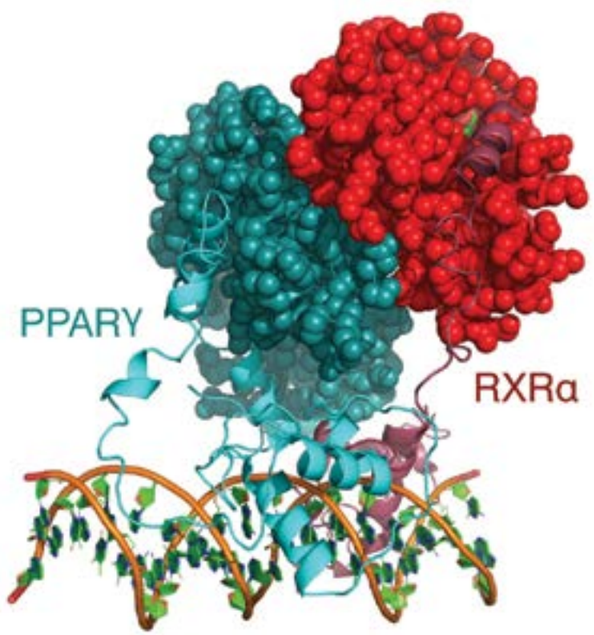

Figure 1. PPARγ (cyan) associated with RXRα (red) bound to DNA. Note the DBDs (helices) fill major grooves on opposite sides of the DNA double helix and the LBDs (displayed in space-filling mode) overlap. From RCSB 3DZY[17]

PPARα is activated by a diverse array of compounds (refer to Table). Importantly, some agonists are specific for this isoform, whereas some also activate PPARβ/δ and/or PPARγ. While receptor activation causes peroxisome proliferation and hepatomegaly in mice and rats, this does not happen in non-rodent (including human) species. Similarly, PPARα agonists, including the fibrates, do not increase the incidence of liver cancer in humans. In fact, lipid-lowering drugs that act through PPARα, including the fibrates gemfibrozil and fenofibrate, have been used for years and their side effects are well-known (and are unique for each drug). For example, gemfibrozil causes a slight but significant increase in gastrointestinal reactions, while fenofibrate may adversely impact liver function tests. In exchange for these potential complications, PPARα activators potently decrease fatty acid and triglyceride levels. They are commonly used in combination with statins, which lower cholesterol by interfering with the cholesterol biosynthetic pathway. While fibrates are best known to stimulate the β-oxidation of long chain and very long chain fatty acids by peroxisomes for the treatment of hyperlipidemia, they are also used to correct atherogenic dyslipidemia in the context of obesity, diabetes, and coronary heart disease.[6] Also, clofibrate has recently been shown to prevent nicotine reward and relapse in rats and squirrel monkeys, suggesting that fibrate medications might promote smoking cessation.[7] Remarkably, although fibrates activate PPARα, direct binding has not been demonstrated.[6] Moreover, clofibrate activates peroxisomal proliferation in plants like *Arabidopsis thaliana*, although *Arabidopsis* lacks a PPARα homolog.[8]

Compound	Murine Receptor EC_{50} (μM) PPARα	PPARα	PPARα/α	Human Receptor EC_{50} (μM) PPARα	PPARα	PPARα/α
WY-14643†	0.63	32	na	5.0	60	35
clofibrate†	50	~500	na	55	~500	na
fenofibrate†	18	250	na	30	300	na
bezafibrate†	90	55	110	50	60	20
GW 9578†	0.005	1.5	2.6	0.05	1.0	1.4
troglitazone†	na	0.78	na	na	0.55	na
pioglitazone†	na	0.55	na	na	0.58	na
rosiglitazone†	na	0.076	na	na	0.043	na
CAY10573†				8	70	500
CAY10599†				4.0	0.05	na
GW 0742†				1.1	2.0	0.001
GW 9578†	0.005	0.15	2.6	0.05	1.0	1.4
GW 7647†	0.001	1.3	2.9	0.006	1.1	6.2
GW 590735†				0.004	2.83	na
CAY10514†				0.173	0.642	

Table. Activity of various PPAR agonists in cell-based transactivation assays.[16] na = not active; †available from Cayman

Nuts and Bolts

As noted earlier, PPARs contain distinct domains for DNA and ligand binding. These domains are separated by a stretch of over 100 aa. The amino terminus, referred to as activation function-1 (AF-1), is thought to have a transactivation function, folding back above the DBD to stabilize heterocomplex formation between the LBD and associating proteins. The large (189 aa) LBD contains a leucine zipper region of some 130 aa that is required for heterodimerization of PPARα with retinoic acid receptor-α (RXRα). RXRα similarly contains a DBD and LBD separated by a hinge region (Figures 1,2). In the classical model of PPARα signaling, PPARα is heterodimerized with RXRα on a PPAR response element (PPRE) consisting of direct repeats of AGGTCA separated by a single intervening nucleotide; this direct repeat PPRE is called DR-1 and is one of several that bind RXRα heterodimers.

In the absence of ligand, the PPARα-RXRα dimer associates with a multiprotein complex that blocks the initiation of transcription, including nuclear receptor corepressors (*e.g.,* NCoR1, SMRT), histone deacetylases (HDACs, SIRTs), and G protein pathway suppressor 2. The addition of ligand leads to dissociation of the corepressor complex followed by the recruitment of coactivators, such as PPAR coactivator-1 and the histone acetyltransferases p300 and CREB binding protein. Formation of the PPAR activation complex leads to histone modification (*e.g.,* through acetylation), chromatin relaxation, and altered gene expression. PPARα affects gene expression relevant to altered lipid metabolism, lowering triglycerides and raising high-density lipoprotein in dyslipidemia (see related article on page 4). Natural ligands for PPARα include certain fatty acids, including metabolites of arachidonic acid, (*e.g.*, leukotriene B_4).[9]

Evidence suggests that PPARs can act in other ways. PPARα can directly interact with numerous proteins other than RXRα and this can occur in either the cytoplasm or nucleus. For example, PPARα binds directly to c-Jun and p65,[10] proteins which, like PPARα, heterodimerize with other proteins to form functional transcription factors. These interactions prevent each transcription factor from acting. For example, PPARα binding to p65 prevents NF-κB-mediated expression of such genes as iNOS, COX-2, and IL-6, thus diminishing pro-inflammatory signaling. PPARα also forms DNA-binding heterodimers with other nuclear receptors, such as thyroid hormone receptor (TR) and liver X receptor (LXR), to alter gene expression. Notably, RXRα can also partner with nuclear receptors, including TR and vitamin D3 receptors. This competitively prevents signaling through PPARα.

Additional information is available in recent reviews.[11-15]

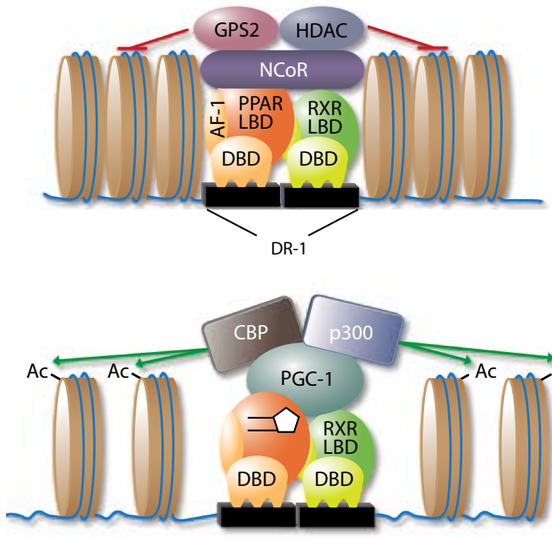

Figure 2. The classical model of PPAR-RXR signaling, showing the PPAR-RXR corepressor complex (above) and the PPAR-RXR coactivator complex after ligand binding (below)

References

1. Hettema, E.H. and Motley, A.M. *J. Cell Sci.* **122,** 2331-2336 (2009).
2. Reddy, J.K., Rao, M.S., and Moody, D.E. *Cancer Res.* **36,** 1211-1217 (1976).
3. Kluwe, W.M. *Environ. Health Perspect.* **65,** 271-278 (1986).
4. Lalwani, N.D., Alvares, K., Reddy, M.K., *et al. Proc. Natl. Acad. Sci. USA* **84,** 5242-5246 (1987).
5. Issemann, I. and Green, S. *Nature* **347,** 645-650 (1990).
6. Pahan, K. *Cell Mol. Life Sci.* **63(10),** 1165-1178 (2006).
7. Panlilio,L.V., Justinova,Z., Mascia,P, *et al. Neuropsychopharmacology* (2012).
8. León, J. *Plant Signal. Behav.* **3(9),** 671-673 (2008).
9. Murakami, K., Ide, T., Suzuki, M., *et al. Biochem. Biophys. Res. Commun.* **260,** 609-613 (1999).
10. Delerive, P., De Bosscher, K., Besnard, S., *et al. J. Biol. Chem.* **274(45),** 32048-32054 (1999).
11. Ament,Z., Masoodi,M., and Griffin,J.L. *Genome Med.* **4,** (2012).
12. Choi, J.-M. and Bothwell, A.L.M. *Mol. Cells* **33,** 217-222 (2012).
13. Nagy,L., Szanto,A., Szatmari,I., *et al. Physiol. Rev.* **92,** 739-789 (2012).
14. Neher,M.D., Weckbach,S., Huber-Lang,M.S., *et al. PPAR Res.* **2012,** 1-13 (2012).
15. Thomas, M.C., Jandeleit-Dahm, K.A., and Tikellis, C. *PPAR Res.* **2012,** 1-10 (2012).
16. Willson, T.M., Brown, P.J., Sternbach, D.D., *et al. J. Med. Chem.* **43(4),** 528-550 (2000).
17. Chandra, V., Huang, P., Hamuro, Y., *et al. Nature* **456(7220),** 350-356 (2008).

Nampt

Nampt is the rate-limiting enzyme in the salvage pathway for the biosynthesis of NAD^+ from nicotinamide. Nampt was first described as a pre-B-cell colony enhancing factor. It was later named visfatin, as it was found to be highly enriched in visceral fat, with plasma levels increasing with obesity. The levels of Nampt in serum correlate with body mass index and body fat mass, are increased during inflammation, and are decreased with liver cirrhosis. Extracellular Nampt regulates insulin secretion in β cells by regulating systemic NAD^+ biosynthesis. Nampt levels and expression in serum, circulating leukocytes, and tissues may be useful biomarkers for inflammation, cancer, obesity, and other diseases.

Nampt/Visfatin (human) EIA Kit 579020

Nicotinamide Phosphoribosyltransferase/Visfatin

Stability: ≥6 months at 4°C **Limit of detection:** 30 pg/ml

Summary: Cayman's Nampt/Visfatin (human) EIA Kit is an immunometric assay which can be used to measure Nampt/Visfatin in human serum.

Specificity:

Visfatin (human)	100%

96 wells

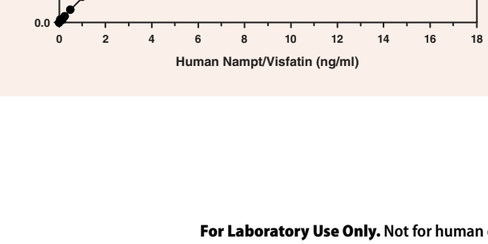

Nampt/Visfatin (intracellular; human) EIA Kit 579030

Nicotinamide Phosphoribosyltransferase/Visfatin

Stability: ≥6 months at 4°C **Limit of detection:** 30 pg/ml

Summary: Cayman's Nampt/Visfatin (intracellular; human) EIA Kit is an immunometric assay which can be used to measure Nampt/Visfatin in human cell lysates.

Specificity:

Visfatin (human)	100%

96 wells

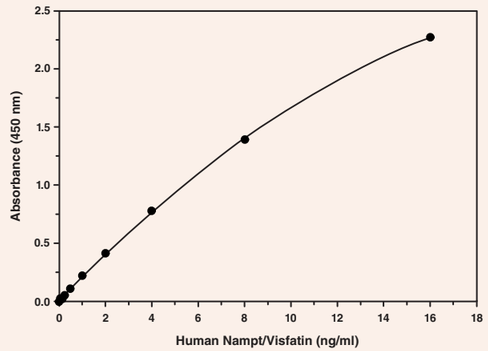

Nampt/Visfatin (mouse/rat) EIA Kit 579040

Nicotinamide Phosphoribosyltransferase/Visfatin

Stability: ≥6 months at 4°C **Limit of detection:** 0.5 pg/ml

Summary: Cayman's Nampt/Visfatin (mouse/rat) EIA Kit is an immunometric assay which can be used to measure Nampt/Visfatin in mouse or rat serum.

Specificity:

Mouse Nampt/Visfatin (mouse)	100%
Mouse Nampt/Visfatin (rat)	100%

96 wells

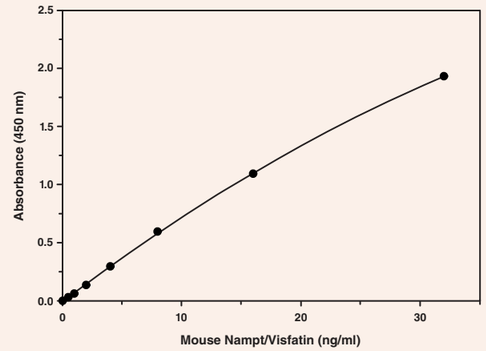

Nampt/Visfatin (intracellular; mouse/rat) EIA Kit 579050

Nicotinamide Phosphoribosyltransferase/Visfatin

Stability: ≥6 months at 4°C **Limit of detection:** 0.5 pg/ml

Summary: Cayman's Nampt/Visfatin (intracellular; mouse/rat) EIA Kit is an immunometric assay which can be used to measure Nampt/Visfatin in mouse or rat cell lysates.

Specificity:

Mouse Nampt/Visfatin (mouse)	100%
Mouse Nampt/Visfatin (rat)	100%

96 wells

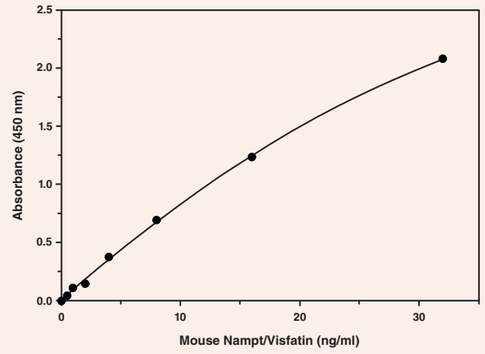

NAD^+/NADH Cell-Based Assay Kit 600480

Nicotinamide adenine dinucleotide/Nicotinamide adenine dinucleotide, reduced

Stability: ≥6 months at -20°C

Summary: NAD exists in an oxidized form, NAD^+, as well as a reduced form, NADH. NAD^+, the main free form in cells, functions in modulating cellular redox status and by controlling signaling and transcriptional events, making it and related enzymes drug targets for various metabolic disorders. Cayman's NAD^+/NADH Cell-Based Assay Kit provides a colorimetric method for measuring intracellular NAD^+/NADH in culture cells. In the assay, alcohol dehydrogenase catalyzes the oxidation of alcohol to acetoaldehyde, in which the formed NADH reduces a tetrazolium salt substrate to a highly-colored formazan which absorbs strongly at 450 nm. The amount of formazan produced is proportional to the amount of NAD^+ in the cell lysate and can be used as an indicator of the cellular NAD^+ concentration.

1 ea

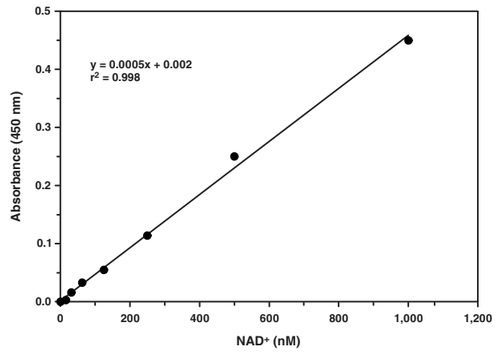

Orexin 1 Receptor STEP Reporter Assay Kit (Luminescence) 600240

OX1R

Stability: ≥1 year at -80°C

Summary: OX1R may be an important therapeutic target for treatment of sleep disorders, obesity, emotional stress, and addiction. This assay consists of a 96-well plate coated with both OX1R and SEAP reporter constructs. Cells grown on the STEP complex will express OX1R at the cell surface. Binding of agonists to OX1R initiates a signal transduction cascade resulting in expression of SEAP. SEAP activity is measured following addition of a luminescence-based alkaline phosphatase substrate provided in the kit.

100 tests

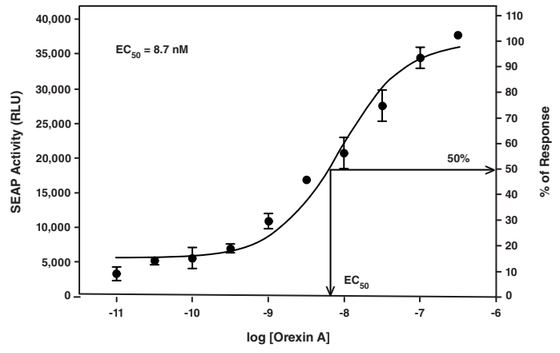

Orexin 2 Receptor STEP Reporter Assay Kit (Luminescence) 600250

OX2R

Stability: ≥1 year at -80°C

Summary: OX2R may be an important therapeutic target for treatment of sleep disorders, obesity, emotional stress, and addiction. This assay consists of a 96-well plate coated with both OX2R and SEAP reporter constructs. Cells grown on the STEP complex will express OX2R at the cell surface. Binding of agonists to OX2R initiates a signal transduction cascade resulting in expression of SEAP. SEAP activity is measured following addition of a luminescence-based alkaline phosphatase substrate provided in the kit.

100 tests

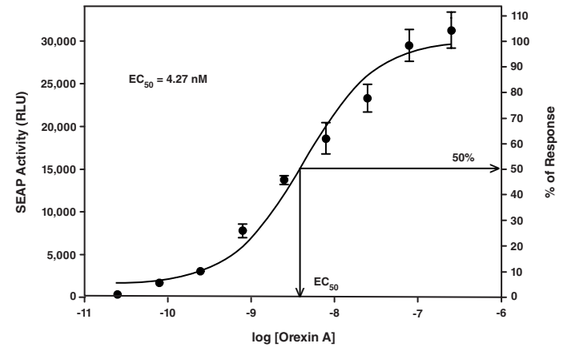

PPAR Transcription Factor Assay Kits

PPARs are ligand-activated transcription factors belonging to the large superfamily of nuclear receptors. PPARα primarily activates genes encoding proteins involved in fatty acid oxidation, while PPARγ primarily activates genes directly involved in lipogenic pathway and insulin signaling. Members of the PPAR family are important direct targets of many antidiabetic and hypolipidemic drugs. Cayman's PPAR Transcription Factor Assays are a non-radioactive, sensitive method for detecting specific transcription factor DNA binding activity in nuclear extracts and whole cell lysates.

PPARα, δ, γ Complete Transcription Factor Assay Kit 10008878

Stability: ≥1 year at -80°C

Summary: A 96-well assay for measurement of PPARα, δ, γ DNA binding activity

96 wells

PPARα Transcription Factor Assay Kit 10006915

Stability: ≥6 months at -80°C

Summary: A 96-well assay for measurement of PPARα DNA binding activity

96 wells

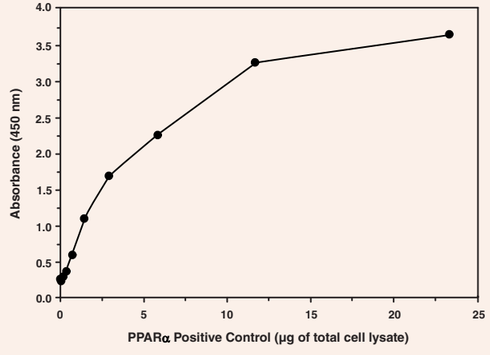

PPARδ Transcription Factor Assay Kit 10006914

Stability: ≥6 months at -80°C
Summary: A 96-well assay for measurement of PPARδ DNA binding activity

96 wells

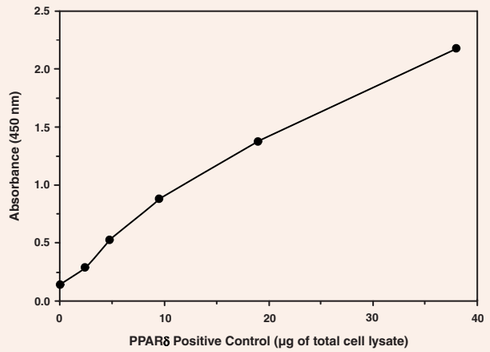

PPARγ Transcription Factor Assay Kit 10006855

Stability: ≥6 months at -80°C
Summary: A 96-well assay for measurement of PPARγ DNA binding activity

96 wells

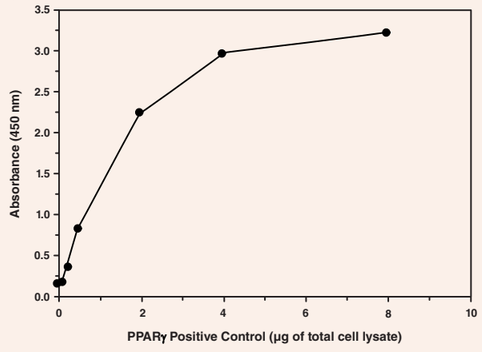

PPARγ Ligand Screening Assay Kit 10007685

Stability: ≥6 months at -20°C
Summary: Cayman's PPARγ Ligand Screening Assay Kit provides a convenient FP-based single step assay for screening PPARγ ligands. In this assay, a ligand of PPARγ was conjugated to FITC and is used as the displacement probe. Agonists, and antagonists of PPARγ will displace the fluorescent probe leading to a decrease in FP. The assay has been validated using known agonists/ligands of PPARγ.

384 wells
1,920 wells

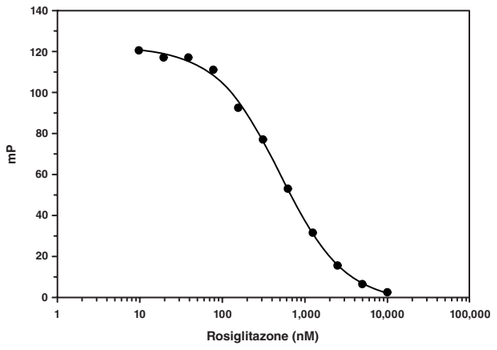

Progranulin

Progranulin (PGRN) is an autocrine growth factor that plays a role in embryonic development, tissue repair, tumorigenesis, and inflammation. Recently, PGRN has been shown to bind directly to tumor necrosis factor receptors where it antagonizes TNF-α signaling, effectively blocking the pathogenesis of inflammatory arthritis in mice. Furthermore, elevated serum concentrations of PGRN are associated with visceral obesity, elevated plasma glucose, and dyslipidemia. In the central nervous system, PGRN is thought to be involved in neurotrophic activity and neuroinflammation.

Progranulin (human) EIA Kit 500940

Stability: ≥6 months at 4°C **Limit of detection:** 32 pg/ml
Summary: Cayman's Progranulin (human) EIA Kit is an immunometric assay which can be used to measure progranulin in human serum, plasma, or cell culture supernatants.
Specificity:

Progranulin (human)	100%

96 wells

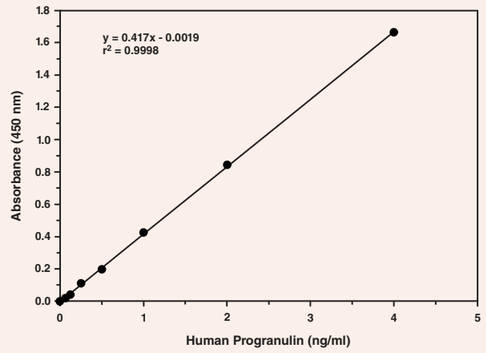

Progranulin (mouse) EIA Kit 500950

Stability: ≥6 months at 4°C **Limit of detection:** 60 pg/ml
Summary: Cayman's Progranulin (mouse) EIA Kit is an immunometric assay which can be used to measure progranulin in mouse serum or cell culture supernatants.
Specificity:

Progranulin (mouse)	100%

96 wells

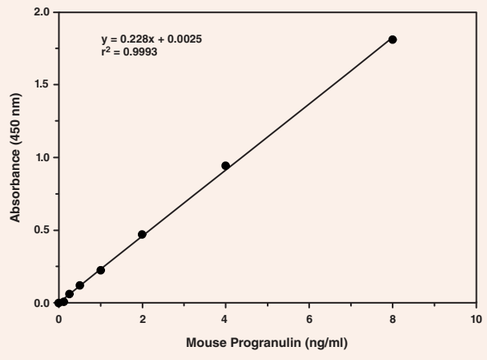

Resistin

Resistin is a peptide hormone belonging to the class of cysteine-rich secreted proteins termed the RELM family, and is also described as adipose tissue-specific secretory factor (ADSF) and Found in Inflammatory Zone (FIZZ3). Resistin impairs glucose tolerance and insulin action in mice and also inhibits adipogenesis of mouse 3T3-L1 cells. Therefore, resistin has been proposed as an adipocyte secreted factor linking obesity and type 2 diabetes.

Resistin (human) EIA Kit† 10007610

ADSF, FIZZ3
Stability: ≥6 months at 4°C **Limit of Detection:** 0.1 ng/ml
Summary: This EIA is based on a double-antibody sandwich technique for quantification of human resistin.
Specificity:
For a full specificity profile, please go to www.caymanchem.com

96 wells

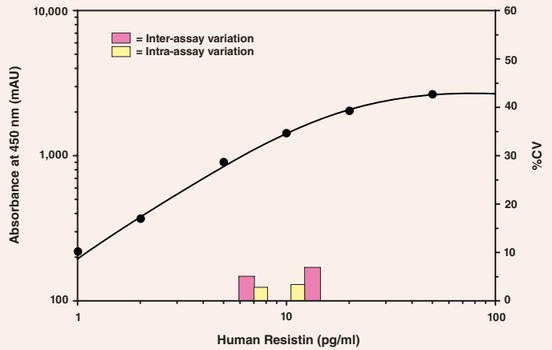

Resistin (rat) EIA Kit† 10007612

ADSF, FIZZ3
Stability: ≥6 months at 4°C **Limit of Detection:** 0.05 ng/ml
Summary: This EIA is based on a double-antibody sandwich technique for quantification of rat resistin.
Specificity:
For a full specificity profile, please go to www.caymanchem.com

96 wells

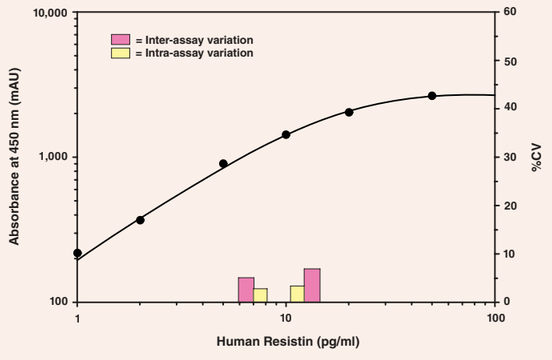

Pyruvate Assay Kit 700470

Pyruvic Acid
Stability: ≥6 months at -20°C
Summary: Pyruvate (pyruvic acid) is a key intermediate in cellular metabolic pathways and is derived primarily from glucose *via* glycolysis. Abnormal blood pyruvate levels are reported in a number of disorders including shock, liver disease, congestive heart failure, diabetes mellitus, thiamine deficiency, and metabolic disorders. Cayman's Pyruvate Assay provides a fluorescence-based method for quantifying pyruvate in biological samples such as serum, plasma, blood, urine, and saliva. It can also be utilized to determine intracellular and extracellular pyruvate concentrations in cell culture samples.

96 wells

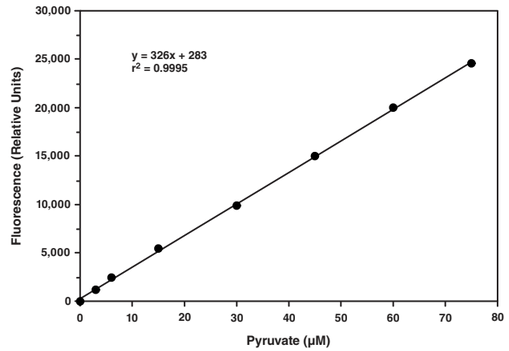

Retinol Binding Protein 4 (human) Competitive EIA Kit 579070

RBP4
Stability: ≥6 months at 4°C **Limit of Detection:** 2.3 ng/ml
Summary: Retinol binding protein (RBP) 4 is a vitamin A transport protein that acts as an adipokine when secreted from adipose tissue. Increased circulating RBP4 levels have been reported in several metabolic complications such as obesity, insulin resistance, metabolic syndrome, and cardiovascular disease. Increased expression of RBP4 positively correlates with increases in pro-inflammatory cytokines and LDL cholesterol in diet-induced obese and hyperlipidemic mice. Reduction of RBP4 has been shown to improve insulin resistance and dyslipidemia. This implicates RBP4 in regulating systemic insulin sensitivity and lipid metabolism, making measurement of serum or plasma RBP4 a useful means to monitor metabolic disorders and to possibly indicate cardiovascular disease risk. Cayman's RBP4 (human) Competitive EIA Kit can be used to measure RBP4 in human plasma, serum, urine, and cell culture supernatants.
Specificity:
For a full specificity profile, please go to www.caymanchem.com

1 ea

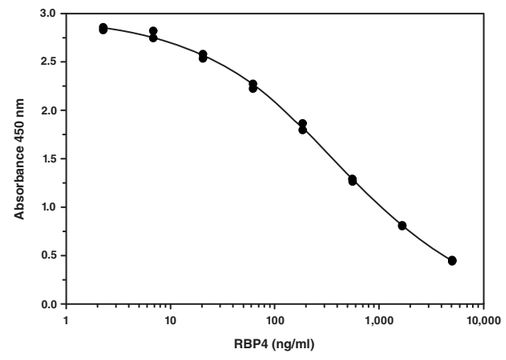

† *SPI-BIO Assays are available through Cayman Chemical only within North & South America and Asia; elsewhere contact Bertin Pharma.*

SREBP-1 Transcription Factor Assay Kit 10010854

Stability: ≥1 year at -80°C
Summary: SREBP-1c acts primarily to activate genes required for fatty acid synthesis, such as acetyl CoA carboxylase, fatty acid synthase, and long chain fatty acid elongase. SREBP-1c has important clinical implications in the treatment of many diseases including obesity, diabetes mellitus, insulin resistance, and non-alcoholic fatty liver disease. Cayman's SREBP-1 Transcription Factor Assay Kit is a non-radioactive, sensitive method for detecting specific transcription factor DNA binding activity in nuclear extracts and whole cell lysates in a 96-well plate format.

96 wells

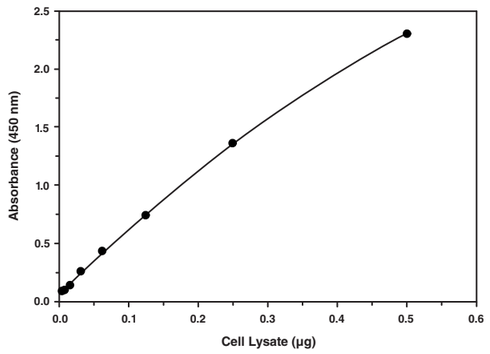

SREBP-2 Cell-Based Translocation Assay Kit 10009239

Stability: ≥1 year at -20°C
Summary: Cayman's SREBP-2 Cell-Based Translocation Assay Kit provides the tools needed to study SREBP-2 movement within whole cells. The kit contains a highly specific SREBP-2 primary antibody together with a DyLight™ (product of Thermo Scientific, Inc.) conjugated secondary antibody in a ready to use format. Also included as a positive control is a cholesterol trafficking inhibitor, U-18666A.

96 wells

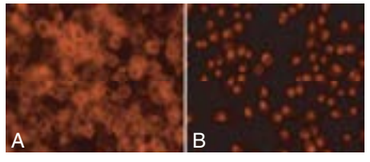

Translocation of SREBP-2 into nuclei by U-18666A. RAW 264.7 cells were treated with DMSO (*vehicle; Panel A*) or 24 µM U-18666A (*Panel B*) for 72 hours.

SREBP-2 Transcription Factor Assay Kit 10007819

Stability: ≥6 months at -80°C
Summary: SREBP-2 is a transcription factor that performs a critical role in the transcriptional regulation of genes involved in cholesterol synthesis and uptake including HMG-CoA synthase, HMG-CoA reductase, and the LDL receptor. Cayman's ChREBP Transcription Factor Assay Kit is a non-radioactive, sensitive method for detecting specific transcription factor DNA binding activity in nuclear extracts and whole cell lysates in a 96-well plate format.

96 wells

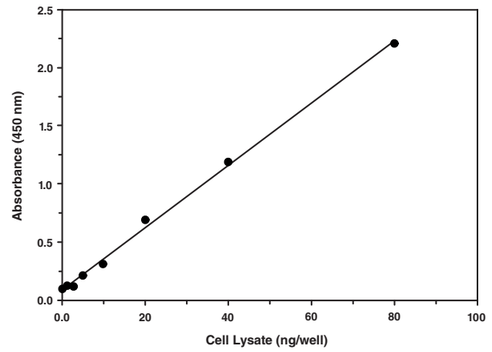

Steatosis Colorimetric Assay Kit 10012643

Stability: ≥1 year at 4°C
Summary: Steatosis, also known as fatty liver, is a pathological process characterized by abnormal accumulation of lipid within cells. Cayman Chemical's Steatosis Colorimetric Assay provides a convenient tool for evaluating the steatosis risk of drug candidates. In this assay, Oil Red O is used to stain neutral lipids in hepatocytes. Lipid accumulation is then quantified using a plate reader after the dye is extracted from the lipid droplets. Chloroquine is included in the kit as a positive control.

1 ea

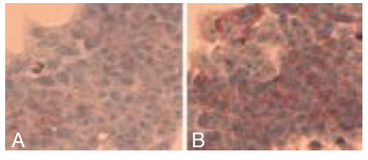

Effect of chloroquine on lipid droplet accumulation in HepG2 cells. *Panel A*: HepG2 cells treated with vehicle. There are a few lipid droplets in the cells, appearing as red dots. *Panel B*: HepG2 cells treated with 25 µM chloroquine show significant accumulation of lipid droplets, evident by abundant appearance of red dots visualized by Oil Red O staining.

Sirtuins

The sirtuins represent a distinct class of trichostatin A-insensitive lysyl-deacetylases (class III HDACs) that catalyze a reaction coupling lysine deacetylation to the formation of nicotinamide and O-acetyl-ADP-ribose. Cayman's Direct Fluorescent Screening Assay Kits provide a fluorescence-based method for screening SIRT inhibitors or activators. The procedure requires only two easy steps, both performed in the same microplate. In the first step, the substrate is incubated with human recombinant SIRT along with its co-substrate NAD^+. Deacetylation sensitizes the substrate such that treatment with the developer in the second step releases a fluorescent product.

SIRT1 Direct Fluorescent Screening Assay Kit 10010401

Stability: ≥1 year at -80°C
Summary: A fluorescence-based method for screening SIRT1 inhibitors or activators

96 wells

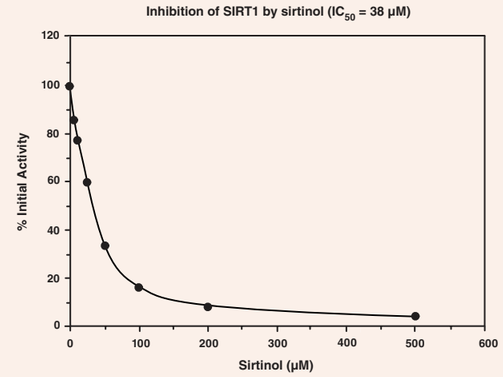

SIRT2 Direct Fluorescent Screening Assay Kit 700280

Stability: ≥1 year at -80°C
Summary: A fluorescence-based method for screening SIRT2 inhibitors or activators

96 wells

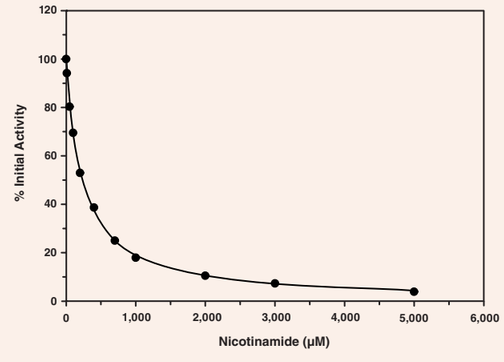

SIRT3 Direct Fluorescent Screening Assay Kit 10011566

Stability: ≥1 year at -80°C
Summary: A fluorescence-based method for screening SIRT3 inhibitors or activators

96 wells

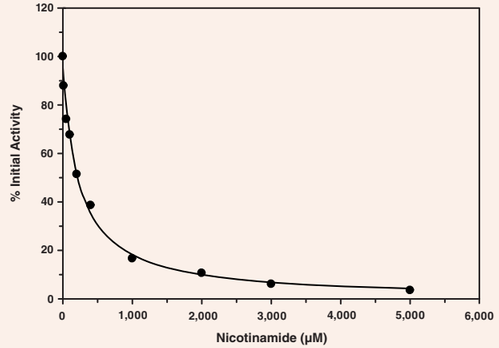

SIRT6 Direct Fluorescent Screening Assay Kit 700290

Stability: ≥1 year at -80°C
Summary: A fluorescence-based method for screening SIRT6 inhibitors or activators

96 wells

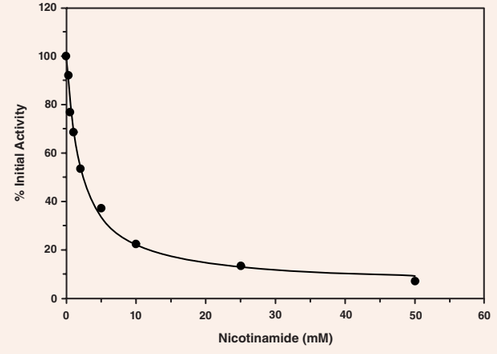

SIRT1 FRET-Based Screening Assay Kit 10010991

Stability: ≥1 year at -80°C
Summary: Cayman's SIRT1 FRET-based Screening Assay Kit provides a fluorescence-based method for screening SIRT1 inhibitors or activators. The procedure requires only two easy steps, both performed in the same microplate. In the first step, the substrate, which is coupled to the fluorophore and quencher, is incubated with human recombinant SIRT1 along with its co-substrate NAD^+. Deacetylation sensitizes the substrate such that treatment with the developer in the second step results in the separation of the quencher and fluorophore. The resulting fluorescence is analyzed using an excitation wavelength of 335-345 nm and emission wavelength of 440-465 nm.

96 wells

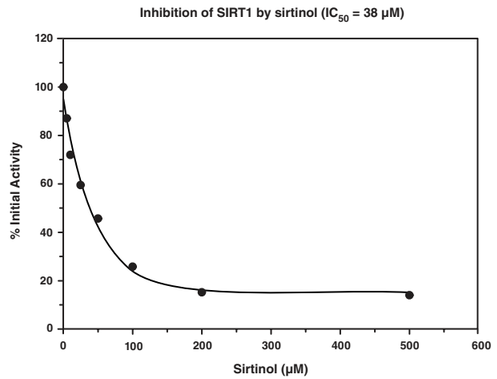

Triglyceride Fluorometric Assay Kit 700730

Stability: ≥1 year at -20°C **Limit of Detection:** 0.3 mg/dL (±0.05 mg/dL)
Summary: Triglycerides are transported in the blood as core constituents of all lipoproteins, but are major components of triglyceride-rich chylomicrons and very low-density lipoproteins. When required, lipases hydrolyze triglycerides from adipose tissue into fatty acids and glycerol, which enter the blood stream leading to fatty acid oxidation in the mitochondria and peroxisomes to produce energy. The measurement of triglyceride levels, in conjunction with other lipid assays, are useful in the diagnosis of primary and secondary hyperlipoproteinemia, dyslipidemia, and triglyceridemia as well as other diseases involving lipid metabolism or various endocrine disorders. Cayman's Fluorometric Triglyceride Assay provides a fluorescence-based method for quantifying triglycerides in plasma and serum.

96 wells

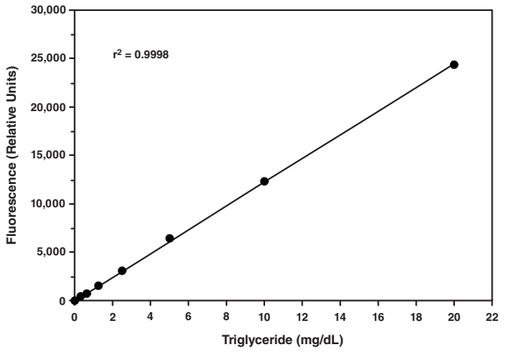

•Also Available: **Triglyceride Colorimetric Assay Kit** (10010303)

Vaspin (human) EIA Kit 579000

Visceral Adipose Tissue-Derived Serpin A12
Stability: ≥6 months at 4°C **Limit of detection:** 12 pg/ml
Summary: Vaspin, designated as visceral adipose tissue-derived serpin A12, is an adipokine with insulin-sensitizing effects. Vaspin mRNA expression is specific for visceral adipose tissues and it is also found circulating in serum. The level of serum vaspin increases with age up to the peak of obesity, body weight, and insulin resistance in OLETF rats, an animal model of abdominal obesity with type 2 diabetes. Treatment with insulin or pioglitazone normalizes serum vaspin concentrations in this model. As such, vaspin may be regarded as a potential biomarker for obesity and impaired insulin sensitivity. Cayman's Vaspin (human) EIA Kit can be used to measure vaspin in human serum, plasma, or cell culture supernatants.
Specificity:

Human Vaspin	100%

96 wells

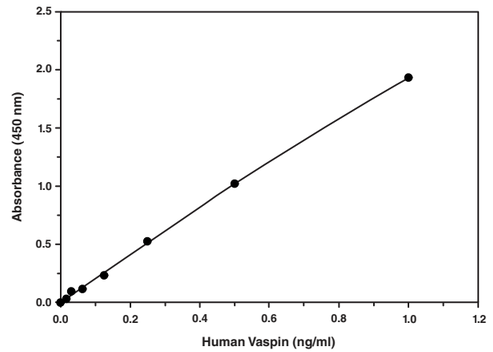

Proteins

ChREBP DBD (human recombinant) 10009524

ChREBP DNA Binding Domain, Williams-Beuren Syndrome Chromosome Region 14, WS-bHLH
M_r: 38.3 kDa **Purity:** ≥85%
Source: Recombinant GST-tagged ChREBP amino acids 648-741 expressed in *E. coli*

5 µg
10 µg
25 µg

•Also Available: **ChREBP DBD Western Ready Control** (10009753)

FABP1 (human recombinant) 10009547

L-FABP, Liver-FABP
M_r: 18.3 kDa **Purity:** ≥90%
Source: Recombinant N-terminal His-tagged protein expressed in *E. coli*

25 µg
50 µg
100 µg

FABP1 (rat recombinant) 10005200

L-FABP, Liver-FABP
M_r: 18.3 kDa **Purity:** ≥95%
Source: Recombinant N-terminal His-tagged protein expressed in *E. coli*

25 µg
50 µg
100 µg

FABP2 (human recombinant) 10009548

I-FABP, Intestinal-FABP
M_r: 19.3 kDa **Purity:** ≥95%
Source: Recombinant N-terminal His-tagged protein expressed in *E. coli*

25 µg
50 µg
100 µg

FABP2 (rat recombinant) 10007938

I-FABP, Intestinal-FABP
M_r: 19.3 kDa **Purity:** ≥95%
Source: Recombinant N-terminal His-tagged protein expressed in *E. coli*

25 µg
50 µg
100 µg

FABP3 (human recombinant) 10007432

H-FABP, Heart-FABP
M_r: 19 kDa **Purity:** ≥95%
Source: Recombinant N-terminal His-tagged protein expressed in *E. coli*

25 µg
50 µg
100 µg

FABP4 (human recombinant) 10009549

Adipocyte-FABP, A-FABP, ALBP, aP2
M: 18.8 kDa **Purity:** ≥95%
Source: Recombinant N-terminal His-tagged protein expressed in *E. coli*

25 µg
50 µg
100 µg

•Also Available: **FABP4 (human recombinant) FITC conjugated** (9001068)
FABP4 (human recombinant) Western Ready Control (10010463)

FABP4 (mouse recombinant) 10005191

Adipocyte-FABP, A-FABP, ALBP, aP2
M_r: 19.5 kDa **Purity:** ≥95%
Source: Recombinant N-terminal His-tagged protein expressed in *E. coli*

25 µg
50 µg
100 µg

•Also Available: **FABP4 (mouse recombinant) Western Ready Control** (10009676)

FABP5 (human recombinant) 10010364

DA11 FABP, E-FABP, Epidermal-FABP, Keratinocyte FABP, Psoriasis-Associated FABP
M_r: 18 kDa **Purity:** ≥95%
Source: Recombinant N-terminal His-tagged protein expressed in *E. coli*

25 µg
50 µg
100 µg

FABP5 (mouse recombinant) 10007433

DA11 FABP, E-FABP, Epidermal-FABP, Keratinocyte FABP, Psoriasis-Associated FABP
M_r: 19.3 kDa **Purity:** ≥95%
Source: Recombinant N-terminal His-tagged protein expressed in *E. coli*

25 µg
50 µg
100 µg

FABP7 (human recombinant) 10009551

B-FABP, Brain-FABP
M_r: 19.1 kDa **Purity:** ≥90%
Source: Recombinant N-terminal His-tagged protein expressed in *E. coli*

25 µg
50 µg
100 µg

Fructose 1,6-bisphosphate (human recombinant) 11104

FBP1, F1,6BPase, FDPase
M_r: 36.8 kDa **Purity:** ≥95%
Source: Recombinant protein expressed in *E. coli*

5 µg
10 µg
25 µg

Glucokinase (human liver recombinant) 10990

ATP:D-Hexose 6-Phosphotransferase GCK, Hexokinase D, Human Hexokinase IV isoform 2
M_r: 53.2 kDa **Purity:** ≥85%
Source: Active recombinant C-terminal FLAG-tagged protein expressed in *E. coli*

5 µg
10 µg
25 µg

Glucokinase (human pancreatic recombinant) 10989

ATP:D-Hexose 6-Phosphotransferase GCK, Hexokinase D, Human Hexokinase IV isoform 1
M_r: 52.8 kDa **Purity:** ≥90%
Source: Active recombinant C-terminal FLAG-tagged protein expressed in *E. coli*

5 µg
10 µg
25 µg

Hormone Sensitive Lipase (human recombinant) 10664

HSL, LIPE
M_r: 118.3 kDa **Purity:** ≥80%
Source: Active recombinant N-terminal His-tagged protein expressed in *Sf*21 insect cells

25 µg
50 µg
100 µg

11β-Hydroxysteroid Dehydrogenase 10007815

11β-HSD, HSD11β
M_r: 31.4 kDa **Purity:** ≥95%
Source: Active recombinant N-terminal His-tagged protein expressed in *E. coli*

25 µg
50 µg
100 µg

PPARα LBD (human recombinant) 10009088

PPARα Ligand Binding Domain
M_r: 34 kDa **Purity:** ≥90%
Source: Recombinant His-tagged protein expressed in *E. coli*

25 µg
50 µg
100 µg

PPARδ (human recombinant) 10007451

FAAR, NUC1, Nuclear Hormone Receptor 1, PPARβ
M_r: 54 kDa **Purity:** ≥95%
Source: Recombinant protein expressed in *Sf*21 cells

10 µg
25 µg
50 µg

- Also Available: **PPARδ Western Ready Control** (10009568)

PPARγ FL (human recombinant from *E. coli*) 61700

PPARγ Full Length
M_r: ~60 kDa **Purity:** ≥90%
Source: Recombinant N-terminal His-tagged protein expressed in *E. coli*

5 µg
10 µg
25 µg
50 µg

PPARγ FL (human recombinant from *Sf*21 cells) 10009987

PPARγ Full Length
M_r: ~60 kDa **Purity:** ≥80%
Source: Recombinant N-terminal His-tagged protein expressed in *Sf*21 cells

5 µg
10 µg
25 µg
50 µg

PPARγ LBD (human recombinant) 10007941

PPARγ Ligand Binding Domain
M_r: 34 kDa **Purity:** ≥90%
Source: Recombinant N-terminal His-tagged protein expressed in *E. coli*

25 µg
50 µg
100 µg

Serum Retinol Binding Protein 4 (human recombinant) 10007818

RBP4, sRBP4
M_r: 21 kDa **Purity:** ≥95%
Source: Recombinant His-tagged protein expressed in *E. coli*

25 µg
50 µg
100 µg

SIRT1 (human recombinant) 10011190

NAD-dependent Deacetylase 1, Silent Information Regulator 2, SIR2L1, SIR2-like Protein 1, Sirtuin 1
M_r: 89.2 kDa **Purity:** ≥60%
Source: Active recombinant N-terminal GST-tagged SIRT1 amino acids 193-747 expressed in *E. coli*

25 units
50 units
100 units

SIRT2 (human recombinant) 10011191

NAD-dependent Deacetylase 2, Silent Information Regulator 2, SIR2L2, SIR2-like Protein 2, Sirtuin 2
M_r: 44.2 kDa **Purity:** ≥90%
Source: Active recombinant N-terminal His-tagged SIRT2 amino acids 2-389 expressed in *E. coli*

25 µg
50 µg
100 µg

SIRT3 (human recombinant) 10011194

Mitochondrial Nicotinamide Adenine Dinuclear-dependent Deacetylase, NAD-dependent Deacetylase 3, Silent Information Regulator 3, SIR2L3, SIR2-like Protein 3, Sirtuin 3
M_r: 37 kDa **Purity:** ≥90%
Source: Active recombinant N-terminal His-tagged SIRT3 amino acids 101-399 expressed in *E. coli*

25 µg
50 µg
100 µg

SIRT4 (human recombinant) 10317

NAD-dependent ADP-ribosyltransferase Sirtuin 4, Silent Information Regulator 4, SIR2L4, Sir2-like Protein 4, Sirtuin 4
M_r: 61.9 kDa **Purity:** ≥95%
Source: Recombinant N-terminal GST-tagged SIRT4 purified from *E. coli*

25 µg
50 µg
100 µg

SIRT5 (human recombinant) 10318

NAD-dependent Deacetylase 5, Silent Information Regulator 5, SIR2L5, SIR2-like Protein 5, Sirtuin 5
M_r: 60.6 kDa **Purity:** ≥90%
Source: Recombinant N-terminal GST-tagged SIRT5 expressed in *E. coli*

25 µg
50 µg
100 µg

SIRT6 (human recombinant) 10315

NAD-dependent Deacetylase 6, Silent Information Regulator 6, SIR2L6, SIR2-like Protein 6, Sirtuin 6
M_r: 43.7 kDa **Purity:** ≥95%
Source: Active recombinant N-terminal His-tagged SIRT6 amino acids 1-355 expressed in *E. coli*

25 µg
50 µg
100 µg

SIRT7 (human recombinant) 10316

NAD-dependent deacetylase 7, Silent Information Regulator 7, SIR2L7, SIR2-like protein 7, Sirtuin 7
M_r: 49.3 kDa **Purity:** ≥85%
Source: Recombinant N-terminal His-tagged SIRT7 expressed in *E. coli*

25 µg
50 µg
100 µg

Alphabetical Index

A

B

C

D

E

F

G

H

I

J

K

L

M

Catalog Number Index


vol. 16
Me
Metabolism and Metabolic Disease
(800) 364 9897
www.caymanchem.com